Kinetic Study of Torrefaction Process of Oil Palm Biomass

by

Nik Nor Azrizam Bin Nik Norizam

Dissertation submitted in partial fulfilment of

the requirements for the

Bachelor of Engineering (Hons)

(Chemical Engineering)

MAY 2011

Universiti Teknologi PETRONAS

Bandar Seri Iskandar

31750 Tronoh

Perak Darul Ridzuan

CERTIFICATION OF APPROVAL

Kinetic Study of Torrefaction Process of Oil Palm Biomass

by

Nik Nor Azrizam Bin Nik Norizam

A project dissertation submitted to the
Chemical Engineering Department
Universiti Teknologi PETRONAS
in partial fulfilment of the requirement for the
BACHELOR OF ENGINEERING (Hons)
(CHEMICAL ENGINEERING)

Approved by,

_____

(DR. Khalik M. Sabil)

UNIVERSITI TEKNOLOGI PETRONAS

TRONOH, PERAK

May, 2011

CERTIFICATION OF ORIGINALITY

This is to certify that I am responsible for the work submitted in this project, that the original work is my own except as specified in the references and acknowledgements, and that the original work contained herein have not been undertaken or done by unspecified sources or persons.

_____

(NIK NOR AZRIZAM BIN NIK NORIZAM)

ABSTRACT

Torrefaction is thermal pretreatment process for biomass at temperature range from 200 to 300°C which carried out at under inert atmosphere. This process is aiming to produce solid fuel which increased energy density, lowered moisture content and easy to comminute into small particle size by decomposing hemicellulose. In this study, three types of oil palm biomass namely empty fruit bunch (EFB), palm mesocarp fiber (PMF) and palm kernel shell are torrefied by using thermogravimetric analyzer (TGA) at different particle sizes, i.e. 250-355µm and 355-500µm. Two steps reaction are found out to give description about decomposition for EFB, PMF and PKS. For two steps, activation energies, E_a of 58267 kJ/mol and -34247 kJ/mol, respectively and pre-exponential factors, A of $11x10^3$ and $1.24x10^{-6}$, respectively for EFB with particle size 250-355 µm are found. During the process, only hemicellulose decomposition takes place. The hemicellulose decomposition is more significant compare to cellulose and lignin during torrefaction of oil palm biomass since temperature decomposition of hemicellulose between 225-325°C. TGA process conditions are replicated using tube furnace to determine energy yield and ultimate analysis for torrefied samples. Energy yield is found increasing with torrefaction temperature. Meanwhile, kinetic model is created and verified for predicting amount of torrefied solid. As conclusion, four main parameters give significant towards torrefaction process which are type of biomass, particle size, torrefaction temperature and reaction time.

ACKNOWLEDGEMENT

First of all, I would like to express my thankfulness to Allah the almighty who gave me the strengths to face challenges in completing this final year research project.

I would like to express my sincere thanks and deep appreciation to Dr. Khali M. Sabil, my final year research project supervisor for his constant supervision and continuous guidance during completing my research project. Not to forget Mrs. Muafah Abd Aziz as master student for the cooperation and endless help.

I would also like to express my infinite gratitude to all chemical engineering department technicians and technician from biohydrogen, Mr. Syamil for their cooperation given throughout the experiment conducted in the laboratory. I would like to extend my gratitude to FELCRA, Bota, Perak and biohydrogen group for their contribution in my research project.

Lastly, I would like to thanks all parties who were involved directly and indirectly in completing my study on kinetic of torrefaction process of oil palm biomass. All the contributions are highly appreciated.

TABLE OF CONTENTS

LIST OF FIGURES

LIST OF TABLE

ABBREVIATIONS AND NOMENCLATURE

Symbol or Abbreviations	Description
EFB	Empty Fruit Bunch
PMF	Palm Mesocarp Fiber
PKS	Palm Kernel Shell
TGA	Thermogravimetric Analyzer
CHNS Analyzer	Carbon, Hydrogen, Nitrogen, Sulphur Analyzer

CHAPTER 1: INTRODUCTION

1.1. Background of Study

Malaysian palm oil industry has grown tremendously over the last 4 decades and since then, it has maintained its position as the leading world's country in the production of palm oil. Nevertheless, the industry has also generated vast quantities of palm biomass, mainly from milling and crushing palm kernel. Generally, most of this biomass can be used as combustion fuels. Currently, the shell and fiber are the main sources of energy in palm oil mills. These fuels are burnt in boiler to produce steam for electricity generation to be used in the milling process. However, EFB, PMF and PKS, due to its physical properties and demands, are not normally utilized as fuel. In order to make use of the resource and expand its usage as fuel in various industries and applications, raw oil palm biomass should be treated and upgraded into uniform and useful fuels [1].

Small Renewable Energy Programme (SREP) Development in Sabah from Malaysian Palm Oil Board (MPOB) Perspective had presented their analysis regarding waste generated by palm at year 2009 where fiber generated 11.14 million tonnes, shell generated 5.14 million tonnes and empty fruit bunch generated 19.71 million tonnes. Over year, accumulated waste of palm causes Malaysia facing huge amount of abundant waste. Environmental issue rise from untreated decomposition of waste from irresponsible industry. As a concern, many researchers found out method to treat the waste in proper way by converting to solid, liquid and gas fuels.

Over years, amount of fossil fuel in the world starts to decrease and hence, it is needed an alternative renewable energy resource for replacement. Due to that concern, many researches were developed to investigate an alternative energy resource. Conversion of biomass to bio oil is one of the prospective alternative energy resources. Wastes palm such as EFB, PMF, and PKS are used as a sample material and carried out through pyrolysis, gasification or combustion methods in order to decrease abundant waste and environmental problem of waste palm.

Figure 1: Waste Generated after Palm Oil Process. (a) Empty Fruit Bunch (EFB), (b) Palm Mesocarp Fiber (PMF) and (c) Palm Kernel Shell (PKS). (Taken from FELCRA, Bota, Perak)

Unfortunately, after going through either method, product produced is worst in term of properties such as low energy density and high moisture content. It leads researchers to find out an alternative way to enhance the properties. A new method recently has been found and it has been proved to improve properties of bio oil to be used as a fuel. It is a pretreatment process, called as torrefaction process.

The study on torrefaction has attracted a few researchers' focus in order to find replacement for fossil fuel. However, this study is still not widely used and the data regarding torrefaction process is less and limited. In order to continue further research on effectiveness of torrefaction process, research on kinetic study of torrefaction process of oil palm biomass has carried out and studied.

1.2. Problem Statement

Torrefaction had been reported as one of the pretreatment method for improving properties of agricultural wastes. Despite all the reported data, the fundamental studies on torrefaction process for oil palm wastes; namely empty fruit bunch (EFB), palm mesocarp fiber (PMF) and palm kernel shell (PKS) are rather limited. Specifically, study on the optimum torrefaction conditions and parameters and kinetics of oil palm wastes is not widely discovered.

However, the use of raw biomass materials as a fuel entails several problems, such as its high bulk volume, high moisture content and relatively low calorific value, which make raw biomass an expensive fuel to transport [2].

Besides, untreated biomass has a relatively low energy density, high moisture content and is difficult to comminute into small particles. Those problems contribute in storage complications such as degradation and self-heating, lower combustion efficiencies and gasifier design limitations.

Furthermore, enhancement of the energy yield is required to replace an equivalent amount of coal in applications such as combustion and gasification.

1.3. Objective and Scope of Study

The objectives of this research are:

1. to analyze weight loss of oil palm biomass (EFB, PMF and PKS) during torrefaction process

2. to analyze temperature affect towards different types of oil palm biomass and decomposition of hemicellulose, cellulose and lignin during torrefaction process.

3. to analyze energy yield of oil palm biomass before and after torrefaction process.

4. to analyze carbon, nitrogen, hydrogen, sulphur and oxygen contents before and after torrefaction process.

5. to create model for torrefaction process through relationship between weight loss and reaction kinetic.

This research is studied and carried out through experimental and modeling works. For experimental work, oven, grinder and sieving will used for sample preparation. TGA will be used to identify weight loss of waste palm, tube furnace will be used for process condition replication same as in TGA, CHNS analyzer will used to determine percent of carbon, hydrogen, nitrogen and sulphur contents (ultimate analysis) of oil palm biomass and bomb calorimeter will be used for identify calorific value of torrefied sample.

Meanwhile for modeling, MATLAB software will be used for calculating reaction kinetics involved during torrefaction process. After that, model will be verified for predicting amount of torrefied product (solid fuel).

CHAPTER 2: LITERATURE REVIEW

2.1. Torrefaction of Biomass

Torrefaction is a thermochemical treatment method in the first place earmarked by an operating temperature within the range of 200 to 300 °C. It is carried out under atmospheric condition and in the absence of oxygen. The name torrefaction is adopted from the roasting of coffee beans, which is, however, done at lower temperature and does allow the presence of oxygen. Nevertheless, the mechanical effects of torrefaction on biomass are supposed to be similar to its effect on coffee beans, which is their brittle structure afterwards. Torrefaction has many synonyms. Some examples are roasting, slow and mild pyrolysis, wood cooking and high-temperature drying. Especially the link with pyrolysis is easy to make as torrefaction covers part of the initial decomposition reactions of pyrolysis.

The main torrefaction product is the solid phase, which is similar to pyrolysis referred to as the charred residue. In the field of torrefaction the solid product is also frequently called torrefied wood or torrefied biomass. Similar to pyrolysis, during torrefaction the chemical structure of biomass is altered. This leads to the formation of a variety of volatile (decomposition) products of which some are liquids at room temperature (condensable). By mass, important reaction products other than char are carbon dioxide, carbon monoxide, water, acetic acid and methanol [3]. After condensation, liquid products manifest themselves as a yellowish liquid. All these non-solid reaction products contain relatively more oxygen compared to the untreated biomass. Hence the O/C ratio of torrefied biomass is lower than untreated biomass, resulting in an increase of the calorific value of the solid product.

Torrefaction of wood has attracted more interest recently. Pentanunt et al. (1990) carried out torrefaction experiments at the Asian Institute of Technology in Bangkok. They compared combustion characteristics of torrefied wood produced after 2-3 hours of torrefaction and concluded that torrefied wood produces less smoke compared with untreated wood. In Brazil, a bench unit was used to determine the effect of raw material, temperature, and residence time on the properties of torrefied wood at the University of Campinas. Torrefaction research is currently carried out at the National Renewable

Energy Centre (NREL) in Golden, Colorado [8] and the Royal Institute of Technology (KTH) in Stockholm, Sweden. However, torrefaction of palm waste is still not widely focused and data available is limited. As an incentive and concern about environmental issues in Malaysia, research on palm waste is carried out in this report.

Lignocellulose is another word for biomass that originates from plants. It generalizes the structure of plants to the three main sugar-based polymeric structures; cellulose, hemicellulose and lignin. These three polymeric structures are mainly considered in most of the studies aiming for the understanding of decomposition mechanisms of woody and herbaceous biomass. In plant structures lignocellulose normally forms the most dominant group of constituents on a mass basis. Its main role is found in the cellular structure of plants and forms the foundation of cell walls and their mutual coherence. Lignocellulose provides mechanical strength and tenacity (toughness) to plant structures and so provides body and the opportunity to grow in height for optimal photosynthesis.

A typical plant cell is structured as illustrated by figure 2. A single cell is typically described by a primary and a secondary wall. Subsequently, three individual layers describe the secondary wall. Individual cells are connected through a glue layer called the middle lamella.
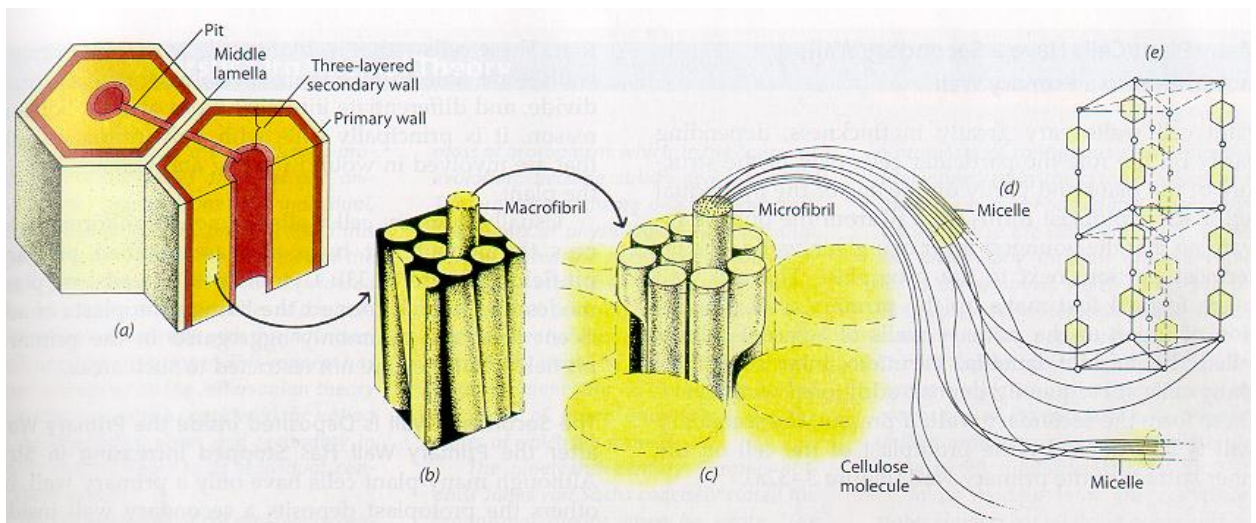
Figure 2: Detailed impression of the structure of a cell wall. (a) Part of the cell wall and middle lamella, primary wall and secondary wall, (b) macrofibrils mutual structure, (c) microfibrill structure, (d) individual cellulose polymers including micelles, and (e) mutual coherence of individual cellulose polymers on a micro level (Taken from Bergman et al., 2005)

The second layer of the secondary wall is the thickest one and is built from vertically oriented macrofibrils. The macrofibril is on its turn composed from macrofibrils, which predominantly consist of evenly oriented cellulose molecules of certain length. The cellulose chains comprise amorphous parts, but also crystalline parts whereby subsequent cellulose molecules are connected.

The polymeric composition of the different walls and layers varies strongly and each wall has different tasks. Figure 3 and 4 illustrate how the polymeric composition varies throughout the cell wall. The middle lamella predominantly contains lignin. Lignin acts as a binding agent and can be considered a glue to bind adjacent cells. While the lignin fraction decreases cell inwards, the fraction of hemicellulose increases. Cellulose meets a maximum content in the S2 of the secondary layer and hemicellulose in S3.
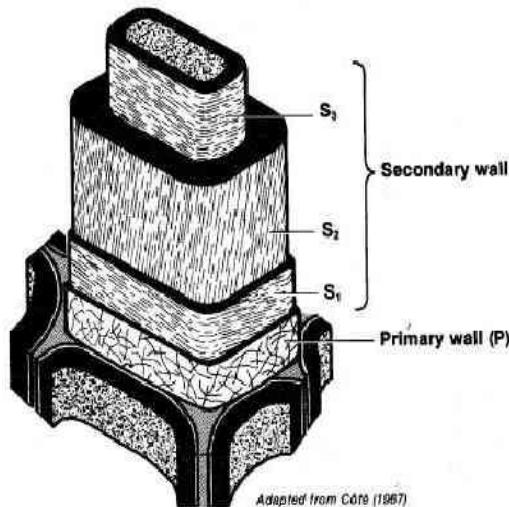
Figure 3: Distribution of lignocellulose within the three layered secondary wall (Taken from Bergman et al., 2005)
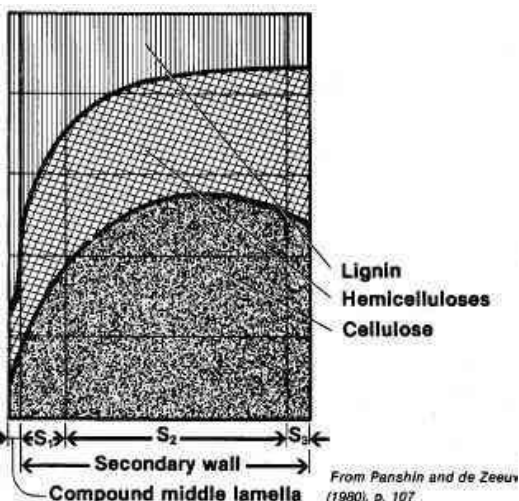
Figure 4: Distribution of lignocellulose within the three layered secondary wall (Taken from Bergman et al., 2005)

The three-layered secondary cell wall mainly consists of cellulose and is very well organized by nature. The cellulose macrofibrils are embedded in a matrix of (disoriented) hemicellulose that bonds the macrofibrils mechanically, but also through hydrogen bonding. The cell wall has a repetitive pattern in which hemicellulose binds macrofibrils of a cell wall and lignin binds adjacent cells. The function of hemicellulose is often well illustrated by comparing its function to concrete in reinforced concrete. Without the concrete the iron rods lose their mutual coherence and orientation.

Each layer of the three-layered cell wall has a different fiber orientation. The main body of the cells (S2) is a vertical oriented structure of fiber kept in a compact form by an outer husk (S1) and annular (inner) husk (S3) both with near perpendicular fiber orientation. The wood structure consists of many of these cellular units 'glued' together by the lignin-rich primary walls. The anisotropic nature of wood, the fibrous structure, is caused due to the differences in thickness and orientation of the different layers. The way cell walls are mechanically organized is copied multiple times from nature because of the high strength and tenacity it provides.

From the three main polymeric constituents of biomass, cellulose has received most attention considering the thermal decomposition of biomass. Especially since the cellulose fraction is large. Therefore, in pyrolysis research cellulose decomposition is very important. During torrefaction, mass loss will predominantly come from the decomposition (devolatilisation) of particularly hemicellulose and some of lignin.

20

Xylan-based hemicellulose generally has its peaking rate in decomposition around 250 to 280°C. Lignin decomposition proceeds slower, but shows a gradual increase of decomposition rate starting from temperatures of about 200 °C or even lower.

Hemicellulose decomposition can be well described by a two-step mechanism as was found by Di Blasi and Lanzetta (1997). The first reactions usually taking place below 250°C (first step) are depolymerisation reactions leading to altered and rearranged polysugar structures. The decomposition of these oligosaccharides and monosaccharide are at higher temperatures (250-300°C) results in the formation of chars, CO, CO_2 and water. The formation of light volatiles like carbonyl compounds result from the fragmentation of the carbon skeleton.

Up to 250 °C, thermal decomposition of cellulose is hardly accompanied with a serious mass loss. The most important mechanism occurring is found to be depolymerisation. Depolymerisation of cellulose has been observed at even 70 °C.It is known that depolymerisation of wood is already occurring at significant rates at 150 °C [9]. At 190 °C, the rate of depolymerisation is already seriously fast. A variety of permanent gases, condensable liquids and char are formed during this step.

Thermal degradation of lignin takes place over a wide temperature range. At temperatures below 200°C, some thermal softening has been observed resulting in a small weight loss of a few percent. Char formation and the release of volatiles result from a devolatilisation process in the temperature region of 240-600°C. From Mark et al. (2006), temperature decomposition for hemicellulose is from 225-325°C, lignin is from 250-500°C and cellulose is from 305-375°C.

2.2. Torrefaction Temperature and Time (Reaction Time)

Difficulties in interpreting the torrefaction process may arise from the definition of the torrefaction time. The term residence time is frequently used, but it only expresses the hold-up time of biomass in a torrefaction reactor. It does not tell how long actual torrefaction takes place, since part of the residence time is 'lost' due to heating of the biomass possibly incombination with drying. Misunderstanding about the torrefaction time automatically leads toinaccuracies in relating product quality to torrefaction operating conditions. To overcome thisproblem, the use of (reactor) residence time has been abandoned and instead the definition ofreaction time is introduced. [9]

When biomass is processed in a torrefaction reactor, it passes several stages with each having its own time-temperature characteristics. This is illustrated in figure 5 for a typical batchoperation. When moist biomass of ambient temperature is fed into a batch torrefaction reactor, the biomass is first heated to a temperature at which the biomass is dried. Then the temperature further increases until the desired torrefaction temperature is reached. This temperature is maintained until the reactor is cooled again. [9]

The temperature window of torrefaction is generally considered to range from about 200 °C to 300°C. Only in this temperature window the torrefaction decomposition reactions occur. In this temperature window three time temperature phases are recognized. First the biomass is heated from 200 °C to the desiredtorrefaction temperature (T_{tor}) in period $t_{tor, h}$. Then the temperature is hold for period t_{tor} at thetorrefaction temperature, until cooling during period $t_{tor, c}$. During t_{tor} the decomposition reactionswill contribute predominantly, but this will depend on the time contribution of the heating and cooling period. [9]

The reaction time has been defined as the sum of $t_{tor, h}+t_{tor}$ and thus leaving out the cooling time $t_{tor, c}$. The heating period is important, as during this period the most thermally labile parts of the feed biomass will rapidly start to decompose. In contrast to the cooling period when the solid product is much more thermally stable as the highest reactive parts already reacted. It is therefore expected that the decomposition reactions will stop as soon as the temperature isdecreased.Hence the cooling period hardly contributes to the decomposition of the biomass. [9]
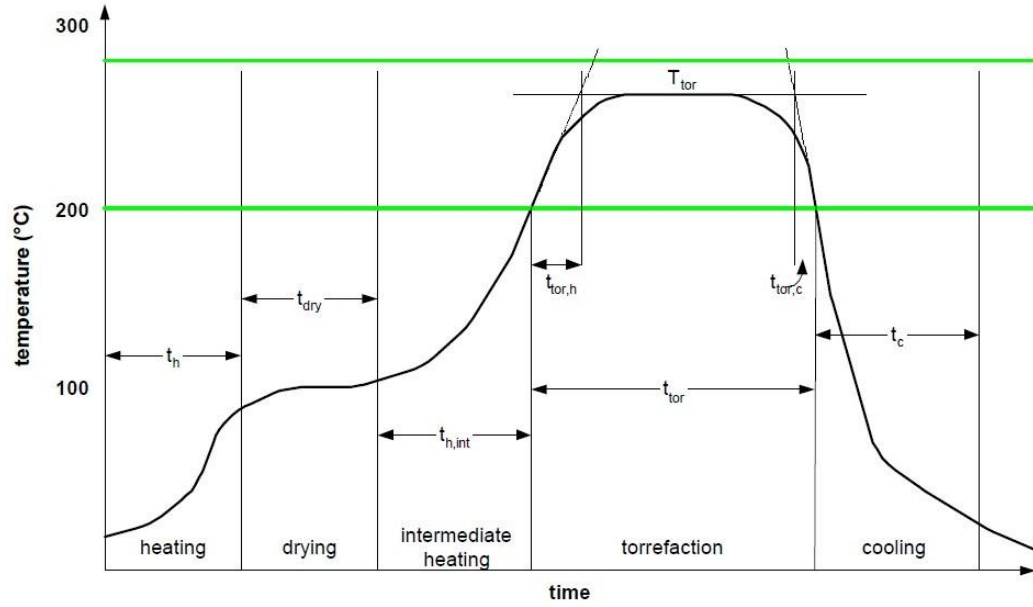
Figure 5: Stages in the heating of moist biomass from 'ambient' temperature to the desired torrefaction temperature and the subsequent cooling of the torrefied product. Temperature-time profile is considered typical for a torrefaction batch process. Explanation: t_h=heating time to drying, t_{dry}=drying time, $t_{h,\,int}$=intermediate heating rate from drying to torrefaction, t_{tor}=reaction time at desired torrefaction temperature, $t_{tor,\,h}$=heating time torrefaction from 200°C to desired torrefaction temperature (T_{tor}), $t_{tor,\,c}$=cooling time from the desired T_{tor} to 200°C, t_c=cooling time to ambient temperature (Taken from Bergman et al., 2005)

2.3. Previous Study on Torrefaction

2.3.1. Torrefaction of reed canary grass, wheat straw and willow to enhance solid fuel qualities and combustion properties

This journal examines torrefaction in nitrogen of two energy crops, reed canary grass and short rotation willow coppice (SRC), and a residue, wheat straw. Product evolution and mass and energy losses during torrefaction are measured using a range of laboratory scale methods. Experiments at different torrefaction conditions were undertaken to examine optimization of the process for the three fuels. Figure 6 gives a comparison of the mass loss profiles at 563 K of different samples. The greatest mass losses at all the temperatures investigated occurred in wheat straw although they were similar to that observed for reed canary grass, whilst the lowest change in mass was observed for willow. The difference in the cell wall composition (table1) provides an explanation for these differences. Hemicellulose is the most reactive of the three lignocellulose components found in biomass and during torrefaction it will undergo the most significant decomposition reactions. [12]

Thus the composition of biomass fuels has a significant impact on the amount of both solid residue remaining and the volatile and gaseous products evolved during torrefaction. Wheat straw and reed canary grass have similar compositions whilst willow has a noticeably lower amount of hemicellulose but higher levels of cellulose and lignin. [12]

Studies conducted using xylan (the prominent hemicellulose found in herbaceous biomass) have concluded that decomposition of hemicellulose starts at temperatures above 473 K and full devolatisation will occur by 623 K, with the major products being H_2O, CO_2, CO, and char, as well as traces or low molecular weight organics. Pure cellulose has a comparatively slower decomposition process at temperatures in excess of 523 K, and the rate of thermal decomposition only becomes more rapid above 573 K. In the 523–573 K range up to 20–30% of the polysaccharide will devolatise. However, a number of studies have concluded that accompanying this

observed mass loss are depolymerisation reactions that reduce the length of the polysaccharide polymers from 1000 to 200 monomer units. [12]

The thermal decomposition of biomass within torrefaction temperatures yields a number of different products. Water is the major product and is released in two different mechanisms, firstly during drying when moisture evaporates and secondly during dehydration reactions between organic molecules. However, there are a number of other organic and inorganic products present in the volatile component liberated during the decomposition of biomass. [12]
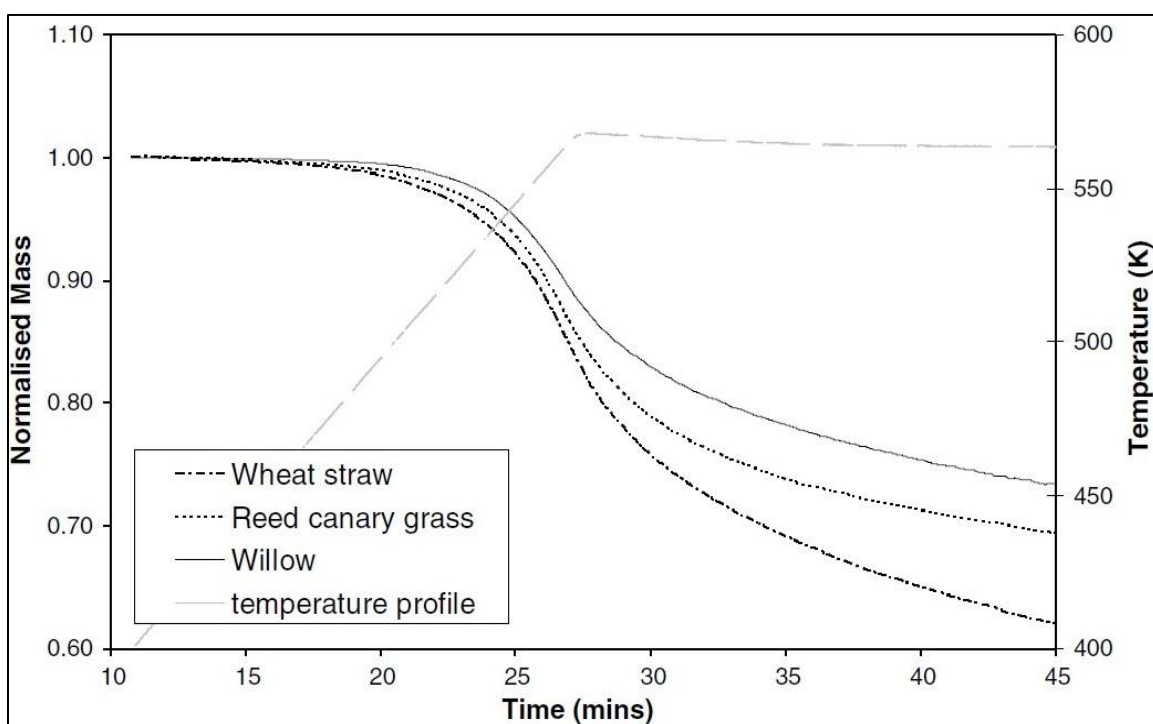
Figure 6: Mass loss of wheat straw, reed canary grass and willow during torrefaction at 563 K (Taken from Bridgeman et al., 2008)

Table 1: Mass % of hemicellulose, cellulose and lignin in raw biomass fuels (dry ash free basis)(Taken from Bridgeman et al., 2008)

	Lignin (%)	Cellulose (%)	Hemicellulose (%)	Total (DMD) (%)
Reed canary gass	7.6	42.6	29.7	80.0
Wheat straw	7.7	41.3	30.8	79.8
Willow	20.0	49.3	14.1	83.4

Progress of torrefaction was also followed by chemical analysis (table 2) and it was seen that the characters of the biomass fuels begin to resemble those of low rank coals in terms of the van Krevelen coal rank parameter. [12]

Table 2: Ultimate analysis, HHV (dry ash free basis), and moisture of untreated and torrefied biomass fuels (Taken from Bridgeman et al., 2008)

	Raw	Torrefaction temperature (K)			
		503	523	543	563
RCG					
C (%)	48.6	49.3	50.3	52.2	54.3
H (%)	6.8	6.5	6.3	6.0	6.1
N (%)	0.3	0.1	0.0	0.1	0.1
O (%)	37.3		37.0	37.3	36.3
Moisture (%)	4.7	2.5	1.9	1.3	1.2
CV (kJ/kg)	19,500	–	20,000	20,800	21,800
Wheat straw					
C (%)	47.3	48.7	49.6	51.9	56.4
H (%)	6.8	6.3	6.1	5.9	5.6
N (%)	0.8	0.7	0.9	0.8	1.0
O (%)	37.7		35.6	33.2	27.6
Moisture (%)	4.1	1.5	0.9	0.3	0.8
CV (kJ/kg)	18,900	19,400	19,800	20,700	22,600
Willow					
C (%)	49.9	50.7	51.7	53.4	54.7
H (%)	6.5	6.2	6.1	6.1	6.0
N (%)	0.2	0.2	0.2	0.2	0.1
O (%)	39.9	39.5	38.7	37.2	36.4
Moisture (%)	2.8	0.5	0.1	0.1	0.0
CV (kJ/kg)	20,000	20,200	20,600	21,400	21,900

In addition, the results indicate that the volatile component of biomass is both reduced and altered producing a more thermally stable product, but also one that produces greater heats of reaction during combustion. The difference between the mass and energy yield was shown to improve for the higher torrefaction temperatures investigated. [12]

The combustion behavior of raw and torrefied fuels was studied further by differential thermal analysis (DTA) and also, for willow, by suspending individual particles in a methane–air flame and following the progress of combustion by high-speed video. It is shown that both volatile and char combustion of the torrefied sample become more exothermic compared to the raw fuels, and that depending on the severity of the torrefaction conditions, the torrefied fuel can contain up to 96%

of the original energy content on a mass basis. Upon exposure to a methane-air flame, torrefied willow ignites more quickly, presumably because its low moisture content means that it heats faster. Torrefied particles also begin char combustion quicker than the raw SRC particles, although char combustion is slower for the torrefied fuel. [12]

2.3.2. Torrefaction of wood

The weight loss kinetics for torrefaction of willow, a deciduous wood type, was studied by isothermal thermogravimetry.
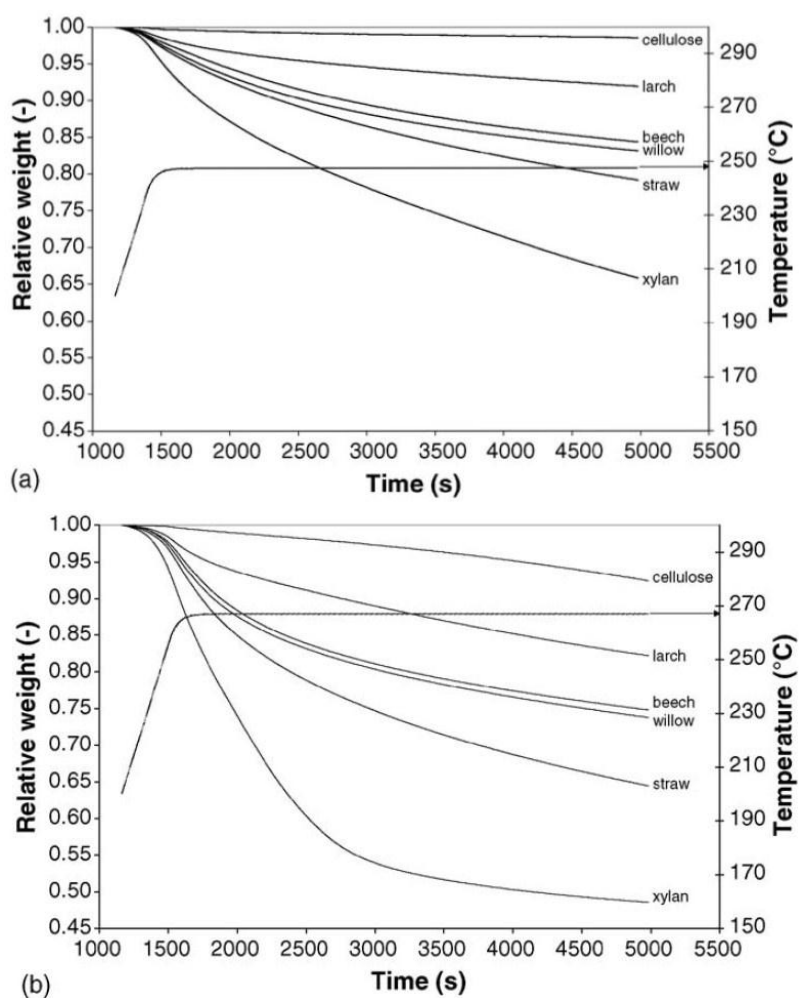

Figure 7: TGA of various biomass compounds, (a) at 248°C and (b) at 267°C. Heating rate 10°Cmin^{-1}, particle size 0.5-2 mm; dotted line is the heating curve (Taken from Prins et al., 2006).

Figure7 showed the weight loss curves of the various biomass types at 248 and 267°C obtained from isothermal TGA experiments. The weight loss observed during heating of the sample from 200°C, the temperature at which thermal decomposition begins to occur, to the required temperature is relatively small, except for xylan. From figure7, it can be concluded that xylan, the main hemicellulose component of deciduous wood, is the most reactive component. It starts decomposing around 200°C and has a high weight loss. At 267°C, limited weight loss of cellulose is found. [5]

The hardwoods beech and willow have comparable reactivity. The weight loss observed lies between that of xylan and cellulose, which was expected as wood contains these fractions. High xylan content also explains the relatively high weight loss of wheat straw, although catalytic effects due to the presence of mineral matter could also play a role. Finally, the coniferous larch reacts a lot slower than the hardwoods. [5]

As a preliminary conclusion, hardwood loses considerably more weight than softwood and therefore a higher increase in energy density (J/g) may be expected. This makes hardwood an attractive feedstock for torrefaction processes. [5]
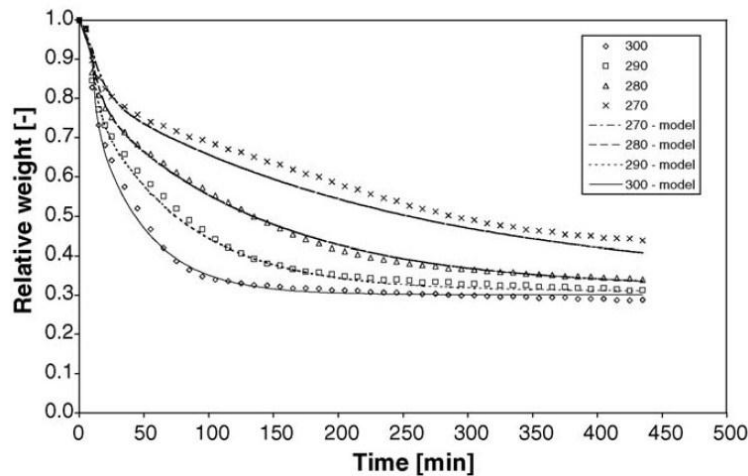

Figure 8: Experimental and modeled relative weight of willow versus time, for various temperatures. Starting weight defined at 200°C; time includes a heating period of 7-10 min (heating rate=10°C min^{-1}) (Taken from Prins et al., 2006)

To verify the final char yield predicted by the model, TGA experiments with a longer reaction time of 435 min were carried out and included a heating period of 7–10 min at a heating rate of 10°C min^{-1}. The results are shown in figure 8. At temperatures of 280–300°C, predicted char yields of 29–31% showed good agreement with experimental data, whereas determination of the final char yield at 270°C was not possible because the weight had not stabilized yet within 435 min. Careful consideration of the experimental weight curves teaches that these do not become completely horizontal, but the weight continues to decrease very slowly. [5]

The final char yield is the product of the solid yield for the first decomposition reaction and the second decomposition reaction. For the temperature range studied, solid yield for the first decomposition decreases from 88% at 230°C to 70% at 300°C, whereas second decomposition is fairly constant at 41%. The first reaction with a relatively low weight loss could very well be representative of decomposition of the reactive xylan in willow wood, since hardwood contains up to 30% of xylan. [5]

The high weight loss in the second reaction can be explained by decomposition of the other fractions contained in the wood, notably the cellulose fraction, perhaps in combination with charring of the remaining hemicellulose fraction. This is also plausible because the activation energy found for the second weight loss step is close to literature values. It may be that the primary decomposition products of xylan decomposition, i.e. acids, initiate decomposition of cellulose fraction. [5]

The kinetics of torrefaction reactions in the temperature range of 230–300°C can be described accurately by a two-step mechanism. The first step is much faster than the second step, so that these steps can be demarcated in time. The first step is representative of hemicellulose decomposition, while the second step represents cellulose decomposition. The solid yield for the first step is higher than for the second step: 70–88% (decreasing with temperature) versus 41%. This may be explained because deciduous wood, such as willow, contains less xylan (the reactive component in its hemicellulose fraction) than cellulose. Xylan reacts approximately one order of magnitude faster than willow, a classical hardwood containing up to

30% xylan. However, initial experiments have shown that softwood is much less reactive and therefore lower rate constants can be expected. [5]

2.4. Reaction Kinetic

For hemicellulose decomposition, a global one-step reaction gives a very rough impression of kinetics of the overall reaction but it is difficult to compare parameters consistently with other researchers. That hemicellulose decomposition could not be modeled by simple kinetics. Research done on multi-step reaction mechanisms gives better results. They found a model of competitive reactions could not describe their data, and proposed a model with two successive reactions, as given in figure 9. In such a model, Xylan is assumed to form an intermediate reaction product, which is a solid with a reduced degree of polymerization. This intermediate then reacts to the final product. The first reaction was found to be substantially faster than the second one. [5]
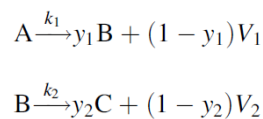
$$A \xrightarrow{k_1} y_1 B + (1 - y_1) V_1$$

$$B \xrightarrow{k_2} y_2 C + (1 - y_2) V_2$$

Figure 9: Equation 1 (Taken from Prins et al., 2006)

The yields of solid product are denoted as the parameters y_1 and y_2 for the first and second reactions, respectively. These parameters as temperature-independent, i.e.for Xylan decomposition, constant values for the solidyields of the first and second reactions were reported. Therefore,the model fails to take into account the change of final charyield (which equals the product of y_1 and y_2) with temperature. Nevertheless, the final char yield can be expected todecrease with temperature, as the hemicellulose componentis dehydrated to a larger extent. [5]

Di Blasi and Lanzetta (1997) used isothermal TGA measurements for evaluation of the kinetic parameters of torrefaction of Xylan. They modeled the kinetics by a combination of a two-step mechanism (figure 9) with parallel reactions for the formation of solids and volatiles.
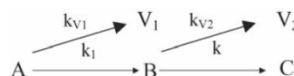

Figure 10: Two-Step Mechanism (Taken from Prins et al., 2006)

The solid yields are given by:

$$y_1 = \frac{k_1}{k_1 + k_{V_1}}$$

$$y_2 = \frac{k_2}{k_2 + k_{V_2}}$$

Figure 11: Equation 2 (Taken from Prins et al., 2006)

When the activation energy of k_{V1} (respectively, k_{V2}) is higher than that of k_1 (respectively, k_2), the solid yield drops withincreasing temperature. So the introduction of separate formation of different product classes, which may be questioned fromthe viewpoint of analytical chemistry, is a mathematical approximation to describe the fact that the ratio between formed solids and volatiles depends on temperature. [5]

The differential rate equations are given for the solids by

$$r_A = \frac{d[A]}{dt} = -(k_1 + k_{V_1})[A]^{n_A}$$

$$r_B = \frac{d[B]}{dt} = k_1[A]^{n_A} - (k_2 + k_{V_2})[B]^{n_B}$$

$$r_C = \frac{d[C]}{dt} = k_2[B]^{n_B}$$

Figure 12: Equation 3 (Taken from Prins et al., 2006)

Similar equations may be derived for the volatile products. If all reactions are assumed to be of first order, the system ofequations can be solved analytically. Integration of thedifferential equations, with the initial condition that only A is present at the beginning of the reactions, and addition givesan expression for the relative solid weight:

$$M = [A] + [B] + [C]$$

Figure 13: Equation 4 (Taken from Prins et al., 2006)

$$\frac{M_t}{M_0} = \left(1 + \left[\frac{k_1 K_1 - k_1 k_2}{K_1(K_2 - K_1)}\right]\right)e^{-K_1 t} + \left[\frac{-k_1 K_2 + k_1 k_2}{K_2(K_2 - K_1)}\right]e^{-K_2 t}$$
$$+ \frac{k_1 k_2}{K_1 K_2}$$

Figure 14: Equation 5 (Taken from Prins et al., 2006)

where:

$$K_1 = k_1 + k_{V_1}$$

$$K_2 = k_2 + k_{V_2}$$

The final char yield, which can be determined experimentally, is equivalent to the last term in figure 14:

$$\frac{C_{t \to \infty}}{M_0} = \frac{k_1 k_2}{K_1 K_2} = y_1 y_2$$

Figure 15: Equation 6 (Taken from Mark et al., 2006)

For higher reaction orders, e.g. a second-order reaction followed by a first-order sequential reaction, the system of equationsis non-linear and of stiff nature. This system can be solved numerically using a suitable algorithm, i.e.in Matlab; a one-step solver based on a modified Rosenbrock formulaof order two may be applied. [5]

CHAPTER 3: METHODOLOGY

3.1. Sample Preparation

    3.1.1.   Drying

Figure 16: Oven

Procedure:

An oven model LHT 4/120 manufactured by Carbolite was used for drying process (figure 16). Fresh oil palm biomass samples (EFB, PMF and PKS) were prepared on aluminium foil before entering the oven. Sample was weighed before entering oven. Oven was set up at temperature 120 °C for 24 hours. After 24 hours, biomass samples were brought out from the oven for weighing. Then, samples were entered oven for next an hour at same temperature. After that, samples were brought out from oven and weighing again until weight of sample was constant.

3.1.2.   Particle Sizing

Figure 17: Grinder

Figure 18: Siever

Procedure:

After drying process, biomass sample was prepared for grinding process. Grinder (model: Upper Part-Pulverisette 25, Bottom Part-Pulverisette 19, Vacuum-Oertzen) manufactured by Fritsch was used (figure 17). Biomass sample was entered into top side for first cutting process (cut samples into small size around 1 to 2 inches). After that, biomass sample was entered into side container for second cutting process (sample size become smaller than 1 inches or powder). After that, sample was sized using siever model BA300N manufactured by CISA (figure 18).Sieve trays were arranged from large into small particle size. Sample collected from grinder was put into sieve tray for sieving process. After that, sample was collected in each tray and put into respectively bottle in order to avoid from moisture.

3.2. Torrefaction Process

3.2.1.   Thermogravimetric Analyzer (TGA)

Figure 19: Thermogravimetric Analyzer

Procedure:

The torrefaction process was carried out using thermogravimetric analyzer model S11-AST-2 manufactured by Diamond TG/DTA (figure 19). The tested sample was loaded in a crucible and measured the weight. For all the experimental runs, approximately 2 mg of samples were used. Nitrogen gas was used as a carrier gas was fixed at 100 ml min^{-1}, so that the samples were torrefied in an inert environment. In this work, the heating rate used was 10°C min^{-1} for two different particle sizes of samples namely 250-355 µm and 355-500 µm. the torrefaction temperatures were 200, 220, 240, 260, 280 and 300°C. Specifically, the temperature of the TG was raised from 50°C to the torrefaction temperature. Once the TG reached the torrefaction temperature, the biomass was torrefied for 2 hours. During torrefaction was performed, a temperature program consisting of a dynamic heating period and an isothermal heating period.

3.2.2.   Tube Furnace

Figure 20: Tube Furnace

Procedure:

Due to limited amount of oil palm biomass sample was produced from TGA; tube furnace was used in order to produce more amount for analyses, i.e. ultimate analysis and calorific value. Tube furnace model TSH17/75/450-2416-2116 manufactured by Elite Thermal Systems Limited was used for torrefaction process (figure 20). Tube furnace conditions were replicated same in TGA. Tube furnace was switched on as well as nitrogen gas. Sample was weighed and placed in crucible (ship shape). Sample was entered into cylinder of the furnace and closed it. Valve was opened for flow the nitrogen gas into tube furnace. Nitrogen flow was controlled based on desired flow rate. Parameters (heating rate, target temperature, reaction time and ending condition) were setup on display screen of tube furnace. After all required parameters were setup, isolated button was pressed followed by run button that locate on display screen of tube furnace.

3.3. Sample Analyses

3.3.1. Calorific Value

Figure 21: Bomb Calorimeter

Procedure:

The calorific value was measured using bomb calorimeter model C2000 series manufactured by IKA-WERKE (figure 21). Bomb calorimeter, oxygen tank and cooling fan are switched on. Sample was weighed and placed into crucible using balance. Cotton thread was tied up at ignition wire and crucible was placed inside decomposition vessel. Vessel was closed. On the main screen of bomb calorimeter, weight of sample was recorded. Vessel was put inside calorimeter system. Start button was pressed for running the bomb calorimeter. Measurement of gross and net calorific value were according to DIN 51900, BS 1016 Part 5 1977, ASTM D3286-91, ASTM D240-87, ASTM E711-87, ISO 1928-1976, ASTM D1989-91 and BSI.

3.3.2. Ultimate Analysis

Figure 22: CHNS Analyzer

Procedure:

CHNS analyzer model CHN-900/CHNS-932 manufactured by LECO was used for ultimate analysis. Biomass sample was prepared using micro balance provided. Sample was prepared in range from 1.5 mg to 2 mg into small tin capsule. After that, tin capsule was fold and weighed again. Sample weight was recorded. The analysis was carried out by technician.

3.4. Kinetic Parameters Calculation through MATLAB

The experimental data obtained from TG was used to create a model for predicting yield of torrefied sample.

In order to identify reaction order of the torrefaction process, graphical method was used by plotting two types of graphs. Graph $\ln \frac{[W(t)]}{[W(0)]}$ versus time for first order reaction and $\frac{1}{[W(t)]} - \frac{1}{[W(0)]}$ versus time for second order reaction were plotted respectively. If straight line was shown, the reaction order was valid for that process.

Meanwhile, graph $\ln k$ versus $1/T$ was plotted for finding activation energy and pre-exponential factor from deriving Arrhenius equation below:

$$k_{1\,or\,2} = Ae^{\frac{-E_a}{RT}}$$

$$\ln k_{1\,or\,2} = \left(\frac{-E_a}{R}\right)\frac{1}{T} + \ln A$$

$$y = mx + c$$

A was pre-exponential factor, E_a was activation energy, R was gas constant and T was temperature. Besides, k_1 and k_2 were determined from Arrhenius equation. Rate of reaction was determined by following equation 1, 2 and 3:

$$r_A = -k_1 W_A^n \qquad \text{(Equation 1)}$$

$$r_B = k_1 W_A^n - k_2 W_B^n \quad \text{(Equation 2)}$$

$$r_C = k_2 W_B^n \qquad \text{(Equation 3)}$$

where r_A, r_B and r_C represented rate of reaction for solid A, B and C. A was initial feedstock, B was intermediate product, C was torrefied product. Meanwhile, W_A, W_B and W_C were weight of solid A, B and C while n was a reaction order.

CHAPTER 4: RESULT AND DISCUSSION

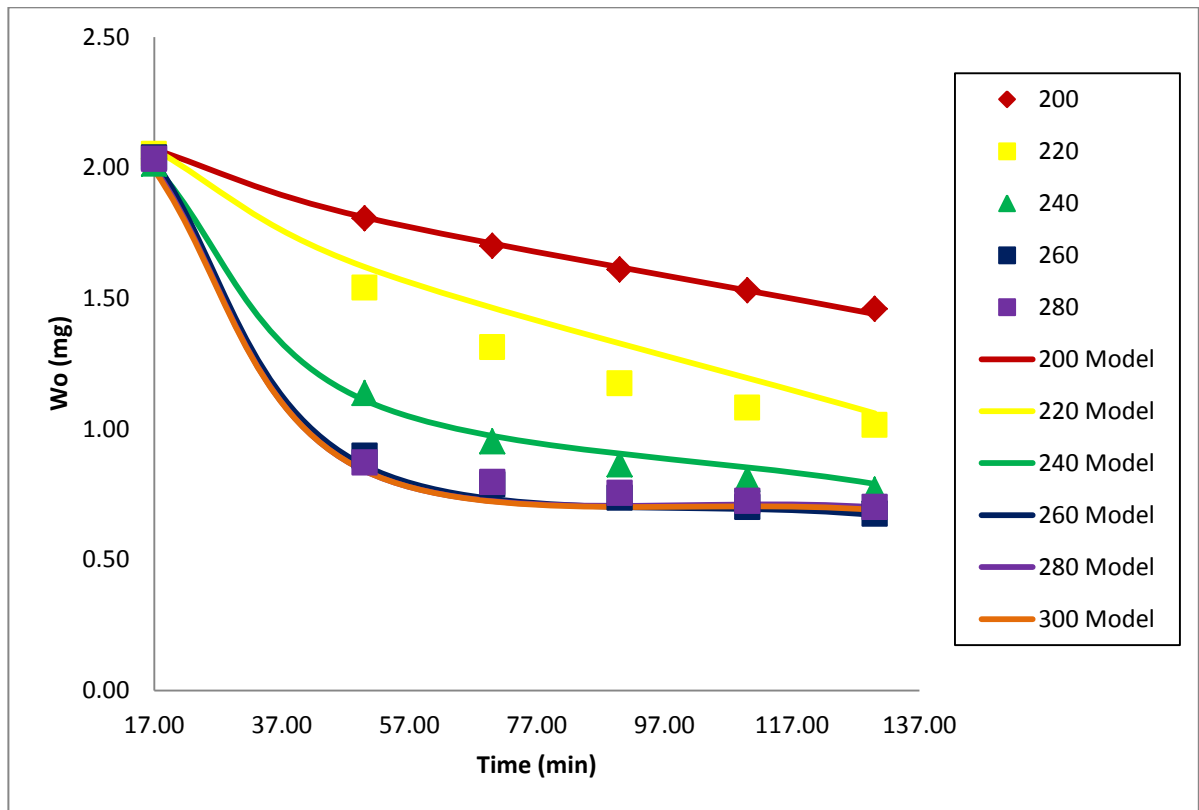## 4.1. Experimental and Model Curves for Different Types of Biomass

Figure 23: Experimental and model curves for EFB at various final torrefaction temperature (°C) and particle size 250-355 μm

Figure 23 showed experimental and model curves at different final torrefaction temperature for EFB particle size between 250-355 μm. The final torrefaction temperature applied: 200, 220, 240, 260, 280 and 300°C. The torrefaction was carried out for 2 hours of reaction time. Line and symbol curves represented modeling data and experimental respectively.

Figure 23 mentioned time axis was started at 17 minutes for all different final torrefaction temperatures. It was due to EFB intrinsic moisture removal during past 17 minutes. Even though the EFB already had drying process but this drying process only managed to remove extrinsic moisture. The existence of intrinsic process was due to xylem structure that located inner side EFB tissues. Xylem was responsible to carried out water and minerals throughout the EFB and provided mechanical support as well. It was important to carry out this intrinsic moisture removal process before going through

40

torrefaction process in order to avoid weight loss due to moisture took place during torrefaction process.

For experimental curves, the weight of EFB decreased with increasing torrefaction temperature. Weight of EFB had less weight loss during temperature 200°C and more weight loss at temperature 260, 280 and 300°C. It was due to decomposition either hemicellulose or cellulose or lignin. Since those three were the main polymeric structures inside the biomass and they had their own temperature decomposition. However, the hemicellulose decomposition was more significant compared to cellulose or lignin during the torrefaction of EFB since temperature decomposition of hemicellulose between 225-325°C [5]. Chen and Kuo (2010) mentioned temperature decomposition of hemicellulose occurred between 150 to 350°C. Both references on hemicellulose temperature decomposition showed most of hemicellulose were decomposed during torrefaction process. Figure 23 showed the decomposition of hemicellulose started reactive at temperature 260°C and above. It concluded most of hemicellulose decomposed at 260°C rather than below 260°C.

Besides, from experimental curves, the weight loss percent can be calculated using equation 4 for identifying amount of weight loss from the original sample during torrefaction process.

$$\text{Weight Loss Percent, \%} = \frac{(\text{Weight before Torrefaction, mg} - \text{Weight after Torrefaction, mg})}{\text{Weight before Torrefaction, mg}} \times 100\%$$

(Equation 4)

For 200, 220, 240, 260, 280 and 300°C, the weight loss percent were 28.23, 50.54, 61.89, 66.85, 65.49 and 42.01 respectively. It showed that, there was decomposition of hemicellulose for every temperature. It seemed that, decomposition of hemicellulose already took place at very beginning of torrefaction process. Each temperature showed different amount of weight loss.

In the other hands, modeling for the torrefaction process of EFB was created for predicting torrefied product and compared with experimental data. Figure 23 represented both experimental and modeling curves. During modeling of torrefaction process, two reactions took place during the process. First process called as fast decomposition while second process called as slow decomposition. Since from above discussion, both two reactions were referred to hemicellulose decomposition.

Average Absolute Deviation (AAD) (equation 5) was introduced in order to identify error between modeling and experimental data before verifying the model.

$$AAD = \frac{1}{n} \sum_{i=1}^{n} |x_i| \text{(Equation 5)}$$

where:

n = Number of Experiment or Modeling Data

x_i = Error Data

Table 3: AAD for EFB 250-355 μm

Temperature	Experimental	Modeling	Error (%)
200.00	1.46	1.44	1.40
220.00	1.02	1.06	4.00
240.00	0.77	0.77	0.00
260.00	0.68	0.67	1.47
280.00	0.70	0.7	0.00
300.00	0.68	0.69	1.47
AAD between Experimental and Modeling			**1.39**

From AAD calculation (table 3) for figure 23, AAD between experimental and modeling data was 1.39. It was less than of 5% of error between experimental and modeling data. As conclusion, figure 23 showed that 260, 280 and 300°C had completed torrefaction reaction while for 200, 220 and 240°C were incomplete reaction.
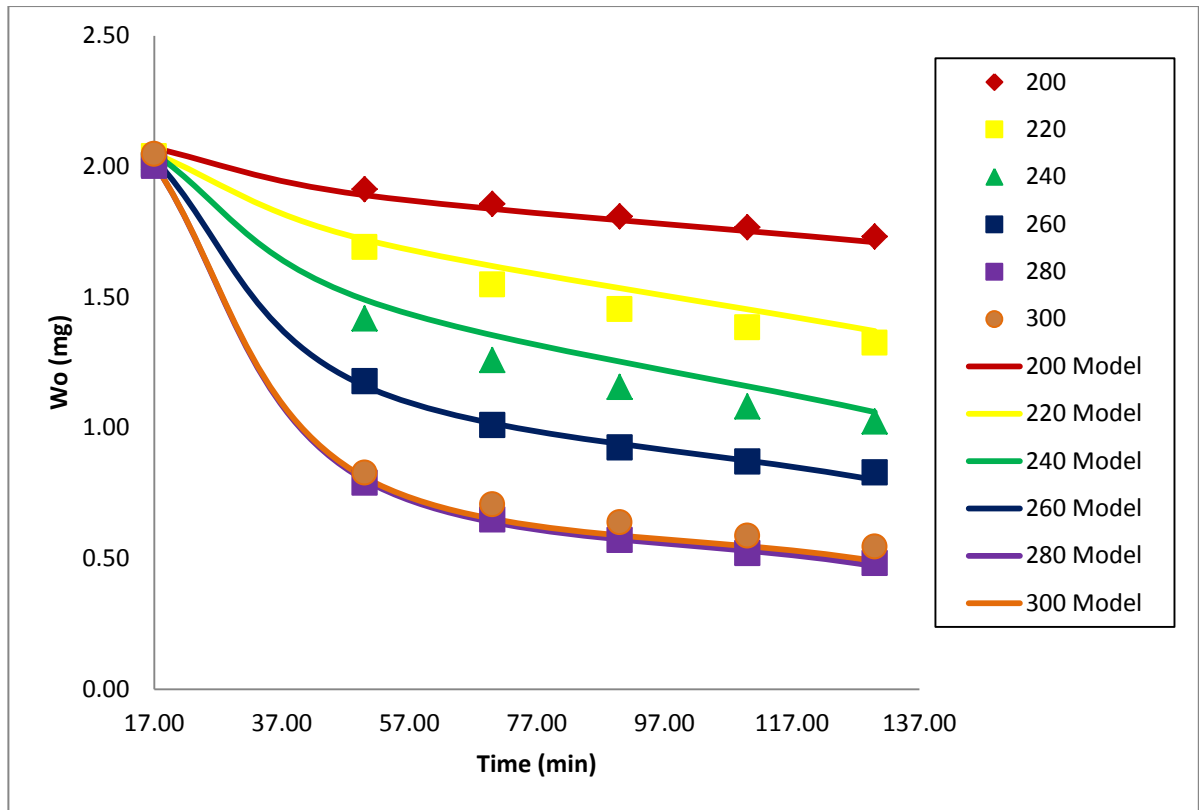
Figure 24: Experimental and model curves for PMF at various final torrefaction temperature (°C) and particle size 250-355 μm

Figure 24 showed experimental and model curves at different final torrefaction temperature for PMF particle sizes between 250-355 μm. The final torrefaction temperature applied: 200, 220, 240, 260, 280 and 300°C. The torrefaction was carried out for 2 hours of reaction time. Line and symbol curves represented modeling data and experimental respectively.

Figure 24 mentioned time axis was started at 17 minutes for all different final torrefaction temperatures. It was due to PMF intrinsic moisture removal during past 17 minutes. Even though the PMF already had drying process but this drying process only managed to remove extrinsic moisture. The existence of intrinsic process was due to xylem structure that located inner side PMF tissues. Xylem was responsible to carried out water and minerals throughout the PMF and provided mechanical support as well. It was important to carry out this intrinsic moisture removal process before going through torrefaction process in order to avoid weight loss due to moisture took place during torrefaction process.

For experimental curves, the weight of PMF decreased with increasing torrefaction temperature. By comparing figure 23 and figure 24, both of EFB and PMF had similar weight loss. For the first four curves, EFB had higher weight loss while for last two curves; it changed to PMF for had higher weight loss. It seemed due to different fraction of polymeric structure (hemicellulose, cellulose and lignin) and structure strength inside the EFB and PMF. PMF had strong structure than EFB and it needed high temperature in order to break the structure of PMF. After the breaking at 280°C, PMF had more weight loss. However, during that time, polymeric structures in EFB almost finish the decomposition.

Weight of PMF had less weight loss during temperature 200°C and more weight loss at temperature 280 and 300°C. It was due to decomposition either hemicellulose or cellulose or lignin. Since those three were the main polymeric structures inside the biomass and they had their own temperature decomposition. However, the hemicellulose decomposition was more significant compared to cellulose or lignin during the torrefaction of PMF since temperature decomposition of hemicellulose between 225-325°C [5]. Chen and Kuo (2010) mentioned temperature decomposition of hemicellulose occurred between 150 to 350°C. Both references on hemicellulose temperature decomposition showed most of hemicellulose were decomposed during torrefaction process. Figure 14 showed the decomposition of hemicellulose started reactive at temperature 280°C and above. It concluded most of hemicellulose decomposed at 280°C rather than below 280°C.

Besides, from experimental curves, the weight loss percent can be calculated using equation 4 for identifying amount of weight loss from the original sample during torrefaction process. For 200, 220, 240, 260, 280 and 300°C, the weight loss percent were 14.64, 35.02, 49.66, 58.69, 75.87 and 73.38 respectively. It showed that, there was decomposition of hemicellulose for every temperature. It seemed that, decomposition of hemicellulose already took place at very beginning of torrefaction process. Each temperature showed different amount of weight loss.

In the other hands, modeling for the torrefaction process of PMF was created for predicting torrefied product and compared with experimental data. Figure 24 represented both experimental and modeling curves. During modeling of torrefaction process, two reactions took place during the process. First process called as fast decomposition while second process called as slow decomposition. Since from above discussion, both two reactions were referred to hemicellulose decomposition.

Average Absolute Deviation (AAD) (equation 5) was introduced in order to identify error between modeling and experimental data before verifying the model.

Table 4: AAD for PMF 250-355 μm

Temperature	Experimental	Modeling	Error (%)
200.00	1.73	1.71	1.16
220.00	1.33	1.37	3.00
240.00	1.02	1.06	3.92
260.00	0.83	0.8	3.61
280.00	0.48	0.47	2.08
300.00	0.55	0.49	10.90
AAD between Experimental and Modeling			**4.11**

From AAD calculation (table 4) for figure 24, AAD between experimental and modeling data was 4.11. It was less than of 5% of error between experimental and modeling data. As conclusion, figure 24 showed that 280 and 300°C had completed torrefaction reaction while for 200, 220, 240 and 260°C were incomplete reaction.
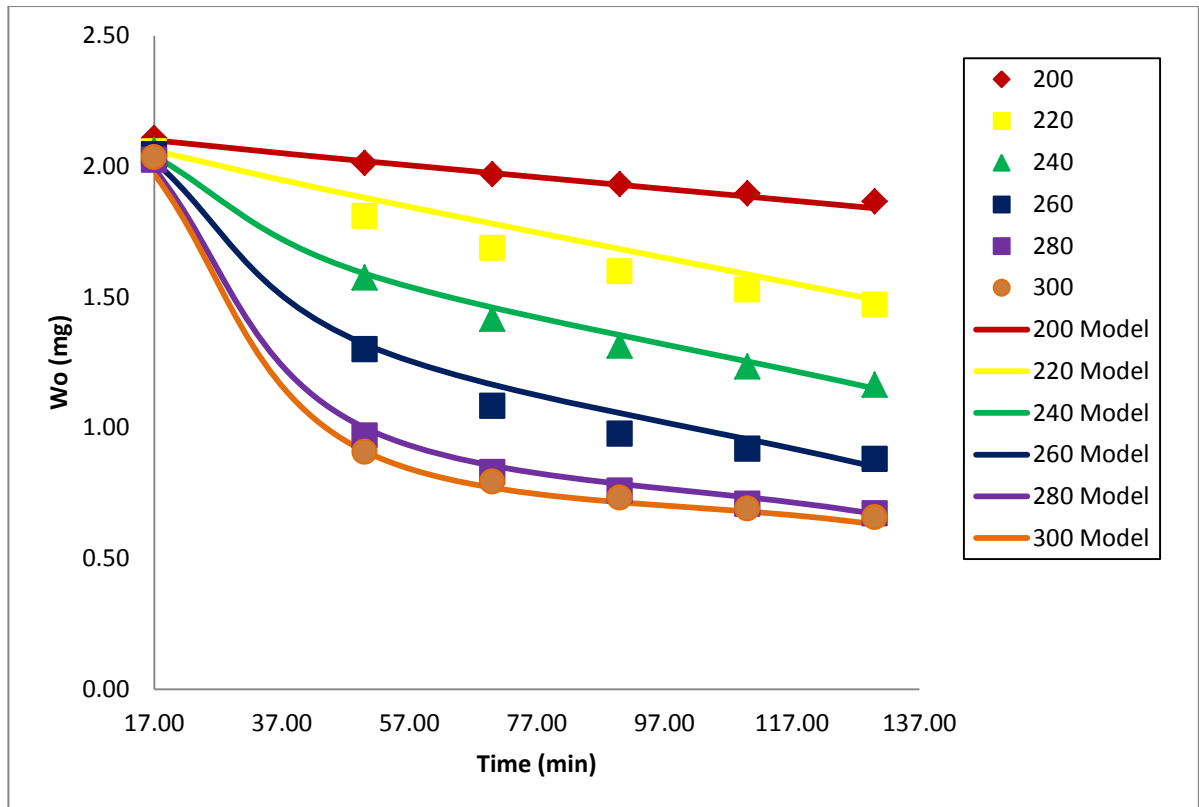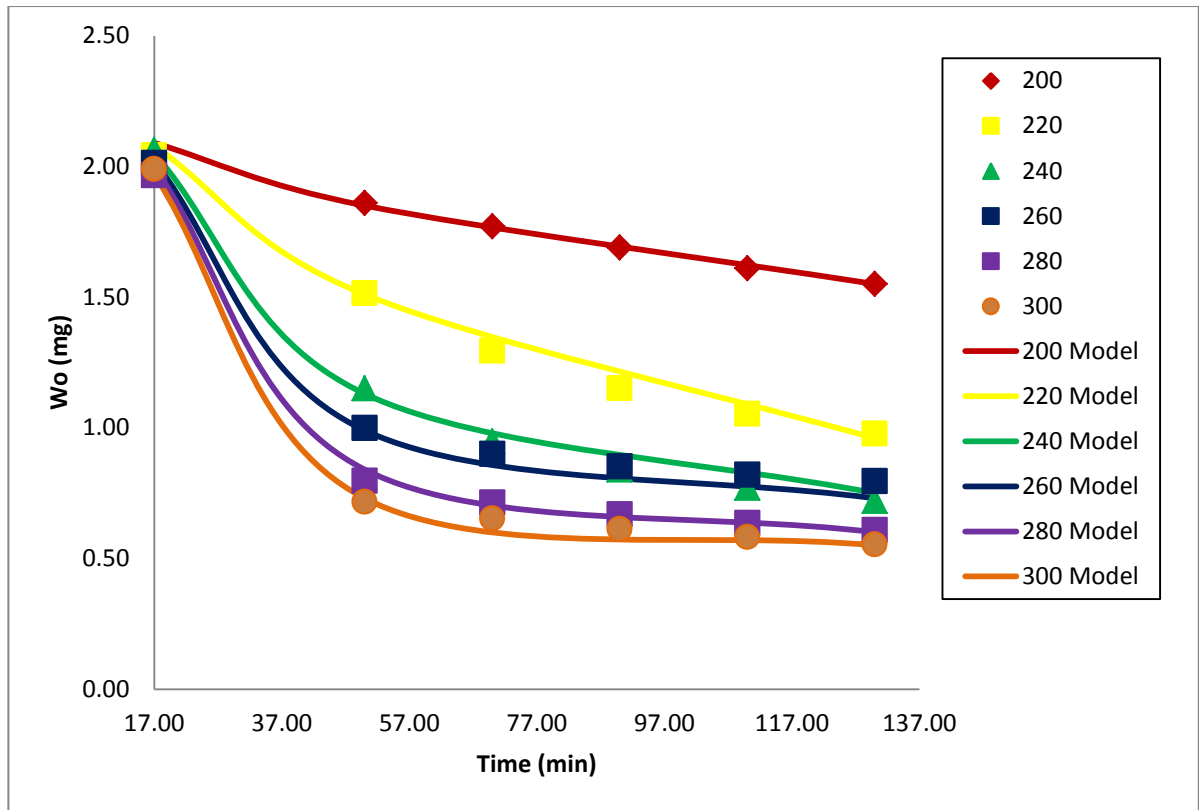
Figure 25: Experimental and model curves for PKS at various final torrefaction temperature (°C) and particle size 250-355 μm

Figure 25 showed experimental and model curves at different final torrefaction temperature for PKS particle sizes between 250-355 μm. The final torrefaction temperature applied: 200, 220, 240, 260, 280 and 300°C. The torrefaction was carried out for 2 hours of reaction time. Line and symbol curves represented modeling data and experimental respectively.

Figure 25 mentioned time axis was started at 17 minutes for all different final torrefaction temperatures. It was due to PMF intrinsic moisture removal during past 17 minutes. Even though the PKS already had drying process but this drying process only managed to remove extrinsic moisture. The existence of intrinsic process was due to xylem structure that located inner side PMF tissues. Xylem was responsible to carried out water and minerals throughout the PMF and provided mechanical support as well. It was important to carry out this intrinsic moisture removal process before going through torrefaction process in order to avoid weight loss due to moisture took place during torrefaction process.

For experimental curves, the weight of PKS decreased with increasing torrefaction temperature. By comparing figure 23, figure 24 and figure 25, PKS had less weight loss compare to EFB and PMF. It seemed due to different fraction of polymeric structure (hemicellulose, cellulose and lignin) and structure strength inside the EFB, PMF and PKS. PKS had different fraction of polymeric structure and strong structure than EFB and PMF. It needed high temperature in order to break the structure of PKS.

Weight of PKS had less weight loss during temperature 200°C and more weight loss at temperature 280 and 300°C. It was due to decomposition either hemicellulose or cellulose or lignin. Since those three were the main polymeric structures inside the biomass and they had their own temperature decomposition. However, the hemicellulose decomposition was more significant compared to cellulose or lignin during the torrefaction of PMF since temperature decomposition of hemicellulose between 225-325°C [5]. Chen and Kuo (2010) mentioned temperature decomposition of hemicellulose occurred between 150 to 350°C. Both references on hemicellulose temperature decomposition showed most of hemicellulose were decomposed during torrefaction process. Figure 25 showed the decomposition of hemicellulose started reactive at temperature 280°C and above. It concluded most of hemicellulose decomposed at 280°C rather than below 280°C. Other than that, it was found that PKS composed less hemicellulose than EFB and PMF. It was found by observing the way PKS decomposed during torrefaction process.

Besides, from experimental curves, the weight loss percent can be calculated using equation 4 for identifying amount of weight loss from the original sample during torrefaction process. For 200, 220, 240, 260, 280 and 300°C, the weight loss percent were 11.48, 28.54, 43.55, 56.99, 66.81 and 67.67 respectively. It showed that, there was decomposition of hemicellulose for every temperature. It seemed that, decomposition of hemicellulose already took place at very beginning of torrefaction process. Each temperature showed different amount of weight loss.

In the other hands, modeling for the torrefaction process of PMF was created for predicting torrefied product and compared with experimental data. Figure 25 represented both experimental and modeling curves. During modeling of torrefaction process, two

reactions took place during the process. First process called as fast decomposition while second process called as slow decomposition. Since from above discussion, both two reactions were referred to hemicellulose decomposition.

Average Absolute Deviation (AAD) (equation 5) was introduced in order to identify error between modeling and experimental data before verifying the model.

Table 5: AAD for PKS 250-355 μm

Temperature	Experimental	Modeling	Error (%)
200.00	1.87	1.84	1.60
220.00	1.47	1.49	1.36
240.00	1.16	1.15	0.86
260.00	0.88	0.85	3.41
280.00	0.67	0.67	0.00
300.00	0.66	0.63	4.55
AAD between Experimental and Modeling			**1.96**

From AAD calculation (table 5) for figure 25, AAD between experimental and modeling data was 1.96. It was less than of 5% of error between experimental and modeling data. As conclusion, figure 25 showed that 300°C had completed torrefaction reaction while for 200, 220, 240, 260 and 280°C were incomplete reaction.
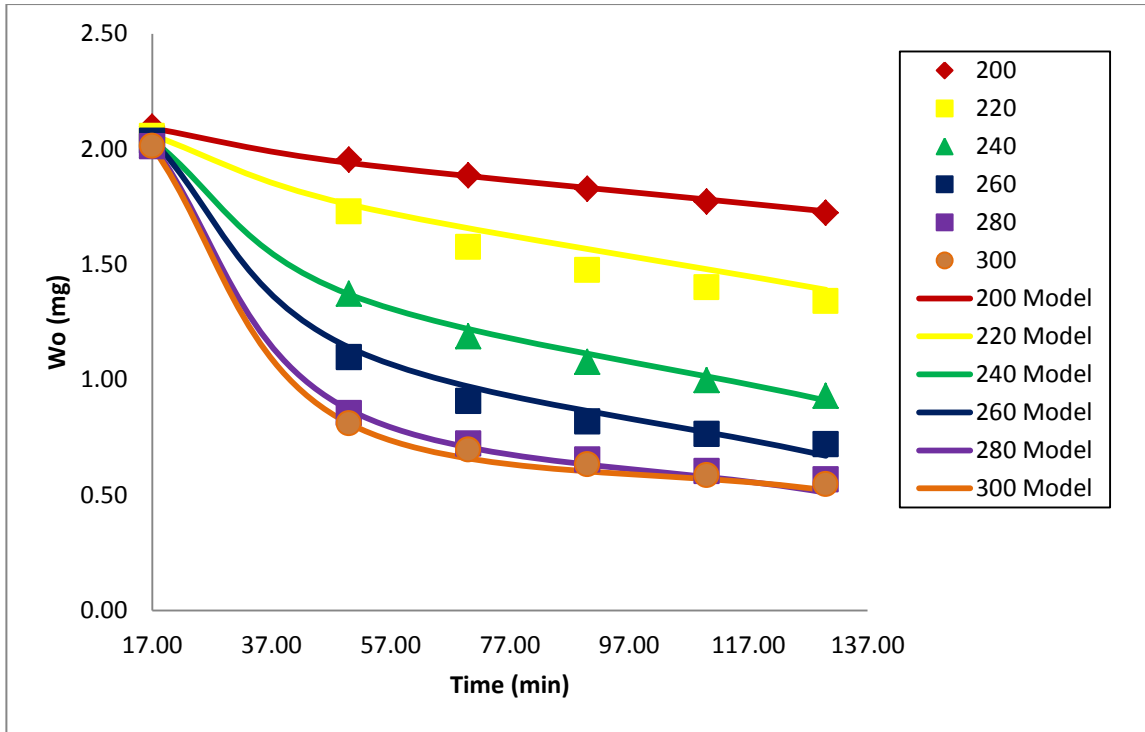
Figure 26: Experimental and model curves for EFB at various final torrefaction temperature (°C) and particle size 355-500 μm

Figure 26 showed experimental and model curves at different final torrefaction temperature for EFB particle size between 355-500 µm. The final torrefaction temperature applied: 200, 220, 240, 260, 280 and 300°C. The torrefaction was carried out for 2 hours of reaction time. Line and symbol curves represented modeling data and experimental respectively.

Figure 26 mentioned time axis was started at 17 minutes for all different final torrefaction temperatures. It was due to EFB intrinsic moisture removal during past 17 minutes. Even though the EFB already had drying process but this drying process only managed to remove extrinsic moisture. The existence of intrinsic process was due to xylem structure that located inner side EFB tissues. Xylem was responsible to carried out water and minerals throughout the EFB and provided mechanical support as well. It was important to carry out this intrinsic moisture removal process before going through torrefaction process in order to avoid weight loss due to moisture took place during torrefaction process.

49

For experimental curves, the weight of EFB decreased with increasing torrefaction temperature. By comparing with figure 23, weight loss of EFB at figure 26was less than figure 23. It was due to different of particle sizes for EFB. 250-355 μm was belonged to figure 23 had larger sample area compare to 355-500 μm in figure 26. As a result, larger area provided more space in sample to absorb heat from outside for decomposition rather than small area. Therefore, figure 26 resulted less weight loss.

Figure 26 had less weight loss during temperature 200°C and more weight loss at temperature 300°C. It was due to decomposition either hemicellulose or cellulose or lignin. Since those three were the main polymeric structures inside the biomass and they had their own temperature decomposition. However, the hemicellulose decomposition was more significant compared to cellulose or lignin during the torrefaction of EFB since temperature decomposition of hemicellulose between 225-325°C [5]. Chen and Kuo (2010) mentioned temperature decomposition of hemicellulose occurred between 150 to 350°C. Both references on hemicellulose temperature decomposition showed most of hemicellulose were decomposed during torrefaction process. Figure 26 showed the decomposition of hemicellulose started reactive at temperature 240°C and above. It concluded most of hemicellulose decomposed at 240°C rather than below 240°C.

Besides, from experimental curves, the weight loss percent can be calculated using equation 4 for identifying amount of weight loss from the original sample during torrefaction process.For 200, 220, 240, 260, 280 and 300°C, the weight loss percent were 24.46, 52.15, 65.10, 60.46, 69.07 and 72.15 respectively. It showed that, there was decomposition of hemicellulose for every temperature. It seemed that, decomposition of hemicellulose already took place at very beginning of torrefaction process. Each temperature showed different amount of weight loss.

In the other hands, modeling for the torrefaction process of EFB was created for predicting torrefied product and compared with experimental data. Figure 26 represented both experimental and modeling curves. During modeling of torrefaction process, two reactions took place during the process. First process called as fast decomposition while second process called as slow decomposition. Since from above discussion, both two reactions were referred to hemicellulose decomposition.

Average Absolute Deviation (AAD) (equation 5) was introduced in order to identify error between modeling data and experimental data before verifying the model.

Table 6: AAD for EFB 355-500 μm

Temperature	Experimental	Modeling	Error (%)
200.00	1.55	1.55	0.00
220.00	0.98	0.96	2.04
240.00	0.72	0.75	4.17
260.00	0.80	0.73	8.75
280.00	0.61	0.6	1.64
300.00	0.55	0.55	0.00
AAD between Experimental and Modeling			**2.77**

From AAD calculation (table 6) for figure 26, AAD between experimental and modeling data was 2.77. It was less than of 5% of error between experimental and modeling data. As conclusion, figure 26 showed that 300°C had completed torrefaction reaction while for 200, 220, 240, 260 and 280°C were incomplete reaction.

Figure 27: Experimental and model curves for PMF at various final torrefaction temperature (°C) and particle size 355-500 μm

Figure 27 showed experimental and model curves at different final torrefaction temperature for PMF particle size between 355-500 μm. The final torrefaction temperature applied: 200, 220, 240, 260, 280 and 300°C. The torrefaction was carried out for 2 hours of reaction time. Line and symbol curves represented modeling data and experimental respectively.

Figure 27 mentioned time axis was started at 17 minutes for all different final torrefaction temperatures. It was due to PMF intrinsic moisture removal during past 17 minutes. Even though the PMF already had drying process but this drying process only managed to remove extrinsic moisture. The existence of intrinsic process was due to xylem structure that located inner side PMF tissues. Xylem was responsible to carried out water and minerals throughout the PMF and provided mechanical support as well. It was important to carry out this intrinsic moisture removal process before going through torrefaction process in order to avoid weight loss due to moisture took place during torrefaction process.

For experimental curves, the weight of PMF decreased with increasing torrefaction temperature. By comparing with figure 24, weight loss of PMF at figure 27 was less than figure 24. It was due to different of particle sizes for PMF. 250-355 μm was belonged to figure 24 had larger sample area compare to 355-500 μm in figure 27. As a result, larger area provided more space in sample to absorb heat from outside for decomposition rather than small area. Therefore, figure 27 resulted less weight loss.

Figure 27 had less weight loss during temperature 200°C and more weight loss at temperature 280 and 300°C. It was due to decomposition either hemicellulose or cellulose or lignin. Since those three were the main polymeric structures inside the biomass and they had their own temperature decomposition. However, the hemicellulose decomposition was more significant compared to cellulose or lignin during the torrefaction of PMF since temperature decomposition of hemicellulose between 225-325°C [5]. Chen and Kuo (2010) mentioned temperature decomposition of hemicellulose occurred between 150 to 350°C. Both references on hemicellulose temperature decomposition showed most of hemicellulose were decomposed during torrefaction process. Figure 27 showed the decomposition of hemicellulose started reactive at temperature 280°C and above. It concluded most of hemicellulose decomposed at 280°C rather than below 280°C.

Besides, from experimental curves, the weight loss percent can be calculated using equation 4 for identifying amount of weight loss from the original sample during torrefaction process.For 200, 220, 240, 260, 280 and 300°C, the weight loss percent were 17.84, 34.82, 53.87, 64.62, 71.82 and 72.88 respectively. It showed that, there was decomposition of hemicellulose for every temperature. It seemed that, decomposition of hemicellulose already took place at very beginning of torrefaction process. Each temperature showed different amount of weight loss.

In the other hands, modeling for the torrefaction process of PMF was created for predicting torrefied product and compared with experimental data. Figure 27 represented both experimental and modeling curves. During modeling of torrefaction process, two reactions took place during the process. First process called as fast decomposition while

second process called as slow decomposition. Since from above discussion, both two reactions were referred to hemicellulose decomposition.

Average Absolute Deviation (AAD) (equation 5) was introduced in order to identify error between modeling data and experimental data before verifying the model.

Table 7: AAD for PMF 355-500 μm

Temperature	Experimental	Modeling	Error (%)
200.00	1.72	1.73	0.58
220.00	1.34	1.39	3.73
240.00	0.93	0.91	2.15
260.00	0.72	0.67	6.94
280.00	0.57	0.51	10.53
300.00	0.55	0.52	5.45
AAD between Experimental and Modeling			**4.90**

From AAD calculation (table 7) for figure 27, AAD between experimental and modeling data was 4.90. It was less than of 5% of error between experimental and modeling data. As conclusion, figure 27 showed that 200, 220, 240, 260 280 and 300°C had uncompleted torrefaction reaction.
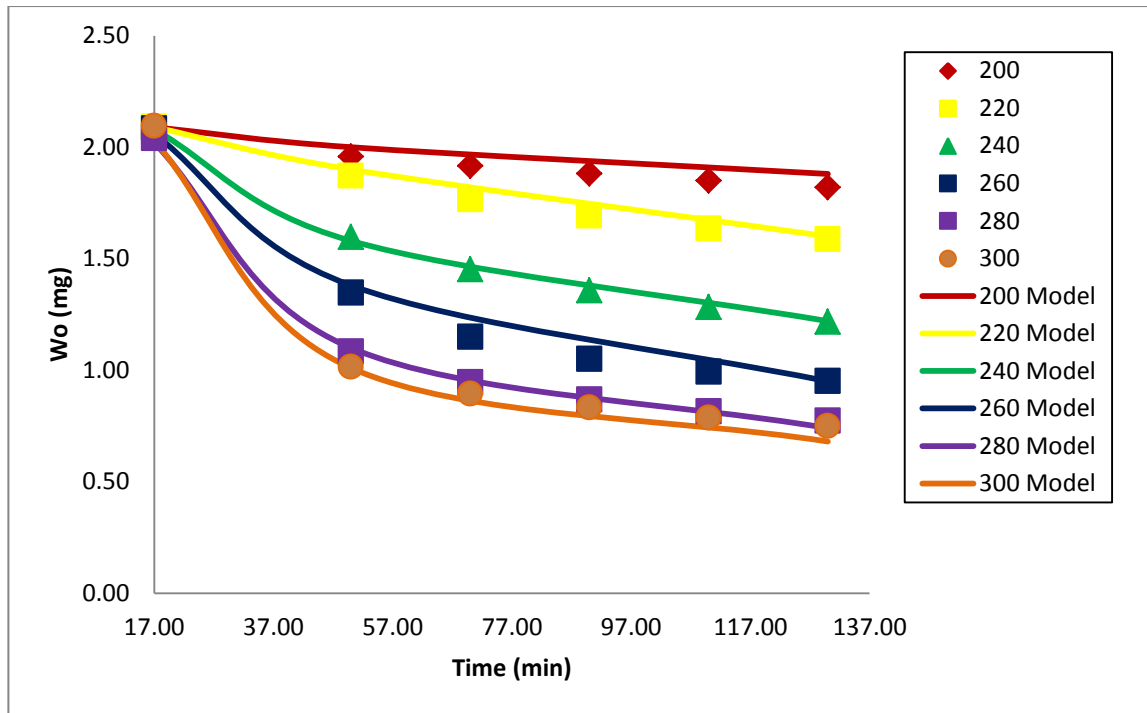
Figure 28:Experimental and model curves for PKS at various final torrefaction temperature (°C) and particle size 355-500 µm

Figure 28 showed experimental and model curves at different final torrefaction temperature for PKS particle size between 355-500 µm. The final torrefaction temperature applied: 200, 220, 240, 260, 280 and 300°C. The torrefaction was carried out for 2 hours of reaction time. Line and symbol curves represented modeling data and experimental respectively.

Figure 28 mentioned time axis was started at 17 minutes for all different final torrefaction temperatures. It was due to PKS intrinsic moisture removal during past 17 minutes. Even though the PKS already had drying process but this drying process only managed to remove extrinsic moisture. The existence of intrinsic process was due to xylem structure that located inner side PKS tissues. Xylem was responsible to carried out water and minerals throughout the PKS and provided mechanical support as well. It was important to carry out this intrinsic moisture removal process before going through torrefaction process in order to avoid weight loss due to moisture took place during torrefaction process.

For experimental curves, the weight of PKS decreased with increasing torrefaction temperature. By comparing with figure 25, weight loss of PKS at figure 28 was less than figure 25. It was due to different of particle sizes for PKS. 250-355 μm was belonged to figure 25 had larger sample area compare to 355-500 μm in figure 28. As a result, larger area provided more space in sample to absorb heat from outside for decomposition rather than small area. Therefore, figure 28 resulted less weight loss.

Figure 28 had less weight loss during temperature 200°C and more weight loss at temperature 280 and 300°C. It was due to decomposition either hemicellulose or cellulose or lignin. Since those three were the main polymeric structures inside the biomass and they had their own temperature decomposition. However, the hemicellulose decomposition was more significant compared to cellulose or lignin during the torrefaction of PKS since temperature decomposition of hemicellulose between 225-325°C [5]. Chen and Kuo (2010) mentioned temperature decomposition of hemicellulose occurred between 170 to 350°C. Both references on hemicellulose temperature decomposition showed most of hemicellulose were decomposed during torrefaction process. Figure 28 showed the decomposition of hemicellulose started reactive at temperature 280°C and above. It concluded most of hemicellulose decomposed at 280°C rather than below 280°C.

Besides, from experimental curves, the weight loss percent can be calculated using equation 4 for identifying amount of weight loss from the original sample during torrefaction process.For 200, 220, 240, 260, 280 and 300°C, the weight loss percent were 11.44, 24.09, 41.21, 54.32, 62.13 and 64.25 respectively. It showed that, there was decomposition of hemicellulose for every temperature. It seemed that, decomposition of hemicellulose already took place at very beginning of torrefaction process. Each temperature showed different amount of weight loss.

In the other hands, modeling for the torrefaction process of PKS was created for predicting torrefied product and compared with experimental data. Figure 28 represented both experimental and modeling curves. During modeling of torrefaction process, two reactions took place during the process. First process called as fast decomposition while

second process called as slow decomposition. Since from above discussion, both two reactions were referred to hemicellulose decomposition.

Average Absolute Deviation (AAD) (equation 5) was introduced in order to identify error between modeling data and experimental data before verifying the model.

Table 8: AAD for PKS 355-500 μm

Temperature	Experimental	Modeling	Error (%)
200.00	1.82	1.88	3.30
220.00	1.59	1.6	0.63
240.00	1.22	1.22	0.00
260.00	0.95	0.95	0.00
280.00	0.77	0.74	3.90
300.00	0.75	0.68	9.33
AAD between Experimental and Modeling			**2.86**

From AAD calculation (table 8) for figure 28, AAD between experimental and modeling data was 2.86. It was less than of 5% of error between experimental and modeling data. As conclusion, figure 28 showed that 200, 220, 240, 260 280 and 300°C had uncompleted torrefaction reaction.

Overall discussion from figure 23 until figure 28 - The weight loss curve found to be constant and stable during torrefaction process. Therefore, 2 hours of the process were enough. The torrefaction process of EFB, PMF and PKS that carried out below 2 hours was not recommended. It was because the time that weight needed to decompose was not enough. By using trial and error for 30, 60, 90 and 120 minutes of reaction time in TGA, it was found that 120 minutes or 2 hours of reaction time gave enough time for weight to decompose for all EFB, PMF and PKS.

Furthermore, as torrefaction temperature increased, the weight loss of each type of sample also increased. It was due to the decomposition of hemicellulose during torrefaction process. Hemicellulose was most reactive and was subjected to limited devolatilisation and carbonisation below 250°C. Above 250°C it was subjected to extensive devolatilisation and carbonisation [10].

Based on experimental and model curves, both EFB and PMF were resulted more weight loss rather than PKS. So, EFB and PMF composed higher fraction of hemicellulose compare to PKS. **However, in order to make deeply investigation on torrefaction process, research on determining composition of hemicellulose, cellulose and lignin for raw and torrefied biomass was strongly recommended (refer chapter 5.2 a) for further explanation).**

In this work, two different particle sizes namely 250-355 μm and 355-500 μm were used. Different particle size resulted different sample area. 250-355 μm had larger area than 355-500 μm. The larger area provided more space in sample to absorb heat for hemicellulose decomposition rather than small area. Therefore, 250-355 μm absorbed more heat than 355-500 μm and resulted more weight loss of hemicellulose. However, for recommendation in industrial, 355-500 μm was recommended than 250-355 μm of particle sizes. It was due to power used for grindability more in 250-355 μm where it caused towards higher of cost.

In addition, by calculating all AAD between experimental and modeling data, it concluded that the error is below than 5%. It showed that model created for all three types of oil palm biomass were applicable and verified since error was ±5%.

By comparing results in figure 23 until figure 28 with literature review in figure 8, the trend of experimental and model curves were same. However, the reaction time, torrefaction temperature and type of biomass were used different. Reason for comparing between research project and previous literature review was to get corresponding and correct result with previous research even though type of biomass used different. The important was ideal of how the torrefaction place took place correspond to reaction time, torrefaction temperature and type of biomass.

4.2. Modeling of Torrefaction Process

4.2.1 Kinetic Parameters

Two steps reaction for decomposition of oil palm biomass were found during torrefaction process in TGA. Based on finding, first step was fast reaction while second step was slow reaction and both were shown below:

First step (Fast reaction)   :$A\,(s) \xrightarrow{k1} B(s) + G_1(g)$

Second step (Slow reaction):$B(s) \xrightarrow{k2} C(s) + G_2(g)$
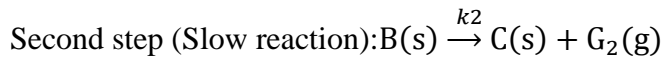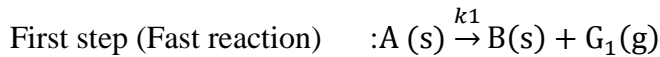
Here A(s) was feedstock in solid, B(s) was intermediate product in solid and C(s) was torrefied product in solid. Both G_1 and G_2 were by-product in gas form. $k1$ and $k2$ represented rate constant for both steps reaction in unit of min^{-1}.

Reaction order, n for the process was obtained using graphical method. It showed straight line during plotting graph $\ln\frac{[W(t)]}{[W(0)]}$ versus time. So, it was first order for both steps reaction for all oil palm biomass samples. Slope of the graph was rate constant and it will used for next determining of activation energy and pre-exponential factor. Meanwhile, for rate constant was obtained by plotting ln k versus $1/T$ from derivation of Arrhenius equation.

$$k_{1\,or\,2} = Ae^{\frac{-E_a}{RT}}$$

$$\ln k_{1\,or\,2} = \left(\frac{-E_a}{R}\right)\frac{1}{T} + \ln A$$

$$y = mx + c$$

where E_a was activation energy in J mol^{-1}, R was gas constant in J mol^{-1} K^{-1}, T was temperature in K and A was pre-exponential factor in min^{-1}. During the plotting, the slope of the graph, m showed value of activation energy over gas constant and the intercept c showed value of pre-exponential factor (figure 29 until figure 40). The expression for k_1 and k_2 were described as follows for all oil palm biomass samples:

a) For EFB (250-355 um):
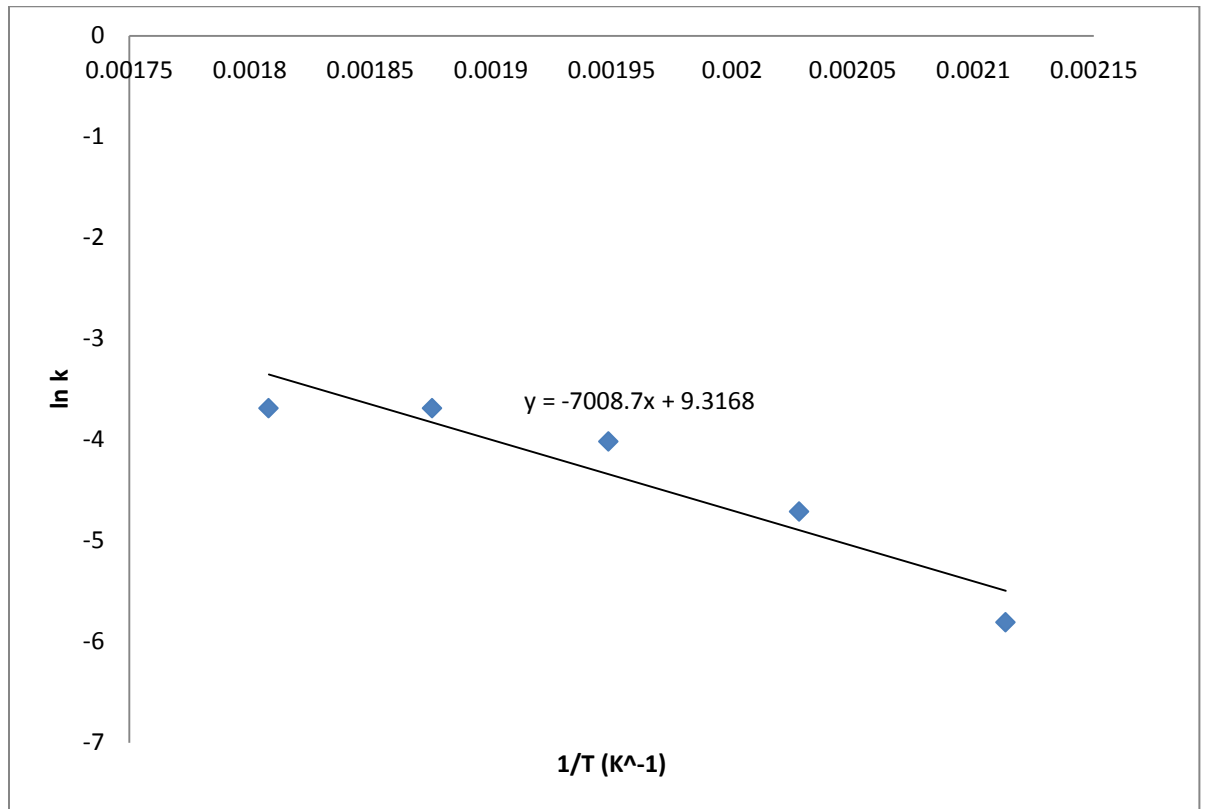
Figure 29: Graph ln k versus 1/T for k_1
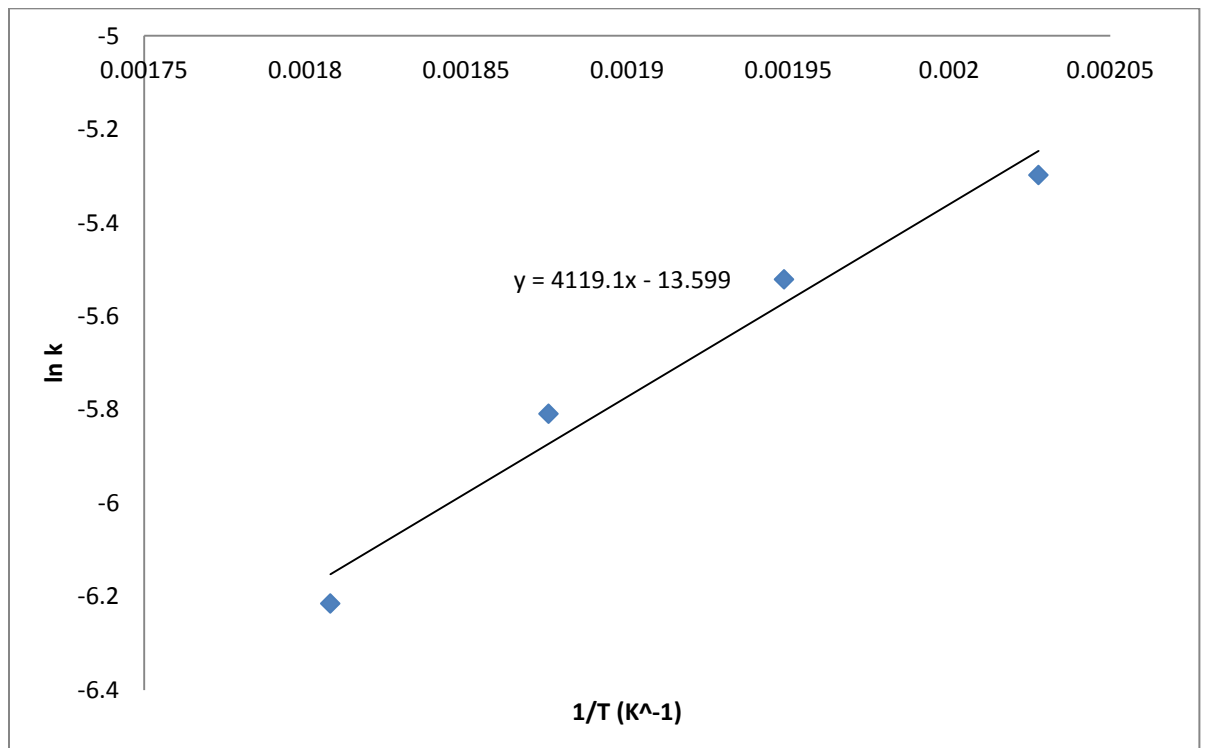
Figure 30: Graph ln k versus 1/T for k_2

60

- $k_1 = 11 \times 10^3 exp\left(\frac{-58267}{RT}\right)$

- $k_2 = 1.24 \times 10^{-6} exp\left(\frac{34247}{RT}\right)$

b) For EFB (355-500 um):

$$y = -2522.8x + 0.9246$$
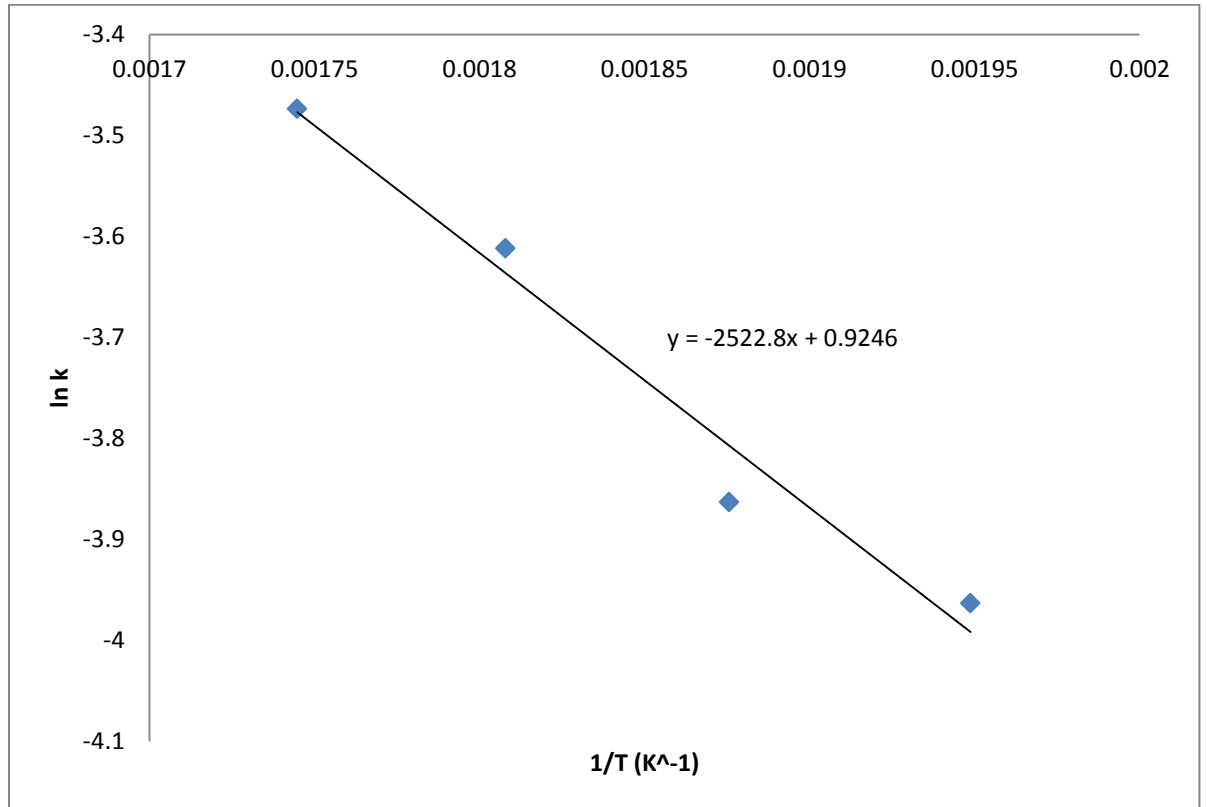
Figure 31: Graph ln k versus 1/T for k_1
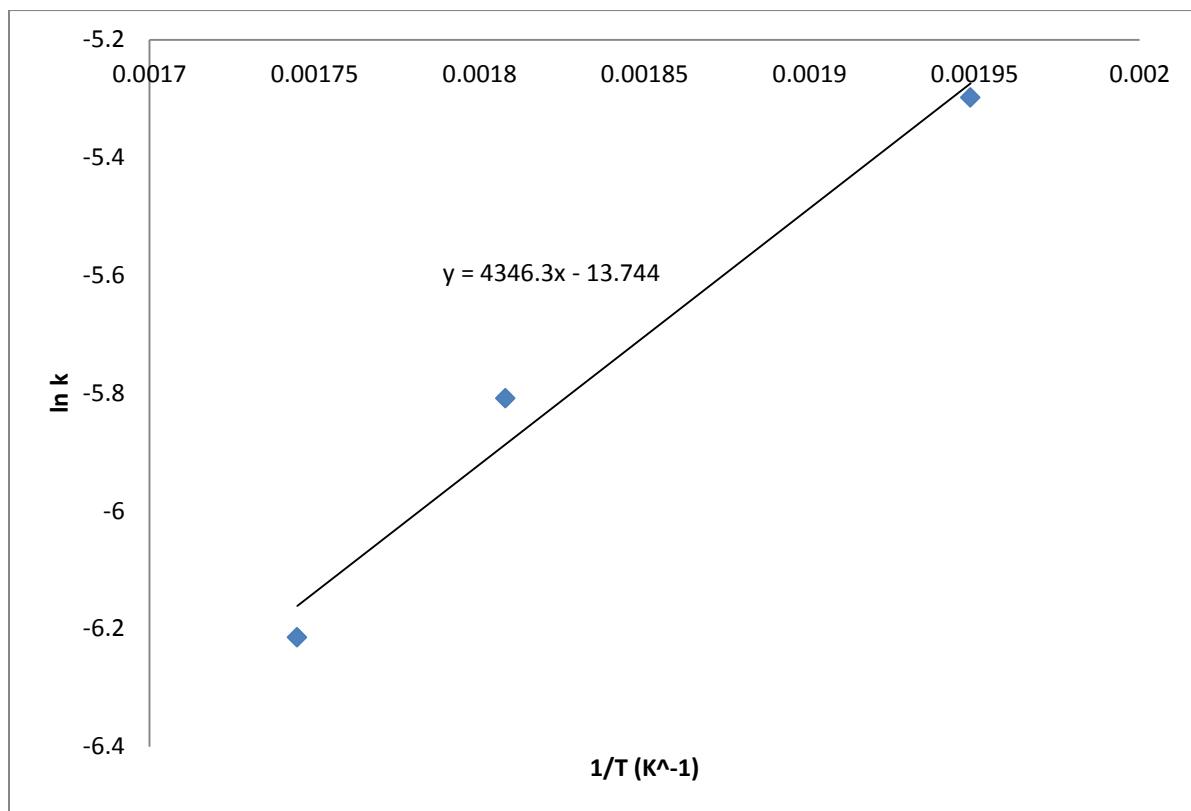
Figure 32: Graph ln k versus 1/T for k_2

- $k_1 = 2.52 exp\left(\frac{-20969}{RT}\right)$

- $k_2 = 1.08 \times 10^{-6} exp\left(\frac{36134}{RT}\right)$

c) For PMF (250-355 um):
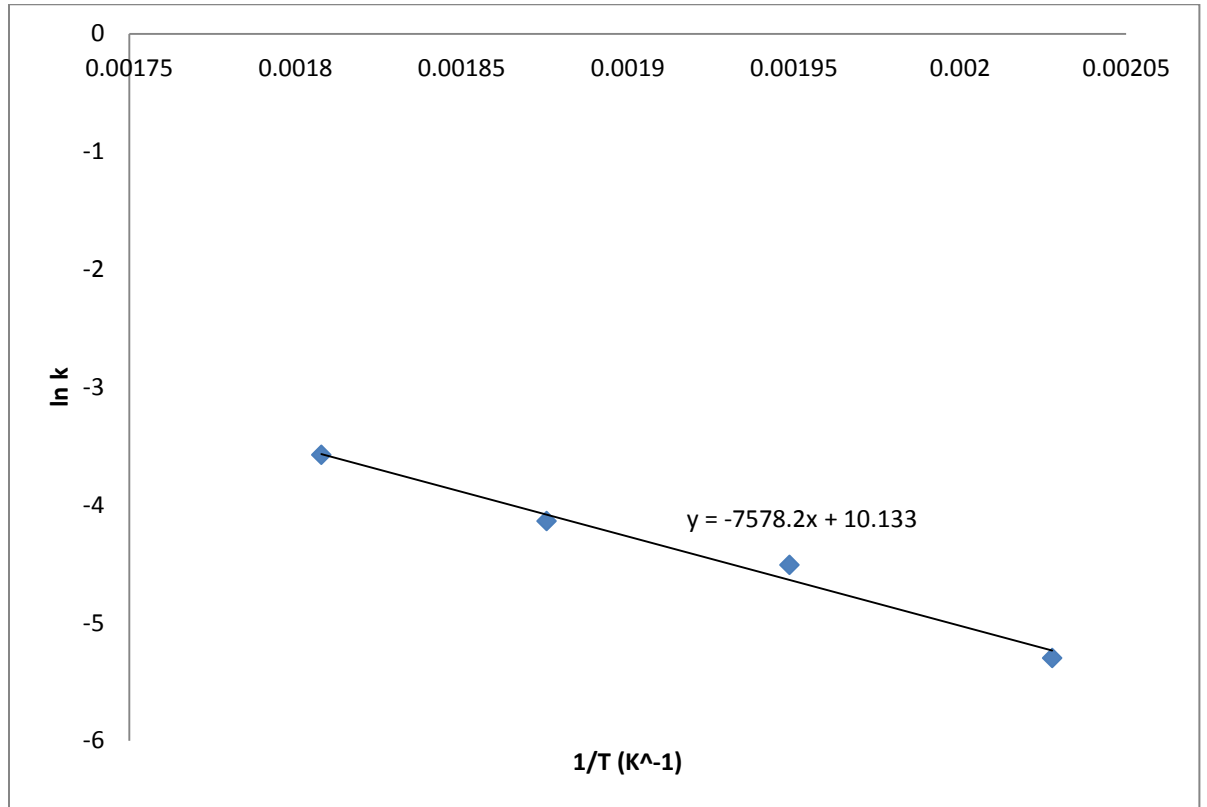
Figure 33: Graph ln k versus 1/T for k_1

The equation in the first graph: $y = -7578.2x + 10.133$

Figure 34: Graph ln k versus 1/T for k_2

The equation in the second graph: $y = -4807.6x + 3.4471$

- $k_1 = 25 \times 10^3 exp\left(\frac{-63007}{RT}\right)$
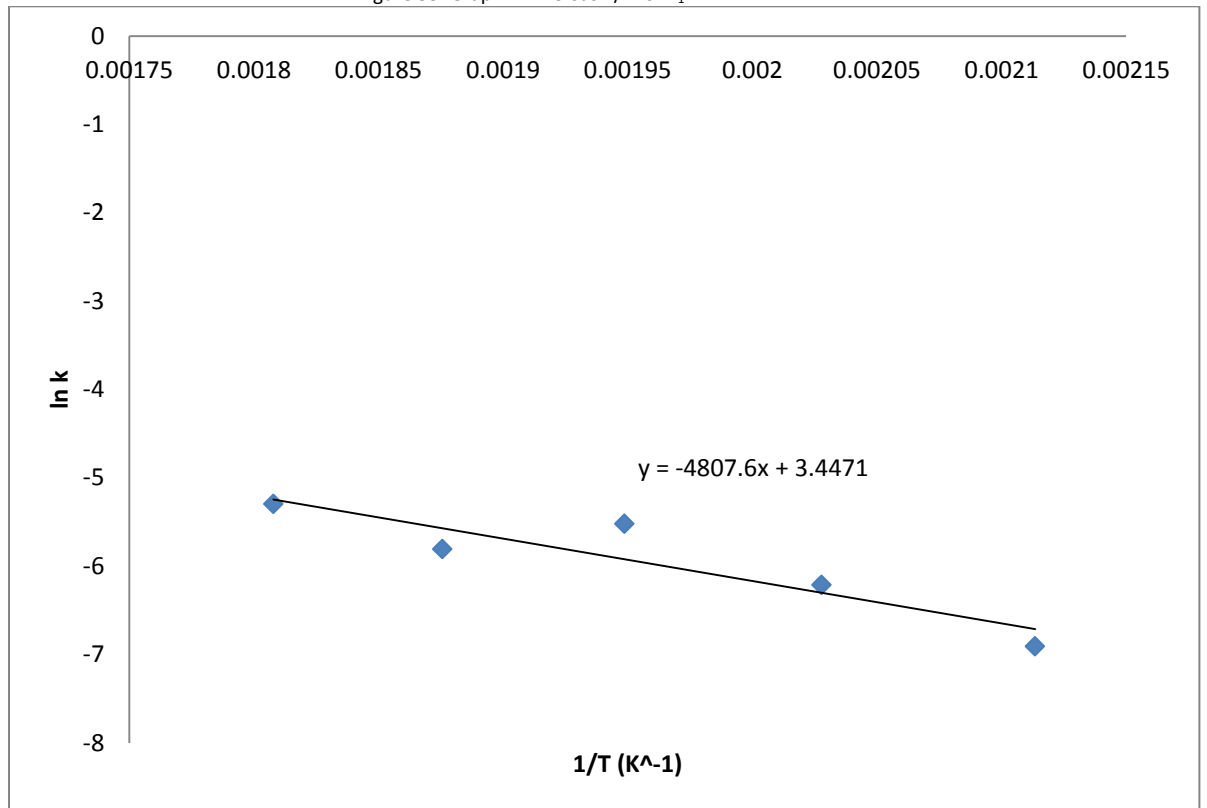
- $k_2 = 31.41 exp\left(\frac{-39967}{RT}\right)$

d) For PMF (355-500 um):
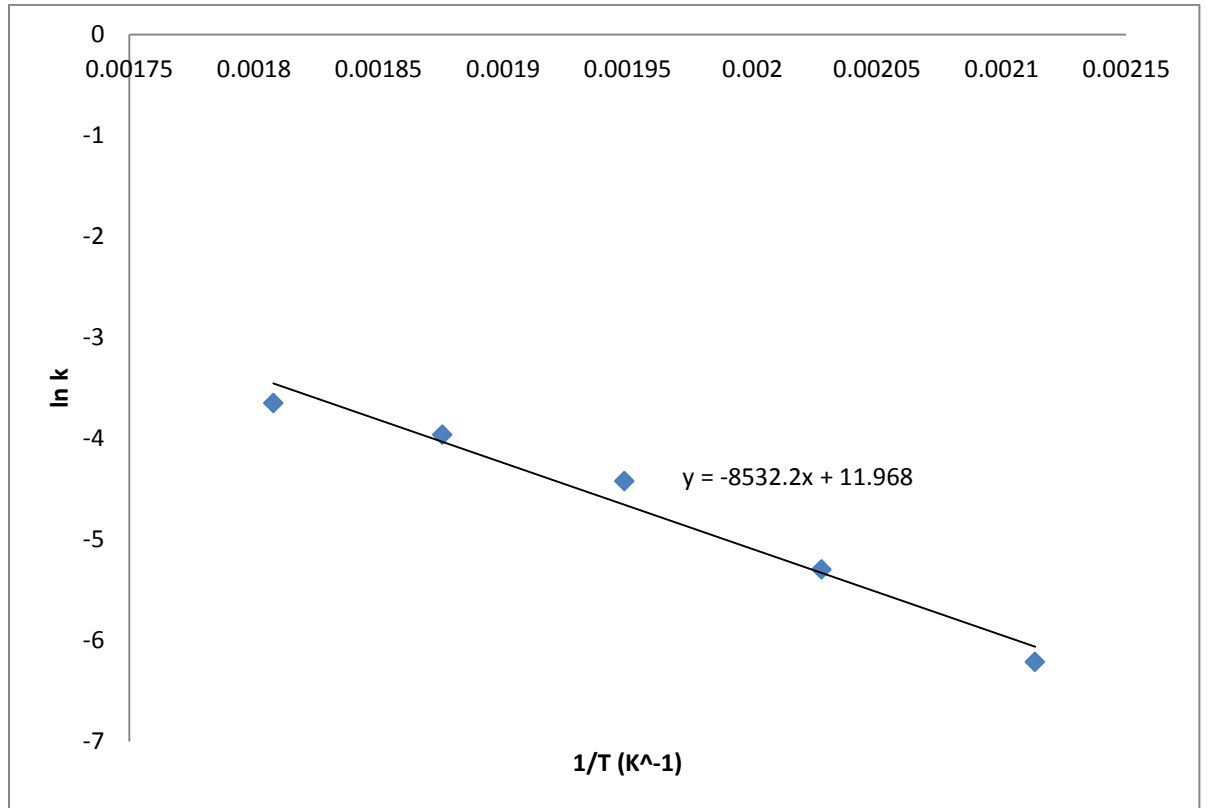
Figure 35: Graph ln k versus 1/T for k_1
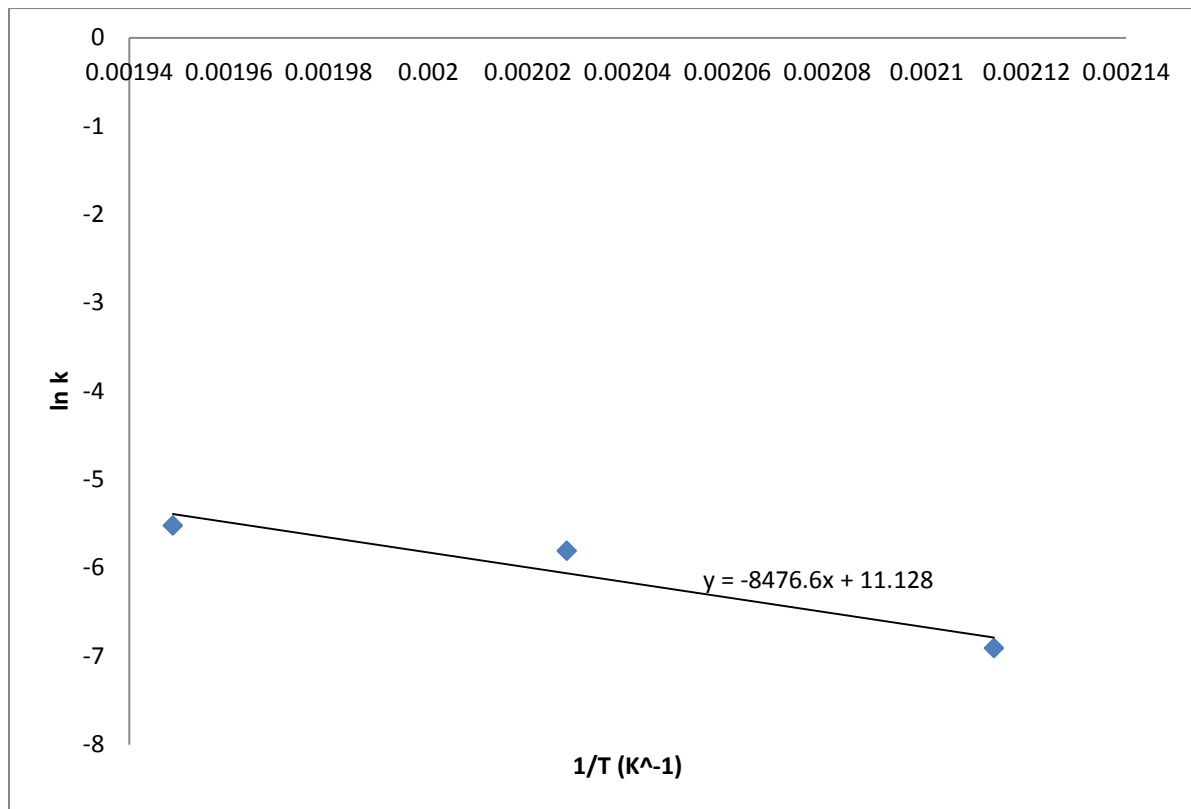
Figure 36: Graph ln k versus 1/T for k_2

- $k_1 = 156 \times 10^3 exp\left(\frac{-70938}{RT}\right)$

- $k_2 = 68 \times 10^3 exp\left(\frac{-70473}{RT}\right)$

e) For PKS (250-355 um):

$$y = -10081x + 14.564$$

Figure 37: Graph ln k versus 1/T for k_1

$$y = -4217.2x + 2.1909$$
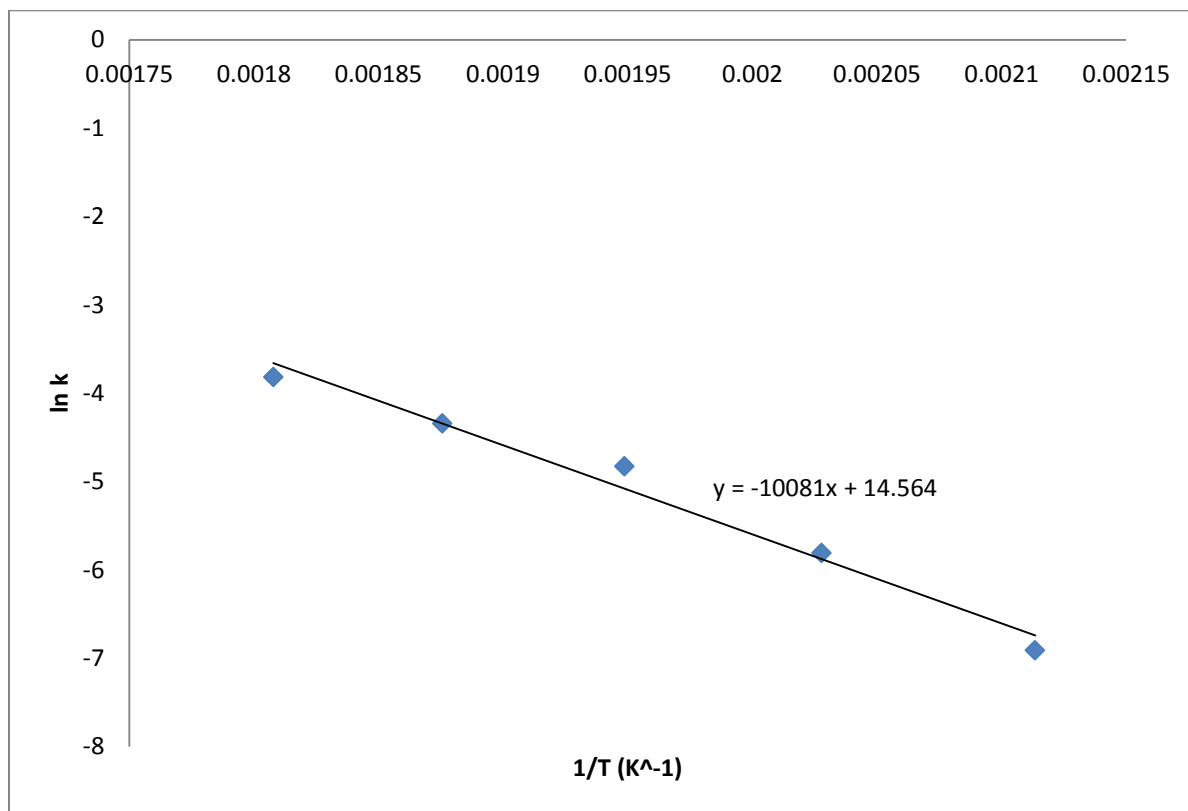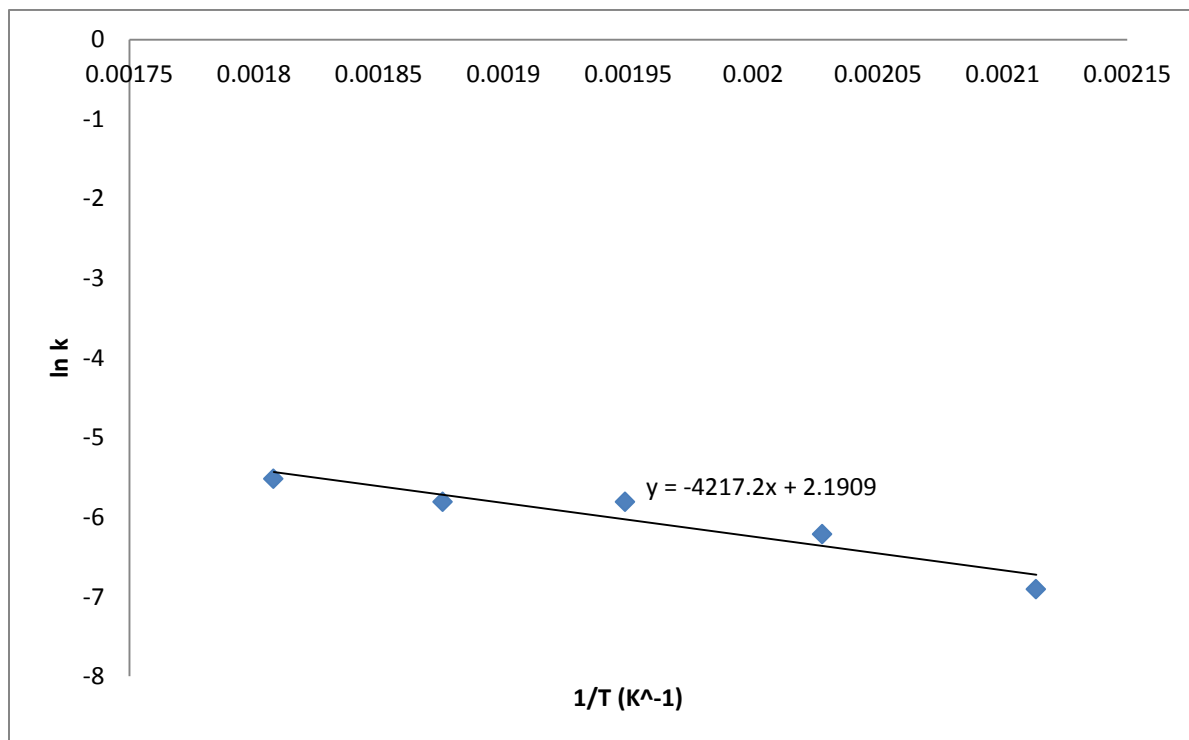
Figure 38: Graph ln k versus 1/T for k_2

- $k_1 = 2.11 \times 10^6 exp\left(\frac{-83817}{RT}\right)$

- $k_2 = 8.94 exp\left(\frac{-35062}{RT}\right)$

f) For PKS (355-500 um):
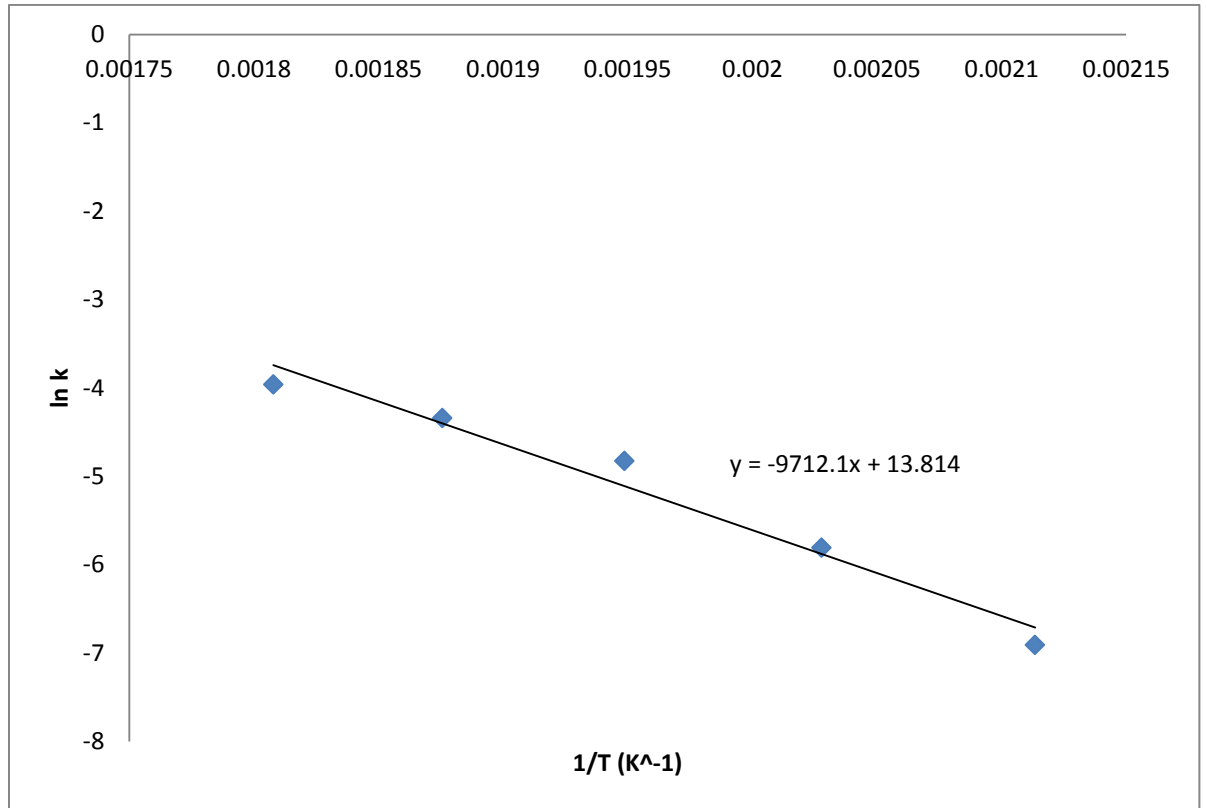
Figure 39: Graph ln k versus 1/T for k_1
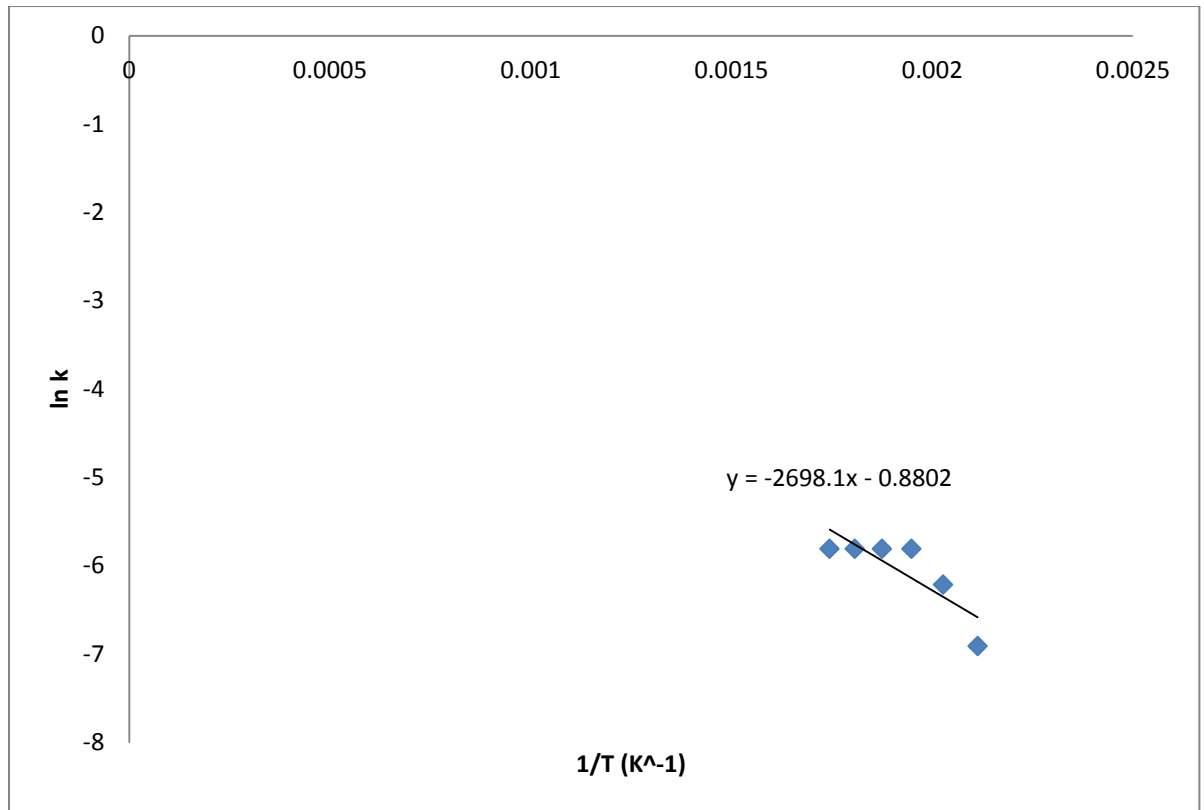
Figure 40: Graph ln k versus 1/T for k_2

- $k_1 = 66 \times 10^3 exp\left(\dfrac{-69550}{RT}\right)$

- $k_2 = 37exp\left(\dfrac{-42536}{RT}\right)$

All kinetic parameters were identified through extraction data from TGA curve.For creating a model for EFB, PMF and PKS at different particle sizes, values of k_1 and k_2 were important in order to solve unidentified rate of reaction. Rate of reaction can be identified using equation 1, 2 and 3. However, the model was developed only can be used on the particle size that range from 250 to 500 um for EFB, PMF and PKS.

4.2.2 Example of Calculation Kinetic Parameters through MATLAB

For EFB with particle size of 250-355 um at temperature 280°C (553 K), MATLAB model will used for predicting rate constant, rate of formation and torrefied product produced at initial weight of 12 kg as below:

$$k_1 = 11 \times 10^3 exp\left(\frac{-58267}{RT}\right)$$

$$= 11 \times 10^3 exp\left(\frac{-58267}{8.3144 \times 553}\right)$$

$$= 0.0346 \text{ min}^{-1}$$

$$k_2 = 1.24 \times 10^{-6} exp\left(\frac{34247}{RT}\right)$$

$$= 1.24 \times 10^{-6} exp\left(\frac{34247}{8.3144 \times 553}\right)$$

$$= 0.0021 \text{min}^{-1}$$

Rate of formation torrefied product at 12 kg,

r = 0.0100 kg/min

Weight of torrefied product with original weight of 12 kg,

w = 3.9031 kg

4.2.3 MATLAB [17, 18]

All kinetic parameters were identified and coded into MATLAB software. Reaction order, n for the torrefaction process was 1. Torrefaction model was created through MATLAB in order to predict amount of torrefied product from different amount of feedstock (EFB. PMF or PKS). Therefore, equation of rate of reaction was derived from chemical equation below before coding:

$$A\,(s) \xrightarrow{k1} B(s)$$

$$B(s) \xrightarrow{k2} C(s)$$
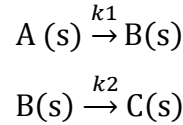
Derivation was done from initial feedstock, $W_A\,(0)$ until final product, W_C as shown below:

$$\frac{dW_A}{dt} = -k_1 W_A(0) \,(\text{Equation 6})$$

$$\frac{dW_A}{W_A} = -k_1 dt$$

Integrate from time 0 to time t1,

$$\int_0^{t1} \frac{dW_A}{W_A} = -\int_0^{t1} k_1 dt$$

$$\ln\frac{W_A(t1)}{W_A(0)} = -k_1 t_{t1}$$

$$W_A(t1) = W_A(0)e^{(-k_1 t_{t1})}$$

Value of $W_A\,(t1)$ will be substituted into equation 7,

$$\frac{dW_B}{dt} = k_1 W_A(t1) - k_2 W_B \,(\text{Equation 7})$$

Integrate from time 0 to time t2,

$$\int_0^{t2} dW_B = \int_0^{t2} \left[(k_1 W_A(0)e^{(-k_1 t_{t1})}) - (k_2 W_B) \right] dt$$

Applying Laplace transform (refer appendix I),

$$W_B(t2) = \frac{k_1}{k_2 - k_1} \times W_A(0) \times \left(e^{(-k_1 t_{t1})} - e^{(-k_2 t_{t2})}\right)$$

Value of W_B (t2) will be substituted into equation 8,

$$\frac{dW_C}{dt} = k_2 W_B(t2) \text{(Equation 8)}$$

Integrate from time 0 to time t3,

$$\int_0^{t3} dW_C = \int_0^{t3} [k_2 W_B(t2)] dt$$

$$\int_0^{t3} dW_C = \int_0^{t3} \left[k_2 \left(\frac{k_1}{k_2 - k_1} \times W_A(0) \times \left(e^{(-k_1 t_{t1})} - e^{(-k_2 t_{t2})}\right) \right) \right] dt$$

Applying Laplace transform (refer appendix I),
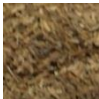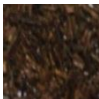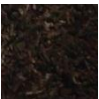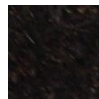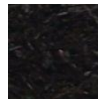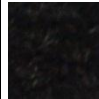
$$W_C(t3) = \frac{k_2 k_1}{k_2 - k_1 + k_2} \times W_A(0) \times \left(e^{(-k_1 t_{t1})} - e^{(-k_2 t_{t2})} - e^{(k_2 t_{t3})}\right)$$

All W_A (t1), W_B (t2) and W_C (t3) were coded into MATLAB. MATLAB was run and values of torrefied product (EFB, PMF and PKS) were predicted by MATLAB. Values were shown in table 3 until table 8 and plotted in figure 23 until figure 28 during discussion on experimental and model curves for different types of biomass.

4.3. Torrefied Biomass from Tube Furnace

Table 9 untiltable14 represented that appearances of EFB, PMF and PKS changed during torrefaction process. The appearances of each set of oil palm biomass sample (EFB, PMF and PKS) turn color from light to dark before and after torrefaction process. It was due to decomposition of hemicellulose that subjected to carbonisation during sample been heated up at different torrefaction temperature. The carbonisation (carbon formation) leads towards dark appearance of all samples.

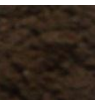Table 9: Appearances for 250-355 μm EFB before and after torrefaction process

Condition	Before Torrefaction Process	After Torrefaction Process (°C)					
Sample	Raw	200	220	240	260	280	300
Type of Biomass	Empty Fruit Bunch (EFB)						
Particle Size	250-355 μm						
Appearance							
Color Intensity	Light ⟶ Dark						

There was some confusion regarding carbonisation process during torrefaction process. For the last poster presentation, people claimed that carbonisation occurred at high temperature around 700-800°C.Regarding the confusion, actually carbonisation started to occur from temperature 200°C and upwards. However, during low temperature, only slow carbonisation process occurred. While during high temperature, it was fast carbonisation process. Therefore, when samples at high and low temperatures were compared, it showed sample at high temperature's appearance darker (more carbon formation) than sample at low temperature. Here, it can concluded that carbonisation can occur at any temperature starting from 200°C and upwards, only the different is amount of carbon formation that directly depending on rate of carbonisation process.

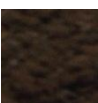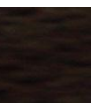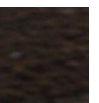Table 10:Appearances for 355-500 μm EFB before and after torrefaction process
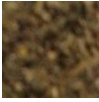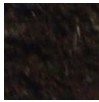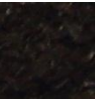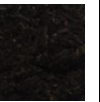
Condition	Before Torrefaction Process	After Torrefaction Process (°C)					
Sample	Raw	200	220	240	260	280	300
Type of Biomass	Empty Fruit Bunch (EFB)						
Particle Size	355-500 μm						
Appearance							
Color Intensity	Light ⟶ Dark						

Table 11: Appearances for 250-355 μm PMF before and after torrefaction process
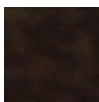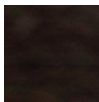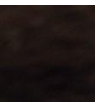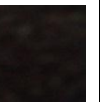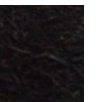
Condition	Before Torrefaction Process	After Torrefaction Process (°C)					
Sample	Raw	200	220	240	260	280	300
Type of Biomass	Palm Mesocarp Fiber (PMF)						
Particle Size	250-355 μm						
Appearance							
Color Intensity	Light ⟶ Dark						

Table 12: Appearances for 355-500 μm PMF before and after torrefaction process
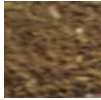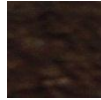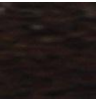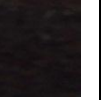
Condition	Before Torrefaction Process	After Torrefaction Process (° C)					
Sample	Raw	200	220	240	260	280	300
Type of Biomass	Palm Mesocarp Fiber (PMF)						
Particle Size	355-500 μm						
Appearance							
Color Intensity	Light ⟶ Dark						

Table 13: Appearances for 250-355 μm PKS before and after torrefaction process
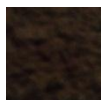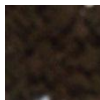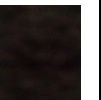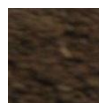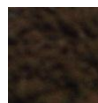
Condition	Before Torrefaction Process	After Torrefaction Process (° C)					
Sample	Raw	200	220	240	260	280	300
Type of Biomass	Palm Kernel Shell (PKS)						
Particle Size	250-355 μm						
Appearance							
Color Intensity	Light ⟶ Dark						

Table 14: Appearances for 355-500 µm PKS before and after torrefaction process

Condition	Before Torrefaction Process	After Torrefaction Process (°C)					
Sample	Raw	200	220	240	260	280	300
Type of Biomass	Palm Kernel Shell (PKS)						
Particle Size	355-500 µm						
Appearance							
Color Intensity	Light ———————————————→ Dark						

However, table 9 until table 14 were not preferable for identify the weight loss during the torrefaction process since, the TGA managed to analyze weight loss of sample accurately during the torrefaction process. Purposed for produced torrefied product through tube furnace was for sample analyses. It was due to limited amount produced by TGA that not enough for sample analyses. Sample loaded into TGA only around 2-10 mg where resulted very little amount only in milligram.

4.4. Ultimate Analyses for Raw and Torrefied Biomass
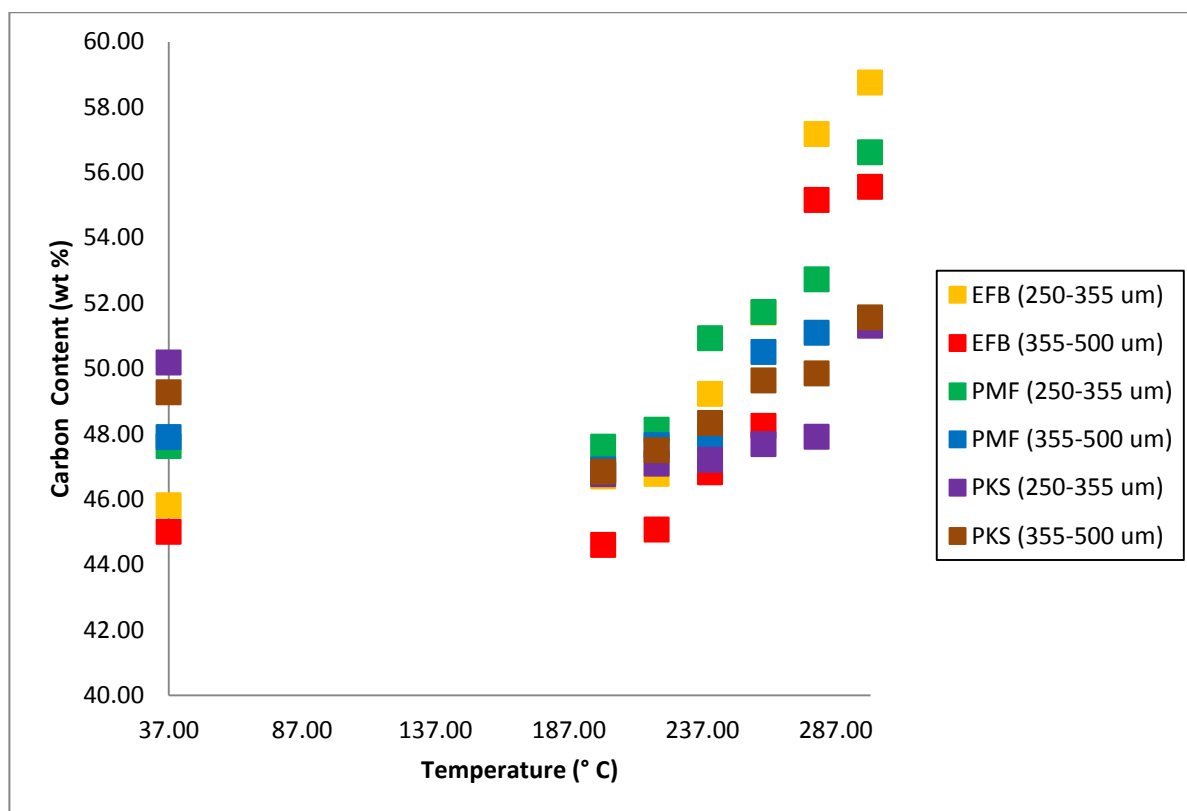
Figure41: ■ Carbon content for raw and torrefied biomass

Figure 41 to figure 45 displayed ultimate analyses for raw and torrefied samples for EFB, PMF and PKS. Theses ultimate analyses revealed the alteration that occurred in the chemical composition of oil palm biomass when it was exposed to torrefaction process.(Refer Appendix II for detail result of carbon, hydrogen, nitrogen, sulphur and oxygen contents)

The carbon content was increased with increasing torrefaction temperature for EFB, PMF and PKS. It caused by devolatilisation and carbonisation that subjected to the decomposition of hemicellulose. Both EFB and PMF had higher amount of carbon content than PKS. It was related with previous discussion on weight loss of EFB, PMF and PKS in part 4.1. Therefore, more weight loss was resulted higher carbon content.

Besides that, figure 41 showed the carbon content was different particle sizes. 250-355 μm of particle size had higher carbon content than 355-500 μm of particle size for each

type of biomass. It was due to 250-355 μm particle size had larger sample area than 355-500 μm. As a result, it caused carbonisation to react faster.
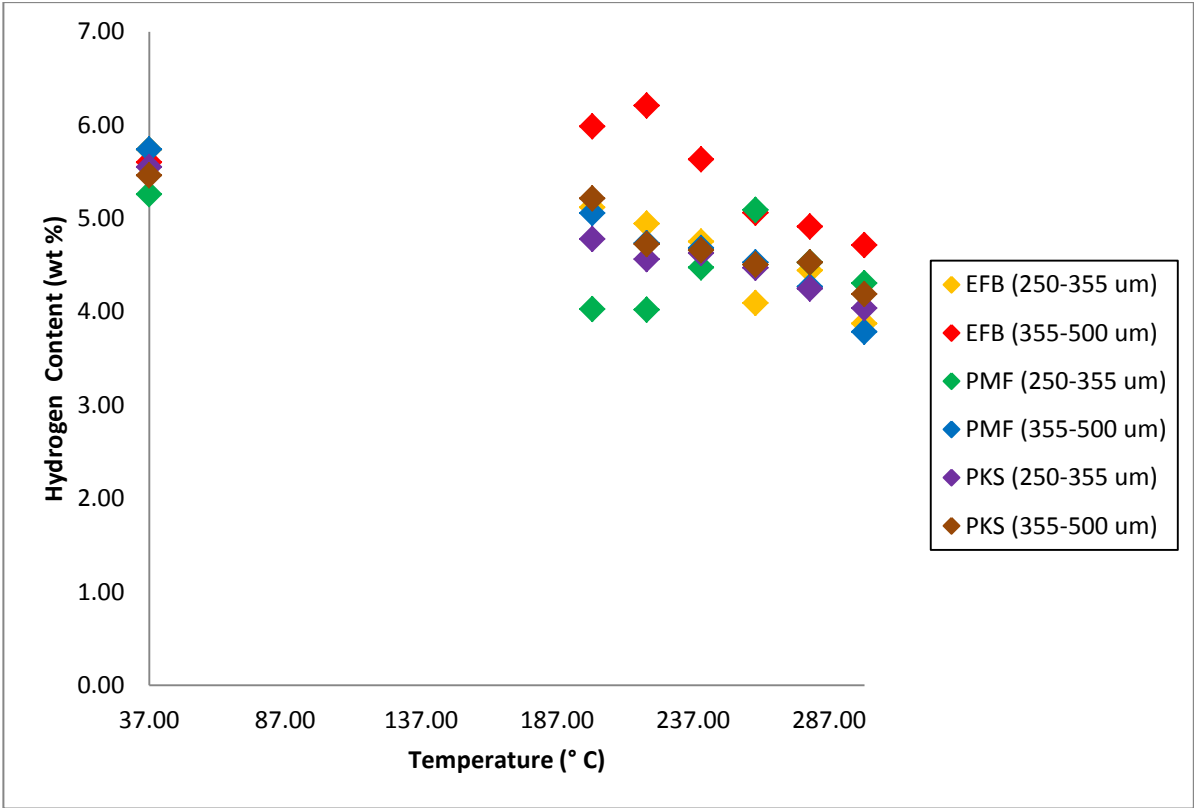
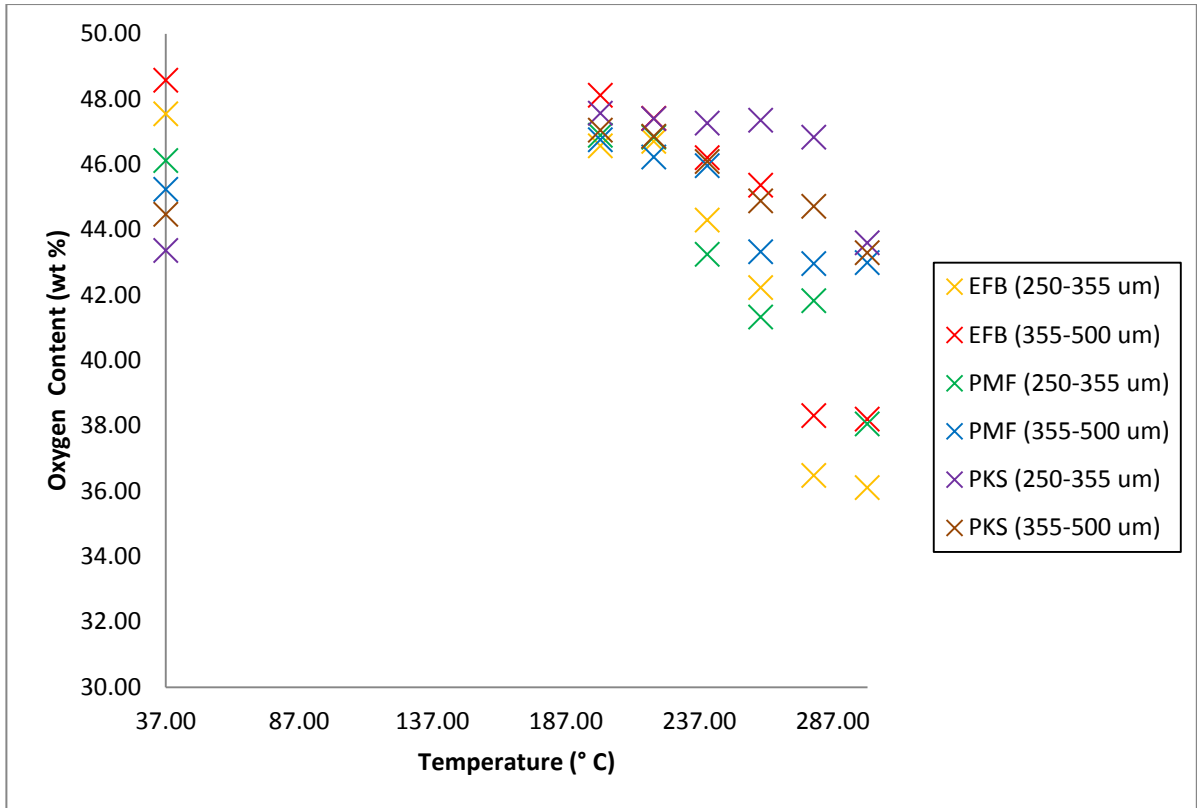

Figure42:♦ Hydrogen content for raw and torrefied biomass

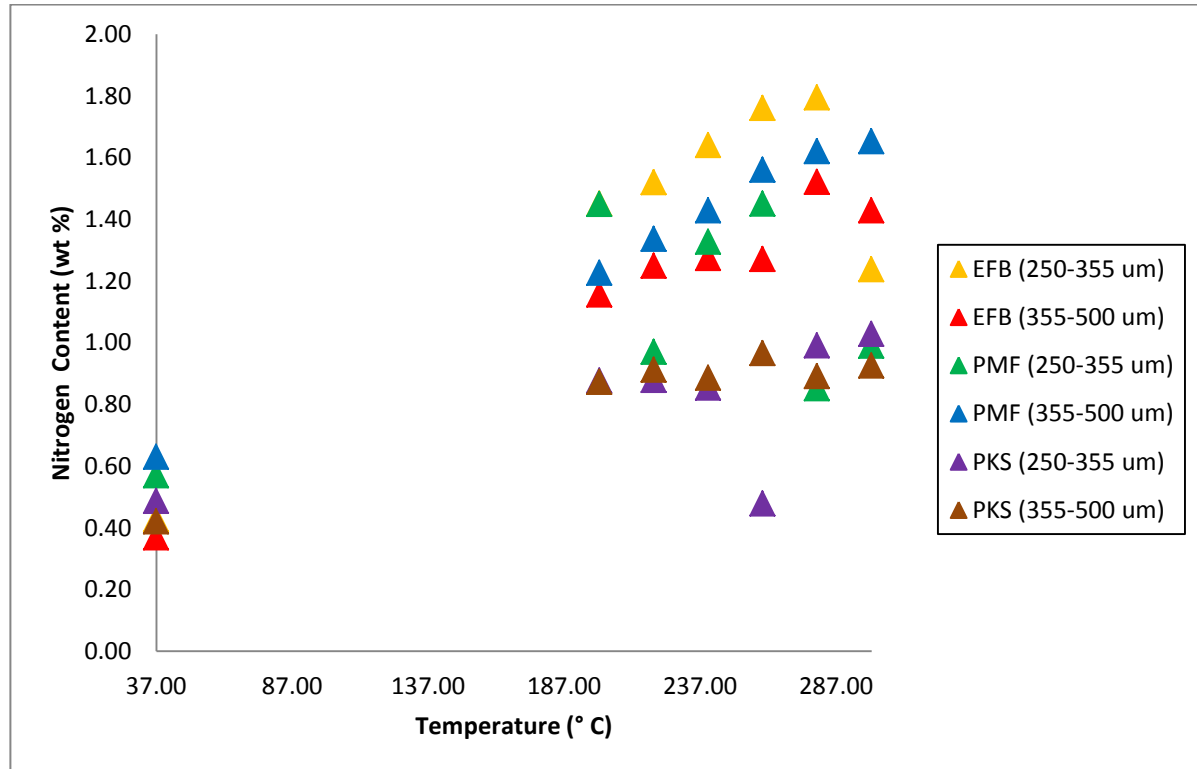Figure43: **x** Oxygen content for raw and torrefied biomass

Figure44: ▲ Nitrogen content for raw and torrefied biomass

Furthermore, figure 42 to figure 43showed hydrogen and oxygen contents were changed due to release of methane (CH_4), ethane (C_2H_6), carbon dioxide (CO_2) and carbon monoxide (CO) during torrefaction process. The exception was nitrogen content while it was remained unchanged from figure 44.
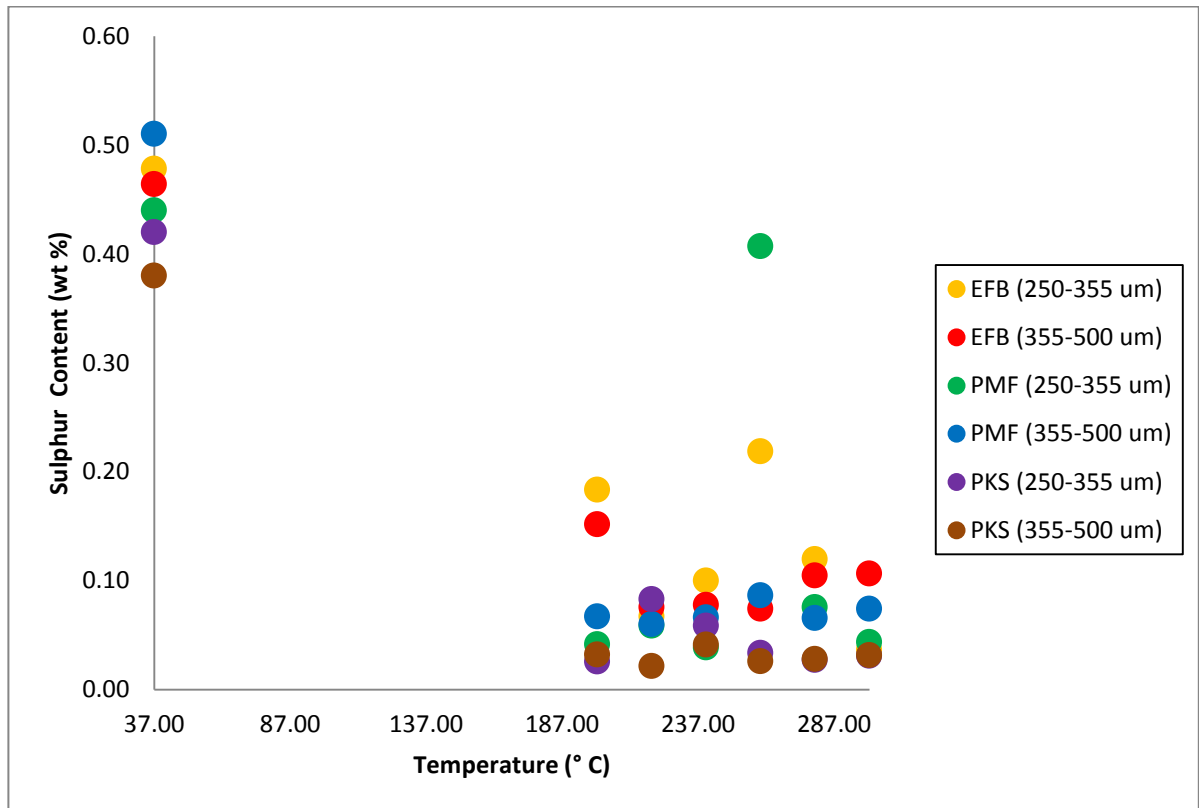
Figure45:● Sulphur content for raw and torrefied biomass

Besides, sulphur content for figure 45 was below than 0.6 wt%. As a result, it showed that oil palm biomass released less sulphur during combustion into atmosphere. Besides, it reduced health problem caused by sulphur.
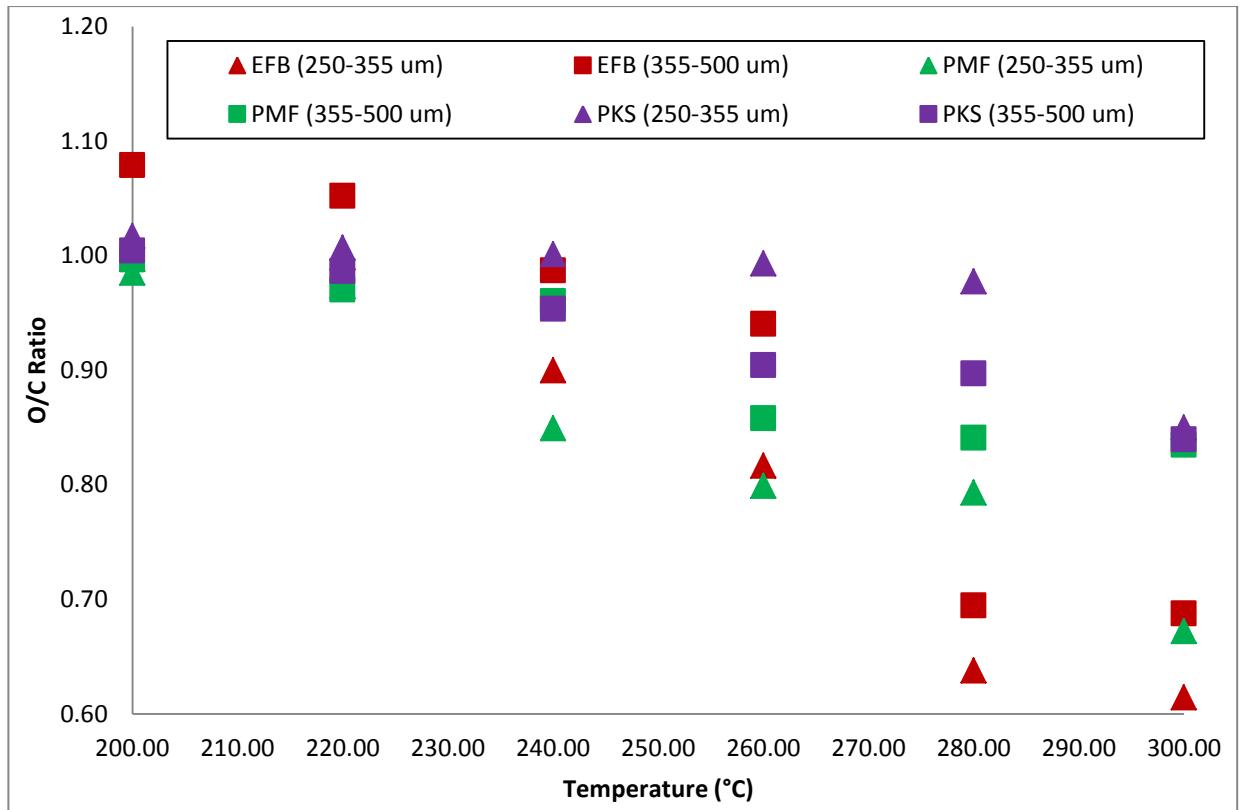
Figure46: O/C ratio for different type of biomass

In the order hand, figure 46 showed O/C ratio for all samples. It decreased over torrefaction temperature and resulted improvement of gasification properties of torrefied biomass [2].The decreasing of O/C ratio was due to removal of water and carbon dioxide during torrefaction process [7]. During the torrefaction process oxygen content was reducing while carbon content was increasing. Increasing of carbon content caused high calorific value during the burning. It resulted less smoke and water vapor were formed. As a result, torrefied products were improved in combustion view.

4.5. Calorific Value fromRaw and TorrefiedBiomass
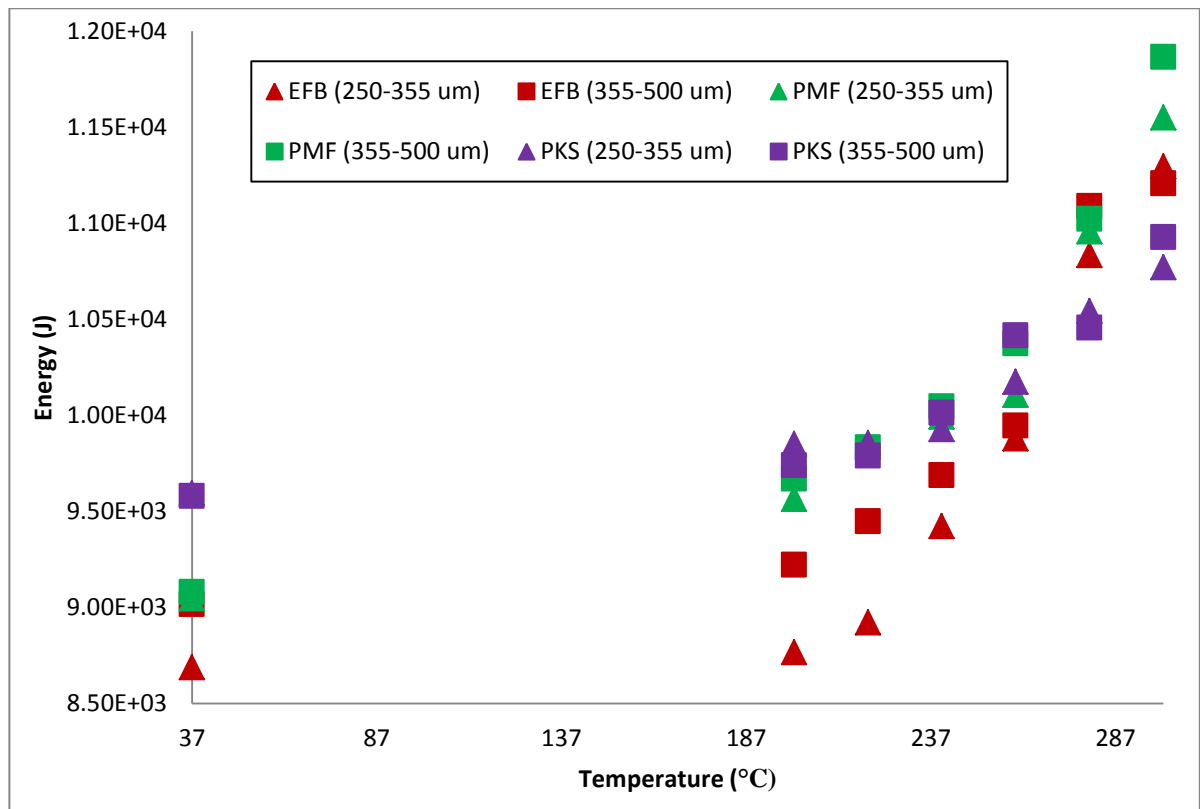
Figure47: Energy yield for different types of oil palm biomass

Figure 47 result represented three types of oil palm biomass (EFB, PMF and PKS) energy variation for raw and torrefied samples. The energy yield was referred to higher heating value (HHV) for both raw and torrefied samples. The graph was plotted at different particle size, torrefaction temperature and type of oil palm biomass.

The energy yield for EFB, PMF and PKS were increased with increasing torrefaction temperature. For all samples, practically all chemical energy was retained in the torrefied product and the energy yield was depended on that torrefied product. It seems torrefied product contained different amount of carbon content that resulted different energy yield.

The influence of biomass type on the energy yield was the best observed in figure 47. It showed PMF had highest energy yield followed by EFB and PKS. It was because of increased carbon content that leads towards high calorific value during burning. PMF had highest increasing of carbon content followed by EFB and PKS. Besides, figure 47

emphasized that particle size gave small influence in energy yield with showing similar trends. Figure 47 most clearly revealed the increase of the energy yield with increasing torrefaction temperature. As proved, torrefaction improved energy density of raw oil palm biomass. (Refer Appendix III for detail result of calorific value for raw and torrefied biomass)

CHAPTER 5: CONCLUSION AND RECOMMENDATION

5.1 Conclusion

The kinetic study from TGA weight loss curve for EFB, PMF and PKS described two steps of reaction involve during torrefaction process. First step was fast hemicellulose decomposition reaction while second step was slow hemicellulose decomposition reaction. Both steps represented hemicellulose decomposition whereas no decomposition of cellulose and lignin. Kinetic model can be used for predicting amount of torrefied product of oil palm biomass from torrefaction process. However, this model limited to EFB, PMF and PKS only with particle size between 250-500 μm.

Torrefaction temperature - Six of torrefaction temperature were applied, i.e. 200, 220, 240, 260, 280 and 300°C for EFB, PMF and PKS. When temperature increased, more weight loss was obtained. From TGA observation, weight loss was resulted from decomposition of hemicellulose only. No cellulose and lignin decompositions were involved. Besides, the hemicellulose decomposition is more significant compare to cellulose and lignin during torrefaction of oil palm biomass since temperature decomposition of hemicellulose between 225-325°C [5].

Type of biomass - Different type of biomass composed different composition of hemicellulose and resulted different weight loss. EFB and PMF composed higher amount of hemicellulose than PKS where both of EFB and PMF torrefied products were resulted more weight loss than PKS.

Particle size - Two particle sizes were used during torrefaction process: 250-355 μm and 355-500 μm. 250-355 μm was resulted higher more weight loss and higher energy density rather than 355-500 μm. It was because of larger sample area of 250-355 μm lead decomposition that subjected to carbonisation, devolatilisation and hemicellulose to react faster than 355-500 μm. EFB, PMF and PKS with 250-355 μm had more weight loss and higher energy density.

Reaction time - During torrefaction process for EFB, PMF and PKS, 2 hours of reaction time was applied for each torrefaction temperature (200, 220, 240, 260, 280 and 300°C). 2 hours of reaction time was enough for EFB, PMF and PKS where there was no more weight loss of sample (weight loss constant). However, reaction time below 2 hours was not suitable for EFB, PMF and PKS. It was due to unfinished reaction showed by TGA for those samples since there was a weight loss (weight loss not constant). It can be concluded that four main parameters give significant to torrefaction process which were torrefaction temperature, type of biomass, particle size, torrefied temperature and reaction time.

Furthermore, applying torrefaction process had resulted towards energy densification for EFB, PMF and PKS. PMF contained highest energy followed by EFB and PKS. Other than that, ultimate analyses for EFB, PMF and PKS showed different carbon, hydrogen, nitrogen, sulphur and oxygen contents before and after torrefaction process.

5.2 Recommendation

During carried out this torrefaction project, there are a few recommendation from my side in order to make improvement and variety focus on torrefaction research, so that it becomes completed with deeply investigation. There are:

a) carried out research on determining composition of hemicellulose, cellulose and lignin for raw and torrefied biomass. Significant on doing this research is to know exact composition of hemicellulose, cellulose and lignin after and before torrefaction process. By doing this, we can know exactly which structure decompose during torrefaction process. It might be hemicellulose, cellulose or lignin. Besides, we can know the starting decomposition of hemicellulose, cellulose and lignin during the torrefaction process.

b) carried out at different particle sizes such as 100-250 µm and 100-200 mm. The important is to identify its affect onto weight loss, energy content and ultimate analysis. By doing that, kinetic model that already created can be modified and applied with different range of particle size.

REFERENCES

1. Nasrin, A.B., Ma, A.N., Choo, Y.M., Mohamad, S., Rohaya, M.H., Azali, A., and Zainal, Z., 2008, "Oil palm biomass as potential substitution raw materials for commercial biomass briquettes production," *American Journal of Applied Sciences* **5 (3):** 179-183.

2. Arias, B., Pevida, C., Fermoso, J., Plaza, M.G., Rubiera, F., and Pis, J.J., 2008, "Influence of torrefaction on the grindability and reactivity of woody biomass," *Fuel Processing Technology* **89:** 169-175.

3. Bourgeois, J., and Guyonnet, R., 1988, "Characterisation and analysis of torrefied wood," *Wood Science Technology* **22 (2):** 143-155.

4. Yang, H., Yan, R., Chin, T., Liang, D.T., Chen, H., and Zheng, C., 2004, "Thermogravimetric analysis-fourier transform infrared analysis of palm oil waste pyrolysis," *Energy and Fuels* **18:** 1814-1821.

5. Prins, M.J., Ptasinski, K.J., and Janssen, F.J.J.G., 2006, "Torrefaction of wood Part 1. Weight loss kinetics," *Journal of Analytical and Applied Pyrolysis* **77:** 28-34.

6. Prins, M.J., Ptasinski, K.J., and Janssen, F.J.J.G., 2006, "Torrefaction of wood Part 2. Analysis of products," *Journal of Analytical and Applied Pyrolysis* **77:** 35-40.

7. Prins, M.J., Ptasinski, K.J., and Janssen, F.J.J.G., 2006, "More efficient biomass gasification via torrefaction," *Energy* **31:** 3458-3470.

8. Nimlos, M. N., Brooking, E., Looker, M.J., and Evans R.J., 2003, "Biomass torrefaction studies with a molecular beam mass spectrometer," *Preprint Papers-American Chemical Society, Division of Fuel Chemistry* **48 (2):** 590-591.

9. Bergman, P.C.A., Boersma, A.R., Kiel, J.H.A., Prins, M.J., Ptasinski, K.J., and Janssen, F.J.J.G., 2005. *Torrefaction for entrained-flow gasification of biomass.* Report ECN-C--05-067, Energy research Centre of th Netherlands (ECN), Petten, The Netherlands

10. Bergman, P.C.A., and Kiel, J.H.A., 2005. *Torrefaction for biomass upgrading.* Proceedings of the 14th European Biomass Conference & Exhibition, Paris, France, October 17-21, 2005.

11. Pentanunt, R., Mizanur Rahman, A.N.M., and Bhattacharya, S.C., 1990, "Upgrading of biomass by means of torrefaction," *Energy* **15:** 1175-1179.

12. Bridgeman, T.G., Jones, J.M., Shield, I., and Williams, P.T., 2008, "Torrefaction of reed canary grass, wheat straw and willow to enhance solid fuel qualities and combustion properties," *Fuel***87:** 844-856.

13. Chen, W.-H., and Kuo, P.-C., 2010, "A study on torrefaction of various biomass materials and its impact on lignocellulosic structure simulated by a thermogravimetry," *Energy***35:** 2580-2586.

14. Sukiran, M.A., Chin, C.M., and Abu Bakar, N.K., 2009, "Bio-oils from pyrolysis of oil palm empty fruit bunch," *American Journal of Applied Sciences***6 (5):** 869-875.

15. Couhert, C., Salvador, S., and Commandré, J-M., 2009, "Impact of torrefaction on syngas production from wood," *Fuel***88:** 2286-2290.

16. Di Blasi, C., and Lanzetta, M., 1997, "Intrinsic kinetic of isothermal xylan degradation in inert atmosphere," *Journal of Analytical and Applied Pyrolysis* **40-41:** 287-303.

17. Houston, P.L., 2001. *Chemical Kinetics and Reaction Dynamics,* New York, McGraw-Hill International Edition

18. Michael J. Pilling, Paul W. Seakins, 1995. *Reaction Kinetics,* New York, Oxford Science Publications

APPENDICES

Appendix I: Laplace Transform

TIME DOMAIN		FREQUENCY DOMAIN
$\delta(t)$	unit impulse	1
A	step	$\dfrac{A}{s}$
t	ramp	$\dfrac{1}{s^2}$
t^2		$\dfrac{2}{s^3}$
$t^n, n > 0$		$\dfrac{n!}{s^{n+1}}$
e^{-at}	exponential decay	$\dfrac{1}{s+a}$
$\sin(\omega t)$		$\dfrac{\omega}{s^2 + \omega^2}$
$\cos(\omega t)$		$\dfrac{s}{s^2 + \omega^2}$
te^{-at}		$\dfrac{1}{(s+a)^2}$
$t^2 e^{-at}$		$\dfrac{2!}{(s+a)^3}$

Appendix II: Ultimate Analyses for Raw and Torrefied Biomass (EFB, PMF, PKS)

Experiment	Content (%)					
	C	H	N	S	O	O/C
EFB_250-355_Raw Sample	45.81	5.74	0.43	0.48	47.55	1.04
EFB_250-355_200	46.69	5.12	1.45	0.18	46.56	1.00
EFB_250-355_220	46.77	4.94	1.52	0.07	46.70	1.00
EFB_250-355_240	49.22	4.75	1.64	0.10	44.29	0.90
EFB_250-355_260	51.70	4.09	1.76	0.22	42.23	0.82
EFB_250-355_280	57.17	4.44	1.80	0.12	36.48	0.64
EFB_250-355_300	58.75	3.87	1.24	0.04	36.11	0.61
EFB_355-500_Raw Sample	45.00	5.60	0.37	0.46	48.57	1.08
EFB_355-500_200	44.60	5.99	1.16	0.15	48.11	1.08
EFB_355-500_220	45.06	6.21	1.25	0.08	47.41	1.05
EFB_355-500_240	46.82	5.63	1.27	0.08	46.20	0.99
EFB_355-500_260	48.24	5.06	1.27	0.07	45.36	0.94
EFB_355-500_280	55.16	4.91	1.52	0.10	38.31	0.69
EFB_355-500_300	55.55	4.71	1.43	0.11	38.20	0.69
PMF_250-355_Raw Sample	45.82	5.26	0.57	0.45	47.90	1.05
PMF_250-355_200	47.60	4.03	1.45	0.04	46.88	0.98
PMF_250-355_220	48.12	4.02	0.97	0.06	46.83	0.97
PMF_250-355_240	50.92	4.47	1.33	0.04	43.24	0.85

PMF_250-355_260	51.73	5.09	1.45	0.41	41.33	0.80
PMF_250-355_280	52.72	4.53	0.85	0.08	41.82	0.79
PMF_250-355_300	56.61	4.30	0.99	0.04	38.05	0.67
PMF_355-500_Raw Sample	47.89	5.74	0.63	0.51	45.23	0.94
PMF_355-500_200	46.91	5.06	1.23	0.07	46.75	1.00
PMF_355-500_220	47.65	4.73	1.34	0.06	46.22	0.97
PMF_355-500_240	47.87	4.68	1.43	0.07	45.96	0.96
PMF_355-500_260	50.50	4.53	1.56	0.09	43.32	0.86
PMF_355-500_280	51.09	4.27	1.62	0.07	42.96	0.84
PMF_355-500_300	51.50	3.78	1.65	0.07	42.99	0.83
PKS_250-355_Raw Sample	50.18	5.55	0.49	0.42	43.36	0.86
PKS_250-355_200	46.76	4.78	0.88	0.03	47.56	1.02
PKS_250-355_220	47.08	4.56	0.88	0.08	47.40	1.01
PKS_250-355_240	47.20	4.63	0.85	0.06	47.26	1.00
PKS_250-355_260	47.68	4.47	0.48	0.03	47.35	0.99
PKS_250-355_280	47.91	4.25	0.99	0.03	46.83	0.98
PKS_250-355_300	51.31	4.04	1.03	0.03	43.60	0.85
PKS_355-500_Raw Sample	49.27	5.46	0.42	0.38	44.47	0.90
PKS_355-500_200	46.84	5.21	0.87	0.03	47.04	1.00
PKS_355-500_220	47.49	4.72	0.91	0.02	46.85	0.99
PKS_355-500_240	48.33	4.66	0.89	0.04	46.08	0.95

PKS_355-500_260	49.63	4.51	0.97	0.03	44.88	0.90
PKS_355-500_280	49.84	4.53	0.89	0.03	44.71	0.90
PKS_355-500_300	51.56	4.19	0.93	0.03	43.29	0.84

*Notation for CHNS Experiment: Sample Name_Particle Size_Torrefaction Temperature

Appendix III: Calorific Value for Raw and Torrefied Biomass (EFB, PMF, PKS)

Experiment	Sample Weight (g)	Calorific Value (J/g)	Energy Yield (J)
EFB_250-355_Raw Sample	**0.5**	**17377.00**	**8.69E+03**
EFB_250-355_200	0.5	17534.00	8.77E+03
EFB_250-355_220	0.5	17844.00	8.92E+03
EFB_250-355_240	0.5	18847.00	9.42E+03
EFB_250-355_260	0.5	19761.00	9.88E+03
EFB_250-355_280	0.5	21669.00	1.08E+04
EFB_250-355_300	0.5	22592.00	1.13E+04
EFB_355-500_Raw Sample	**0.5**	**18035.00**	**9.02E+03**
EFB_355-500_200	0.5	18443.00	9.22E+03
EFB_355-500_220	0.5	18897.00	9.45E+03
EFB_355-500_240	0.5	19377.00	9.69E+03
EFB_355-500_260	0.5	19893.00	9.95E+03
EFB_355-500_280	0.5	22180.00	1.11E+04
EFB_355-500_300	0.5	22415.00	1.12E+04
PMF_250-355_Raw Sample	**0.5**	**18093.00**	**9.05E+03**
PMF_250-355_200	0.5	19129.00	9.56E+03
PMF_250-355_220	0.5	19671.00	9.84E+03
PMF_250-355_240	0.5	19986.00	9.99E+03
PMF_250-355_260	0.5	20214.00	1.01E+04
PMF_250-355_280	0.5	21914.00	1.10E+04
PMF_250-355_300	0.5	23102.00	1.16E+04
PMF_355-500_Raw Sample	**0.5**	**18161.00**	**9.08E+03**
PMF_355-500_200	0.5	19341.00	9.67E+03
PMF_355-500_220	0.5	19667.00	9.83E+03
PMF_355-500_240	0.5	20092.00	1.00E+04
PMF_355-500_260	0.5	20751.00	1.04E+04
PMF_355-500_280	0.5	22046.00	1.10E+04
PMF_355-500_300	0.5	23732.00	1.19E+04

PKS_250-355_Raw Sample	**0.5**	**19191.00**	**9.60E+03**
PKS_250-355_200	0.5	19702.00	9.85E+03
PKS_250-355_220	0.5	19715.00	9.86E+03
PKS_250-355_240	0.5	19856.00	9.93E+03
PKS_250-355_260	0.5	20351.00	1.02E+04
PKS_250-355_280	0.5	21085.00	1.05E+04
PKS_250-355_300	0.5	21542.00	1.08E+04
PKS_355-500_Raw Sample	**0.5**	**19160.00**	**9.58E+03**
PKS_355-500_200	0.5	19481.00	9.74E+03
PKS_355-500_220	0.5	19581.00	9.79E+03
PKS_355-500_240	0.5	20026.00	1.00E+04
PKS_355-500_260	0.5	20833.00	1.04E+04
PKS_355-500_280	0.5	20913.00	1.05E+04
PKS_355-500_300	0.5	21856.00	1.09E+04

*Notation for Bomb Calorimeter Experiment: Sample Name_Particle Size_Torrefaction Temperature

Appendix IV: Raw Data for TGA

a) -Type of biomass: EFB

   -Particle size   : 250 – 355 μm

   -Reaction time   : 2 hours

   -Temperature   : 200, 220, 240, 260, 280 and 300°C
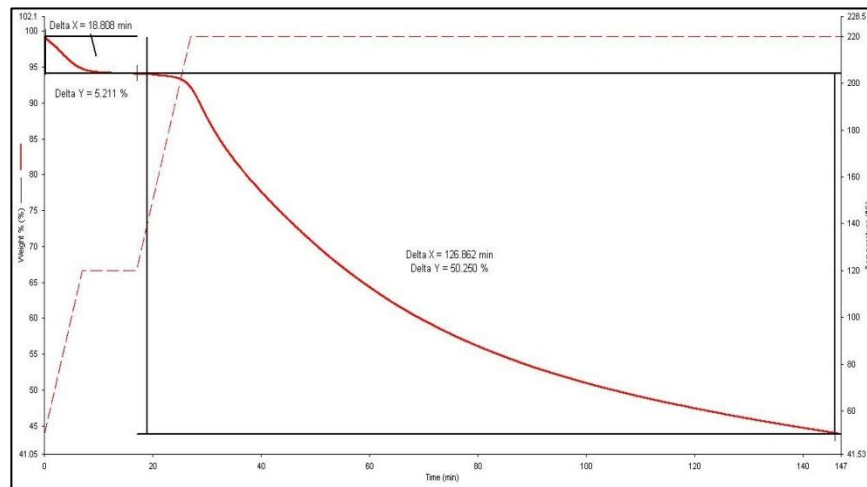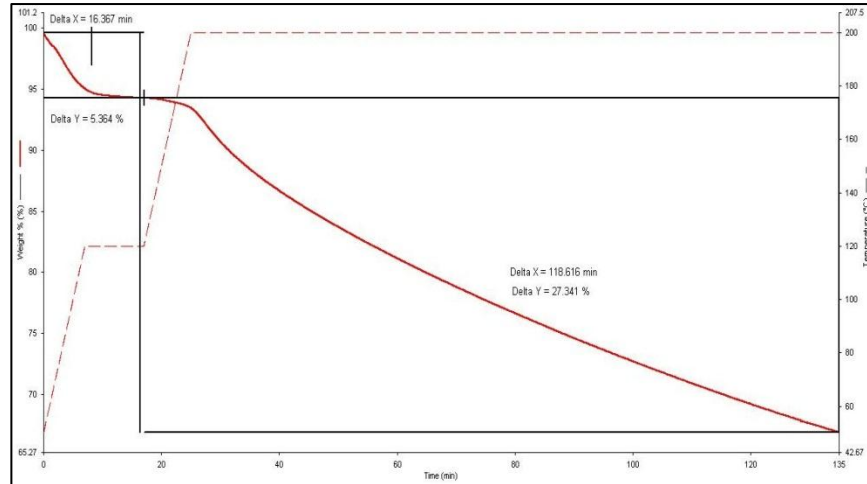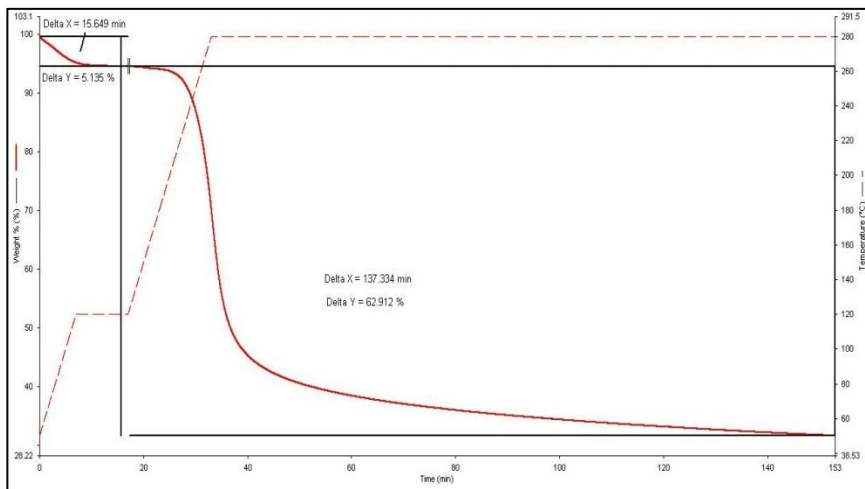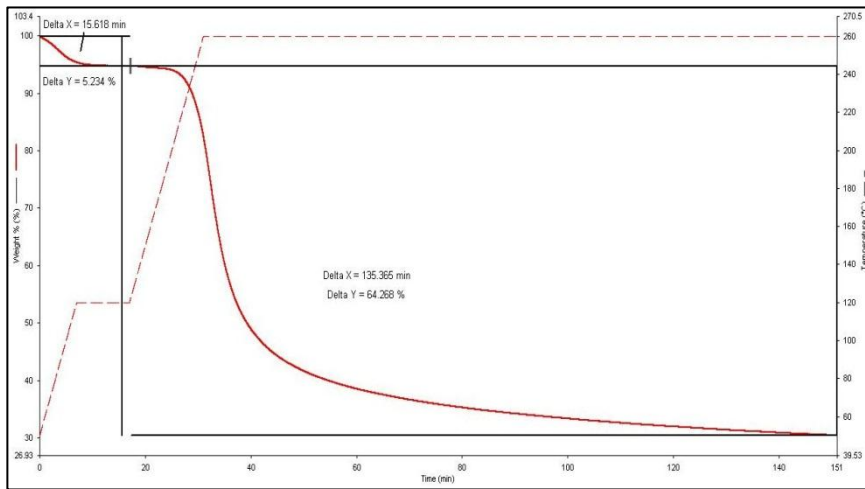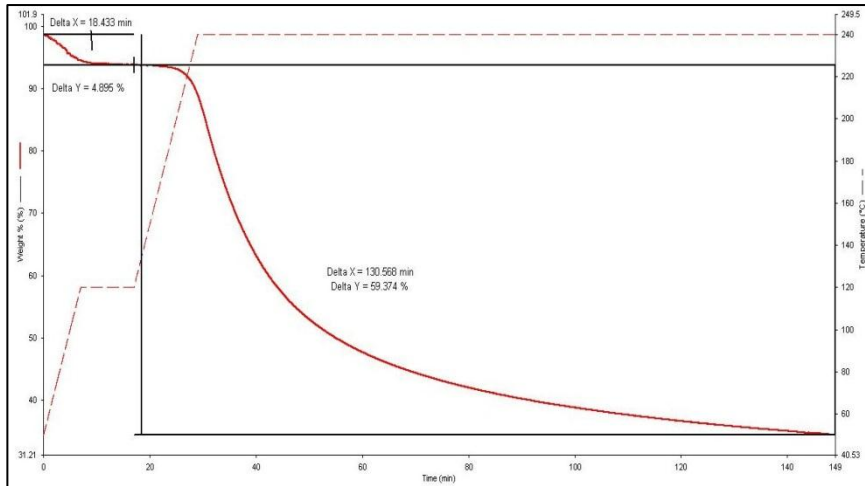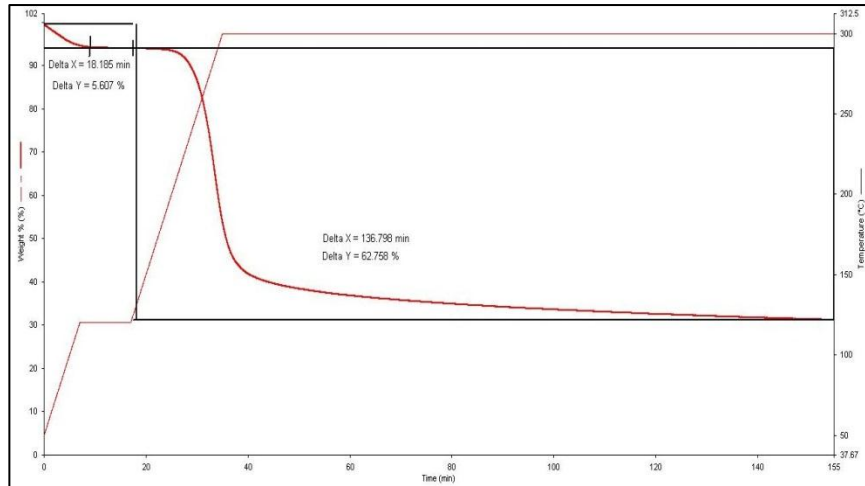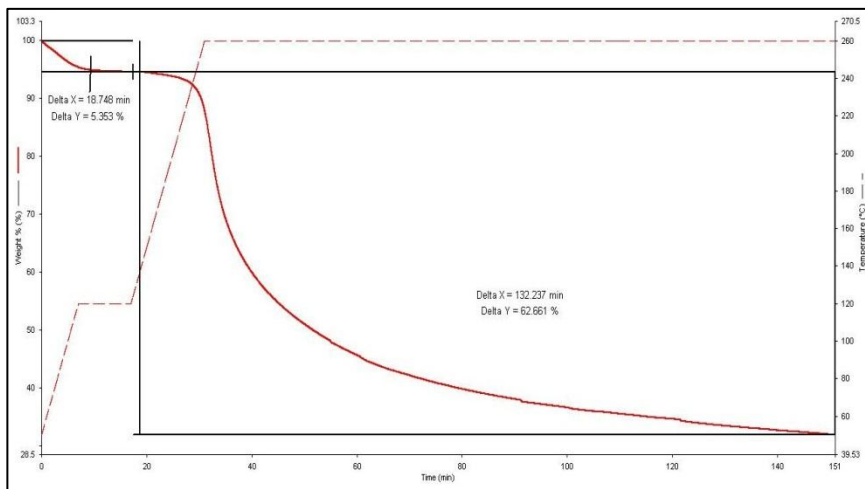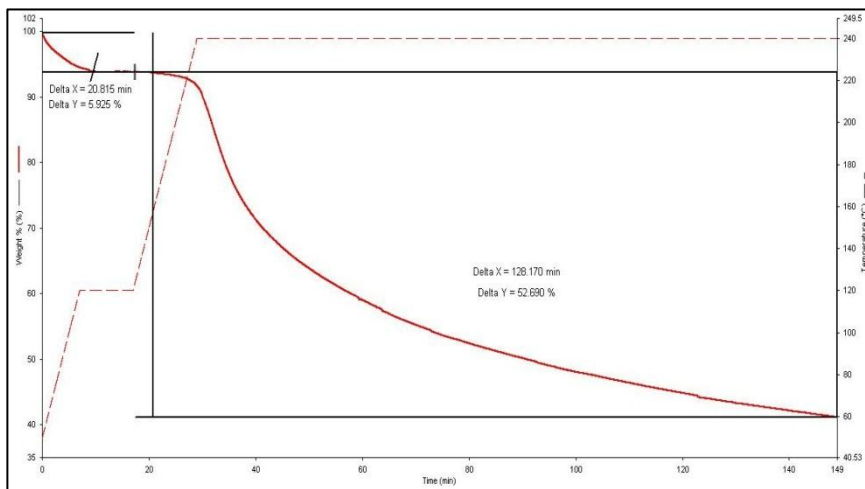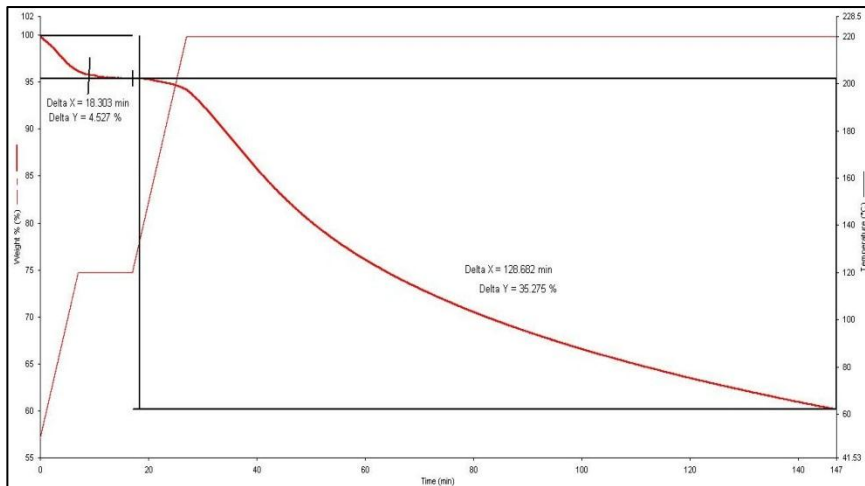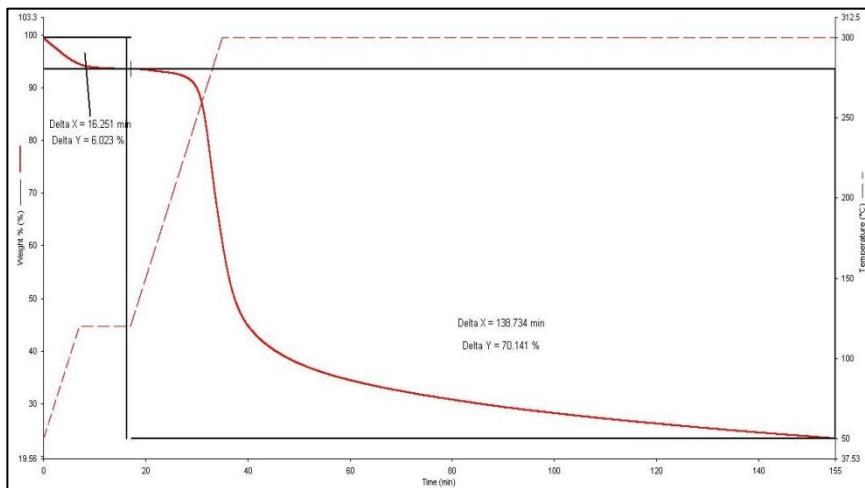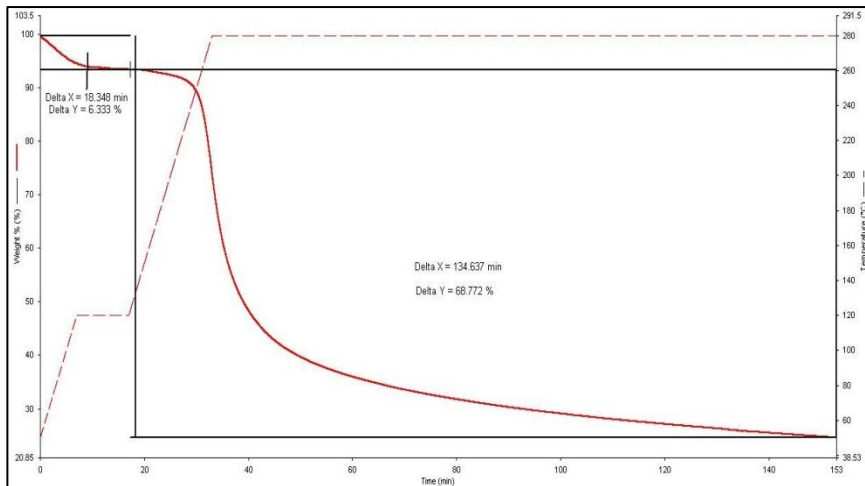
b) -Type of biomass: EFB

-Particle size   : 355 – 500 μm

-Reaction time   : 2 hours

-Temperature   : 200, 220, 240, 260, 280 and 300°C
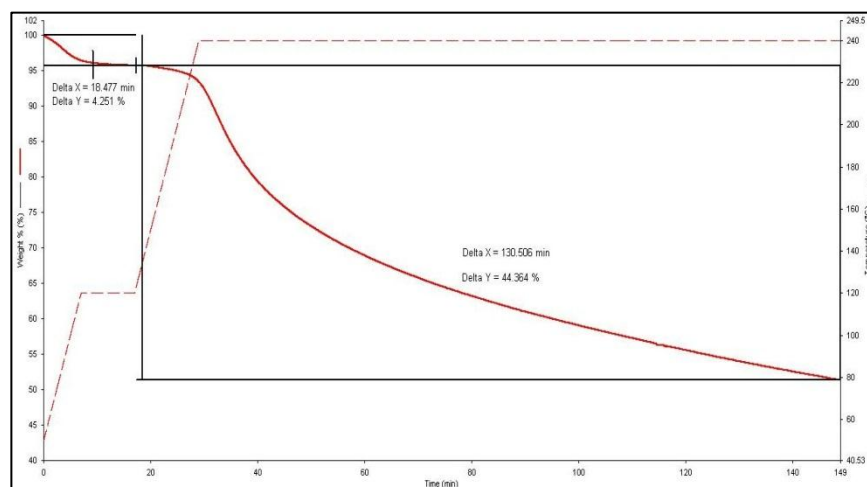

96
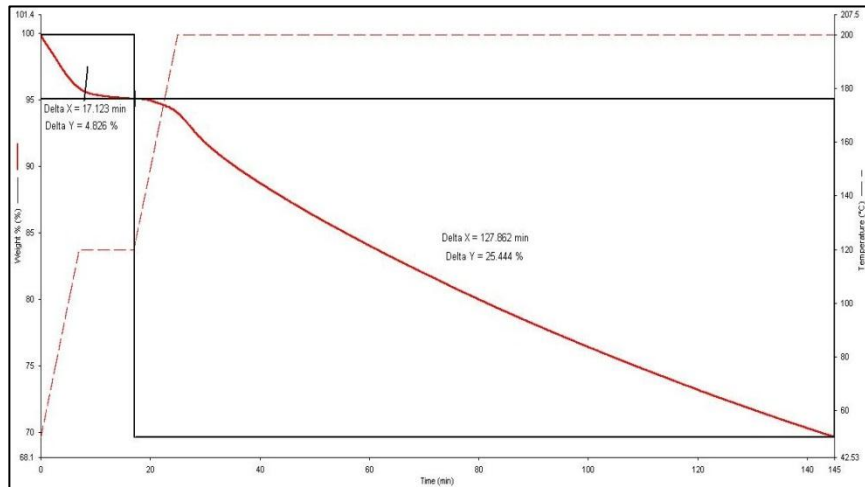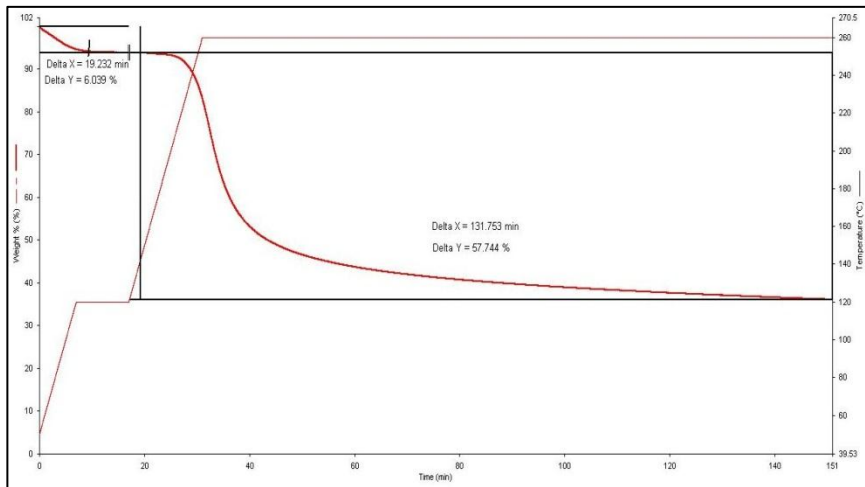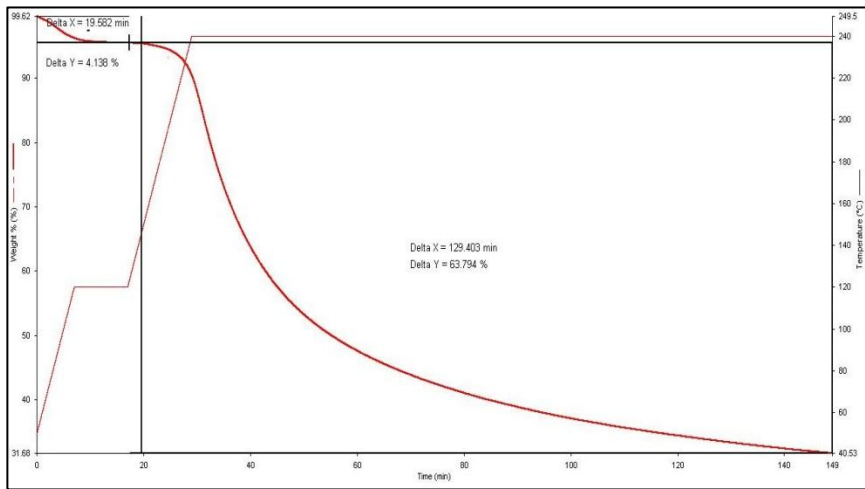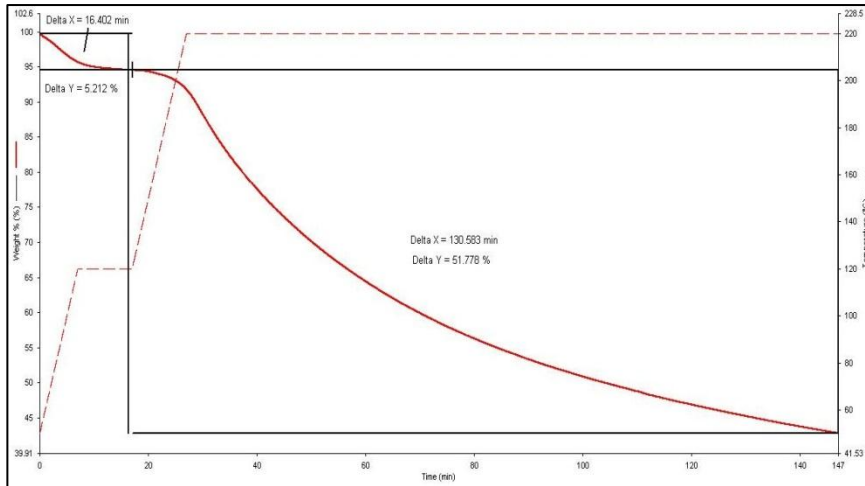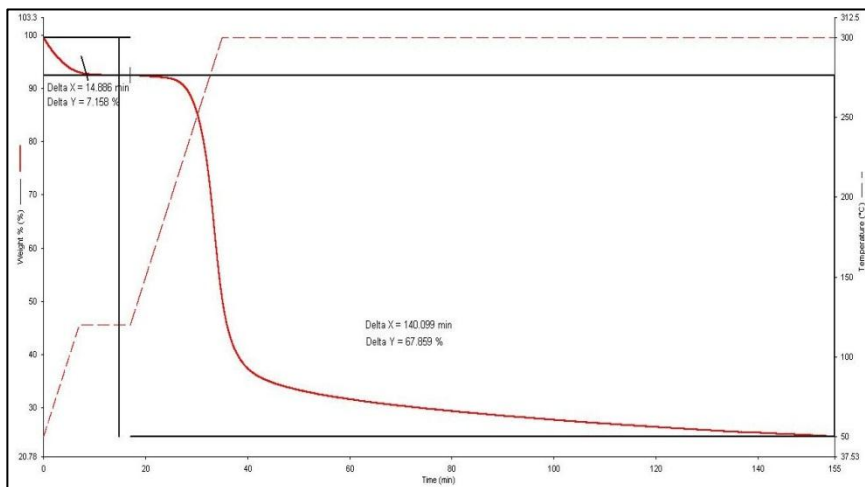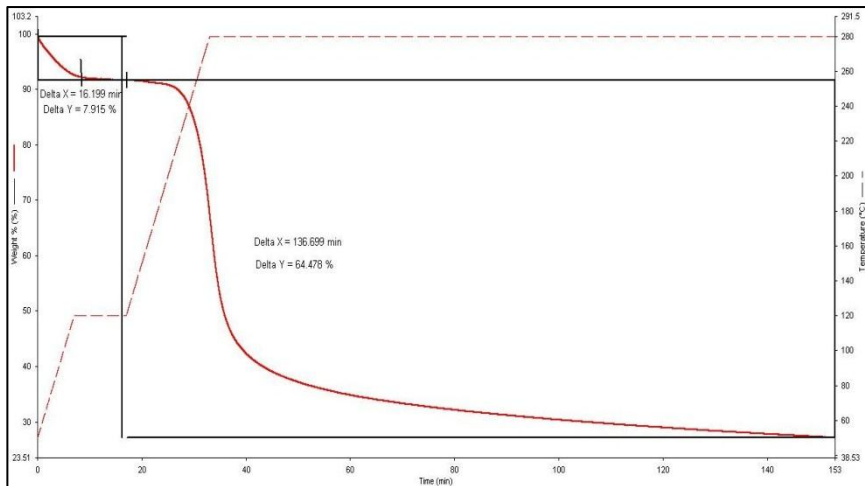
c) -Type of biomass: PMF
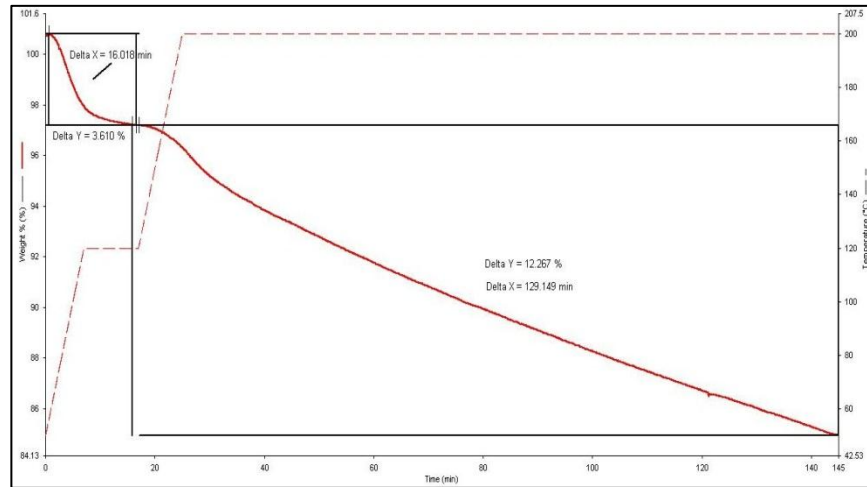
    -Particle size   : 250 – 355 µm

    -Reaction time   : 2 hours

    -Temperature   : 200, 220, 240, 260, 280 and 300°C

d) -Type of biomass: PMF

-Particle size   : 355 – 500 μm

-Reaction time   : 2 hours

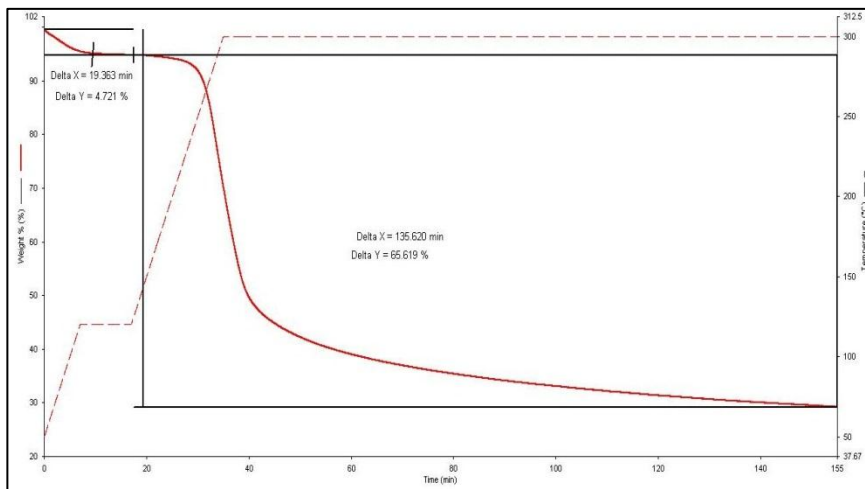-Temperature   : 200, 220, 240, 260, 280 and 300°C

Delta X = 18.348 min
Delta Y = 6.333 %

Delta X = 134.637 min
Delta Y = 68.772 %

Delta X = 16.251 min
Delta Y = 6.023 %

Delta X = 138.734 min
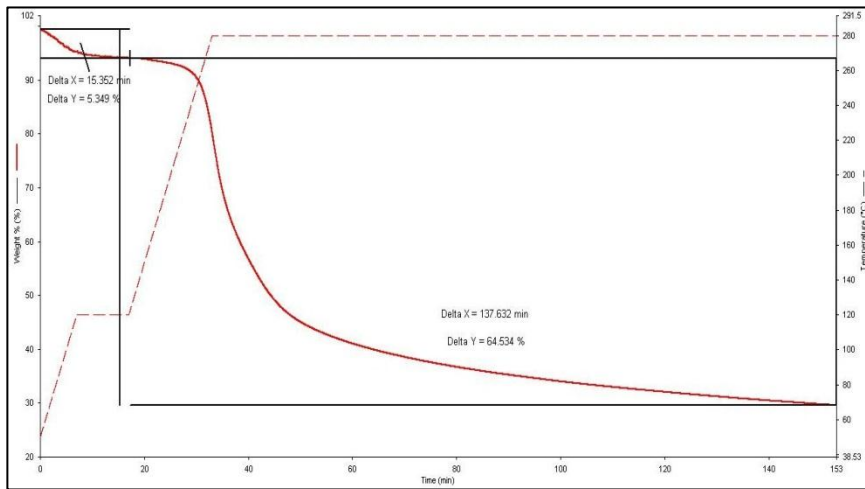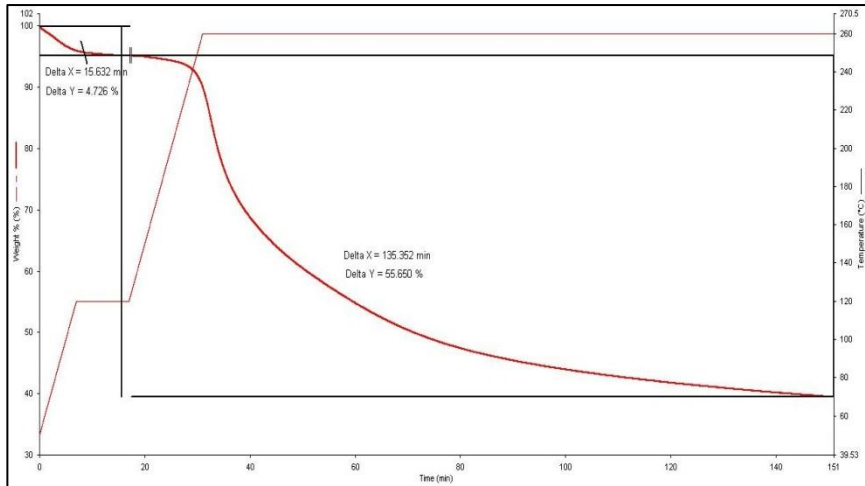Delta Y = 70.141 %
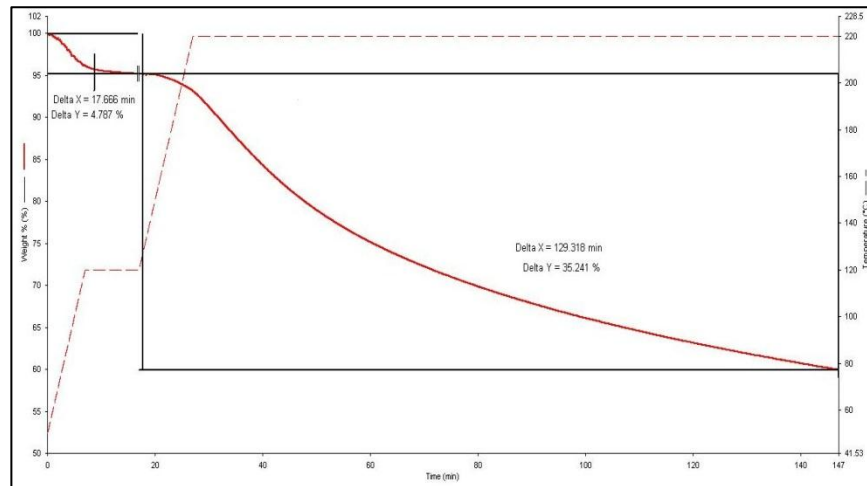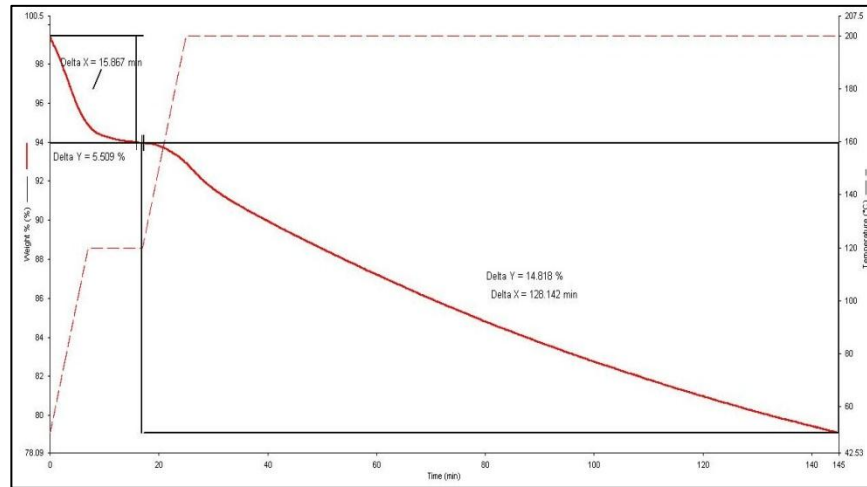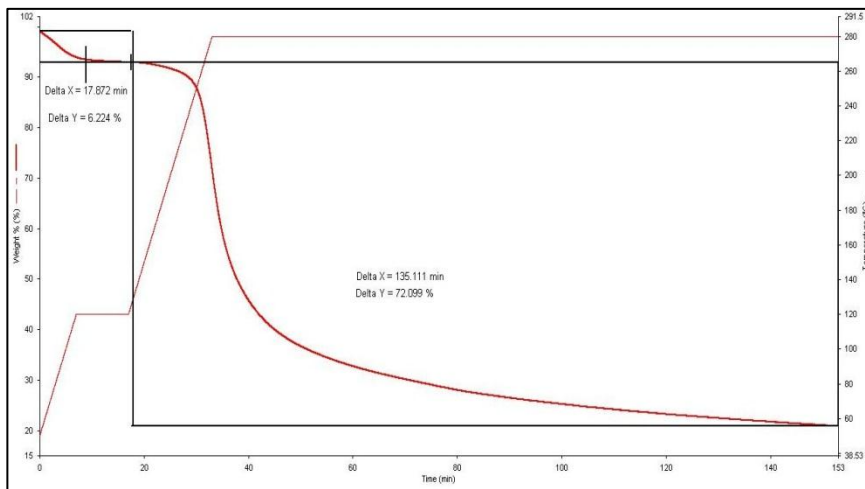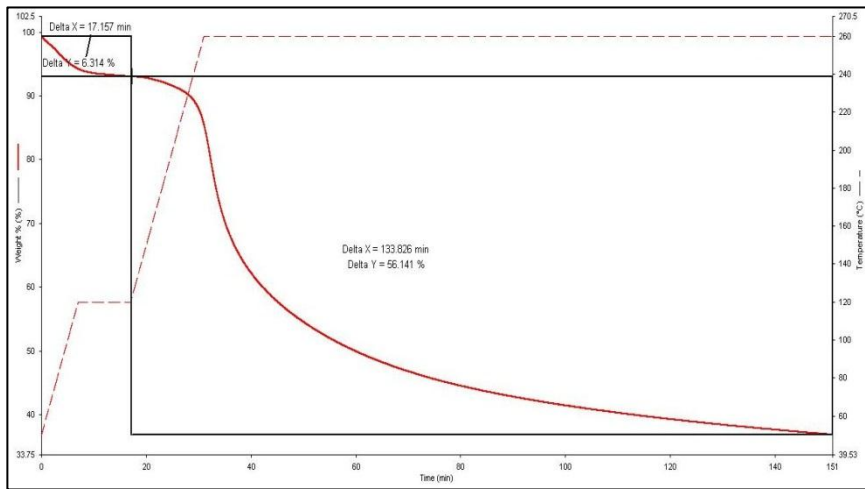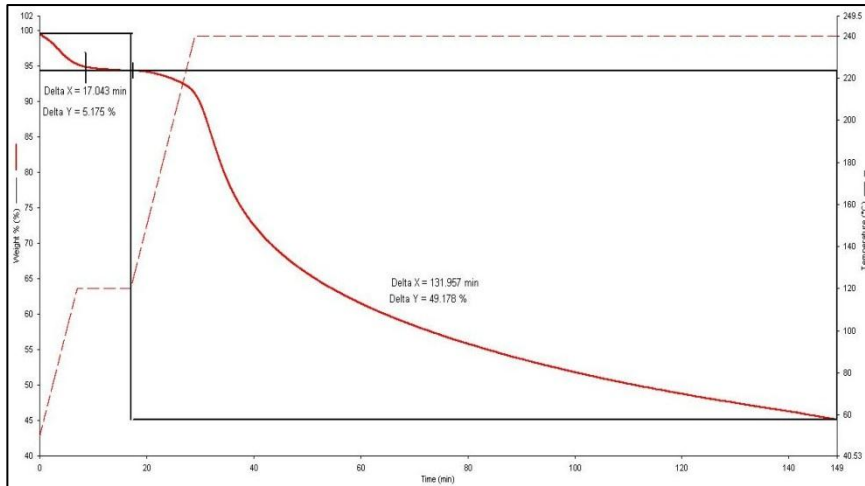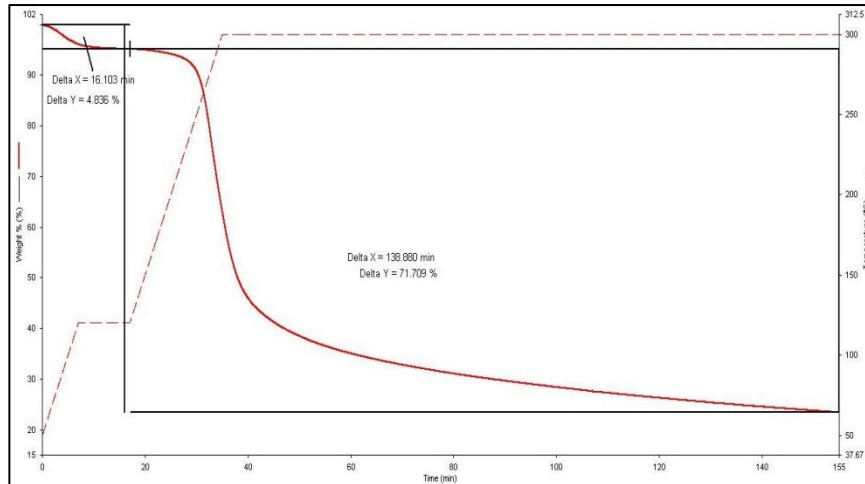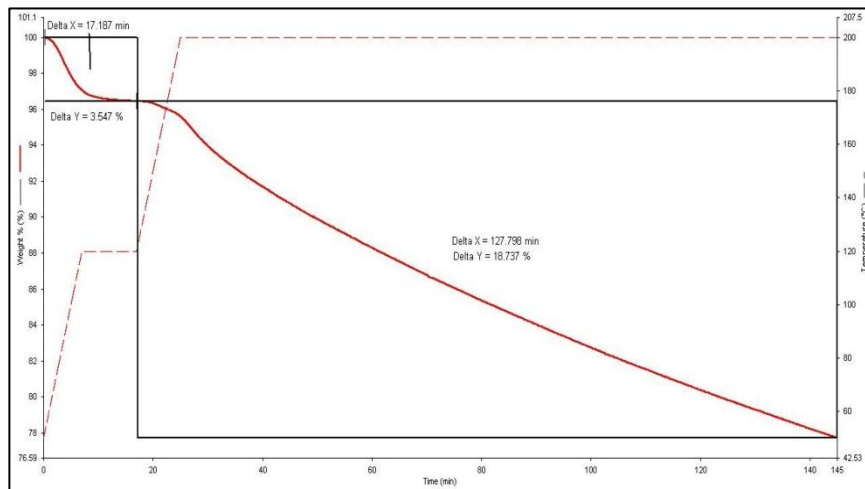
e) -Type of biomass: PKS

    -Particle size   : 250 – 355 μm

    -Reaction time   : 2 hours

    -Temperature   : 200, 220, 240, 260, 280 and 300°C

f) -Type of biomass: PKS

-Particle size   : 355 – 500 μm

-Reaction time   : 2 hours

-Temperature   : 200, 220, 240, 260, 280 and 300°C